https://doi.org/10.5194/egusphere-2026-1193
Preprint. Discussion started: 20 March 2026

Attribution of The Record Breaking 2025 European Fire Season to Climate Change

Theodore R. Keeping[1,2], Mariam Zachariah[1], Olivia Haas[2,3], Manolis Grillakis[2,4], Clair Barnes[1], Gareth D. Clay[5], Bikem Ekberzade[6], Orjeta Jaupaj[7], Andreia Ribeiro[8,9], Ricardo Trigo[10], Apostolos Voulgarakis[2,4], Friederike E. L. Otto[1]

[1]Centre for Environmental Policy, Imperial College London, London, UK
[2]Leverhulme Centre for Wildfires, Environment and Society, Imperial College London, London, UK
[3]Laboratory for Climate Sciences and the Environment, Paris Saclay University, Paris, France
[4]School of Chemical and Environmental Engineering, Technical University of Crete, Chania, Greece
[5]Department of Geography, University of Manchester, Manchester, UK
[6]Eurasia Institute of Earth Sciences, Istanbul Technical University, Istanbul, Türkiye
[7]Institute of Geosciences, Polytechnic University of Tirana, Tirana, Albania
[8]Department of Compound Environmental Risks, Helmholtz Centre for Environmental Research, UFZ, Leipzig, Germany
[9]Institute for Atmospheric and Climate Science, ETH Zurich, Zurich, Switzerland
[10]Instituto Dom Luiz, Faculdade de Ciências, Universidade de Lisboa, Lisbon, Portugal

Correspondence to: Theodore R. Keeping (t.keeping21@imperial.ac.uk)

Abstract. The 2025 European fire season was historically extreme, with record-breaking burned area exceeding 1,400,000 ha, and multiple regionally unprecedented wildfires. Emerging fire regimes and extreme wildfire behaviour in Europe pose increasing adaptation challenges. Extreme event attribution of a recent fire season, combined with analysis of changes in vegetation and land use, provides insight into the effect of climate and environmental change on high impact events. We analyse five regions that experienced particularly extreme wildfire activity in 2025 (northwestern Iberia, western and northern Britain, Occitania, the eastern Adriatic/Ionian, and northern and western Türkiye) capturing a diverse range of driving weather conditions and fire regimes. Strong trends towards drier summer summers and extreme weekly vapour pressure deficit (VPD) were found, with summer drought emergent from natural variability in most southern European regions, and VPD extreme emergent in reanalysis data for all regions. Changes in VPD are the main reason why combined hot, dry, and windy conditions have become more frequent than expected from natural variability. This emergence is seen in both reanalysis data and climate models for the Iberian, Adriatic/Ionian and Turkish regions. In contrast, in the British and Occitanian regions, models do not show observed trends.

https://doi.org/10.5194/egusphere-2026-1193
Preprint. Discussion started: 20 March 2026

1 Introduction

The 2025 European wildfire season saw a record-breaking burned area of over 1.4 million ha (European Commission, 2026), since 2006 when the EFFIS record began (Fig. 1). Many regions across a range of wildfire regimes experienced extreme wildfire activity, with Cyprus, Germany, Kosovo (per UNSCR 1244), Slovakia, Spain and the United Kingdom all seeing their highest annual area burned since 2006, and for 19 countries out of 39 in the European region 2025 was one of the three most severe years for annual area burned (Table G1). This development of several regionally unprecedented wildfires across the European region was associated with extreme fire weather conditions. Galicia experienced its largest wildfire on record, with fires across northwestern Iberia leading to eight direct deaths (France 24, 2025) and 40,000 evacuations (De Ozone, 2025; Viúdez, 2025; Ortiz, 2025). The largest French wildfire in 75 years led to a death (Robins. 2025) and significant losses to vineyards (Mercer, 2025) – a key regional industry. In Türkiye, wildfires were most destructive – resulting in 17 deaths, over 1000 structures destroyed, and over 50,000 people evacuated (Keeping et al., 2025a). 2025 also recorded the highest European wildfire emissions since 2003 when the full global MODIS record began, with the majority of the smoke emitted from large fires in Portugal and Spain leading to poor air quality in that region (Parrington and McNorton, 2025). Wildfire smoke broadens the otherwise localised impacts of wildfire events, harming respiratory and cardiovascular health (Naeher et al., 2006) and causing large numbers of excess deaths globally (Johnston et al., 2012; Chen et al., 2021).

European-wide fire records are relatively short and often begin only after major demographic and economic shifts had already transformed historical human–land interactions. Although longer national records exist in some countries (e.g. France), they provide limited insight into whether recent fire seasons are truly unprecedented beyond the very recent past. Nevertheless, the events examined here were clearly extreme and, in some cases, may lack historical analogue. Detailed description of the driving conditions of 2025's extreme wildfire events coupled with attribution of fire weather conditions and trend analysis of land-use and vegetation allows the contribution of multiple rapidly changing wildfire drivers to extreme wildfire seasons to be assessed in detail, providing insight into the present and future state of the European wildfire hazard.

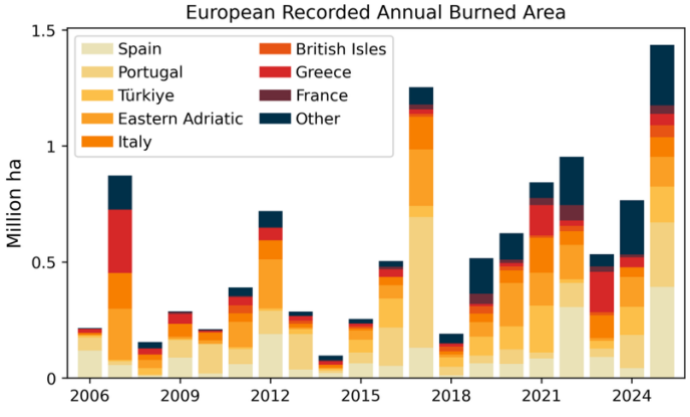

https://doi.org/10.5194/egusphere-2026-1193
Preprint. Discussion started: 20 March 2026

Figure 1: European annual burned area according to EFFIS estimates from 2006-2025 breaking down contributions to total burnt area in the EU + Albania, Andorra, Bosnia and Herzegovina, Kosovo (per UNSCR 1244), Montenegro, North Macedonia, Norway, Serbia, Switzerland, Türkiye, and UK. Major national contributors to the 2025 fire season are colour coded, with 'Eastern Adriatic' aggregating Albania, Bosnia and Herzegovina, Croatia and Montenegro, and 'British Isles' aggregating Great Britain and the island of Ireland – due to smaller individual contributions from these adjacent countries with similar fire ecologies.

Together, extreme heat, winds and drought constitute 'fire weather', which drive the large wildfire events (Potter and McEvoy, 2021) that dominate regional burned area variability (Hantson et al., 2014). With climate change, the incidence of some key ingredients of fire weather, in particular hot-dry extremes, are projected to increase globally and across Europe (De Luca and Donat, 2023). Extreme heat leads to an exponential increase in atmospheric moisture capacity and vapour pressure deficit (VPD), and consequently increased evaporative demand on plants and dead fuels, and has been strongly linked to the largest wildfire events in Europe (Costa-Saura et al., 2025; Little et al., 2025). Such hot extremes are intensifying rapidly with climate change for all of Europe (Seneveratne et al., 2021). Drought leads to lower live and dead vegetation moistures, and in combination with extreme heat can cause vegetation mortality (McDowell et al., 2008), resulting in higher dead fuel loads and more intense wildfires (Stephens et al., 2018). There is a clear increasing drought signal in the western and central Europe, and Mediterranean IPCC regions (Allan et al., 2021). Another important component of fire weather is wind, with extreme winds as a driver of rapid fire spread. Whilst the response of wind to climate change is highly uncertain (Seneveratne et al., 2021), climate change can play a role in novel wind extremes. For example Hurricane Ophelia, the only Hurricane on record to ever have reached Europe, had an important effect on the unprecedented Portuguese wildfires of 2017 (Duane et al., 2021, Ramos et al., 2023). Furthermore, a possible increase in atmospheric instability with climate change (Chen and Dai, 2023) allows for greater vertical motion of the air, leading to fast-spreading, unpredictable and dangerous pyroconvective wildfire behaviour (Tang et al., 2014; Di Virgilio et al., 2019).

Clear increasing trends in fire weather extremes have been identified across Europe (Abatzoglou et al., 2018; Grillakis et al., 2022; Giannaros and Papavasileiou, 2023), with this trend projected to continue with future climate change (Garroussi et al., 2024). These large scale analyses of compound fire weather indices such as the Canadian Fire Weather Index (FWI) are useful in understanding big picture changes in a specific but widely meaningful definition of fire weather. To fully understand how climate change has and could affect wildfires, the gold standard is to understand how multiple components of fire weather and moisture stress are affecting a reasonably ecologically homogeneous region. This has been done for a small number of studies globally (Kirchmeier-Young et al., 2018; Barbero et al., 2020; Li et al., 2021; Lanet et al., 2024; Senande-Rivera et al., 2025), but there is inconsistent coverage across key European fire regimes, including no studies for most of northern Europe and the eastern Mediterranean – including Adriatic, Ionian and Aegean coastal regions that are extremely wildfire prone.

https://doi.org/10.5194/egusphere-2026-1193
Preprint. Discussion started: 20 March 2026

In addition to weather conditions, other factors also play an important role in understanding the unprecedented fire season in 2025. Europe has seen an increasing trend in gross primary production over recent decades, also known as greening (Eisfelder et al, 2025; Kempf et al., 2023). Gross primary production is a key driver of wildfire activity (Pausas and Ribeiro, 2013; Haas et al., 2024), with greater fuel availability causing higher burnt area and fire intensity (Haas et al., 2022). The primary driver of increased gross primary production over Europe is increased photosynthetic activity through the CO2 fertilization effect (Cai and Prentice, 2020). Spring greening in the Mediterranean, Black Sea and Anatolian regions is driven by temperature and precipitation allowing an earlier start to the growing season whereas summer greening in Spain and Türkiye is associated with precipitation affecting mostly grasslands and croplands (Eisfelder et al., 2025). Whilst previous studies have examined overall trends in vegetation productivity over the past decades, attributing seasonal greening and browning patterns directly to specific fire activity within a given year remains challenging. Interactions with climate and land use also complicate our ability to isolate the effect. Here we analyse long-term trends in leaf area index (LAI) alongside vegetation activity in the spring and summer of 2025. This approach allows us to explore the potential for long-term fuel accumulation associated with increased vegetation productivity as well as evaluate whether anomalous vegetation greening or browning in 2025 may have contributed to elevated fuel availability.

Rapid changes in climate, vegetation abundance, rural land abandonment – and its obverse, urban expansion – are all driving increasingly intense European fire per European Environment Agency reporting (Keesstra et al., 2025). In Mediterranean Europe, the widespread abandonment of formerly managed lands has emerged as a major driver of increasing fire hazard through passive vegetation succession (Mantero et al., 2020; Ganteaume et al., 2021). As traditional agricultural and pastoral practices decline, landscapes shift from heterogeneous mosaics of land uses to continuous natural vegetation dominated by flammable shrublands and young forest stands (Moreira et al., 2011; Fernandez-Anez et al., 2021). This vegetation regrowth substantially increases fuel continuity and biomass accumulation, thereby enhancing the potential for rapid fire spread across the landscape (Salis et al., 2022). In addition, the accumulation of dead biomass increases vertical fuel connectivity, and the likelihood that surface fires escalate into crown fires and overwhelm initial suppression efforts. As a result, many Mediterranean regions have transitioned from historically fuel-limited fire regimes to predominantly drought-driven regimes, in which abundant, unmanaged fuels enable the development of high-intensity wildfires during extreme weather conditions (Pausas and Fernández-Muñoz, 2012; San-Miguel-Ayanz et al., 2013).

Considering the continuing emergence of extreme fire behaviour in Europe (Dupuy et al., 2020, Duane et al., 2021) and the underlying but inhomogeneous trends in fire weather, vegetation cover, and land management, we offer a detailed analysis of the changing drivers of wildfire for five spatially diverse regions that experienced extreme wildfire in 2025, and how they are responding to climate and land use change. In section 2, we introduce the five study regions considered in the analysis, including an overview of the fire regime and key drivers of change in wildfire activity for each. In section 3, an overview of the variables, datasets, and attribution methodology used is given. Section 4.1 covers fire weather experienced across Europe

https://doi.org/10.5194/egusphere-2026-1193
Preprint. Discussion started: 20 March 2026

in 2025, with trends in vegetation cover and land-use also presented. Sections 4.2-4.6 give a probabilistic attribution of the changing likelihood and intensity of the drought and fire weather conditions seen in 2025 due to climate change from pre-industrial to present, and from present to +2.6°C, using a synthesis of reanalysis and climate model data per Philip et al. (2020). Time series in overall spring and summer vegetation cover, as well as the managed land fraction, were also aggregated for each case study region. Interpretation of these changes and their implications is given in section 5.

2 Study Area

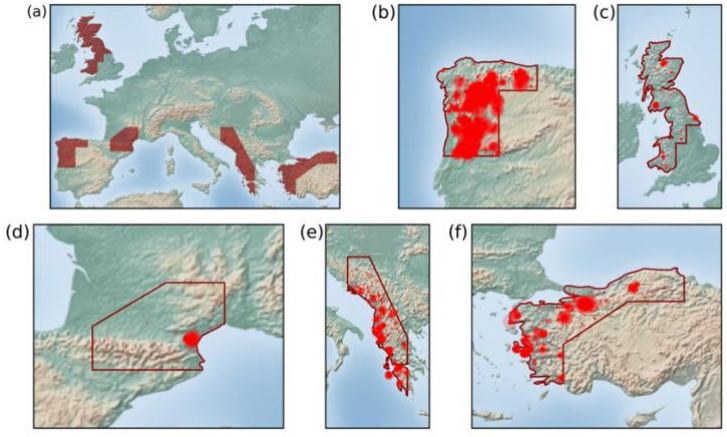

Figure 2: Case study regions considered in this analysis, with daily fire radiative power (per MODIS) events in 2025 overlaid where the size of the dot is proportional to the daily detected FRP. (a), the five case study regions analysed here in greater detail – selected for anomalously severe wildfire behaviour. (b), the case study region referred to hereafter as northwestern Iberia. (c), the case study region referred to hereafter as western and northern Britain. (d), the case study region referred to hereafter as Occitania. (d), the case study region referred to hereafter as the eastern Adriatic/Ionian. (e), the case study region referred to hereafter as northern and western Türkiye.

Different regions of Europe experience highly varied wildfire seasons. Galizia et al. (2021) identify approximately half of the European Economic Area (EEA) – which excludes Türkiye – as being non-fire-prone, meaning very few fires and low burned area, primarily situated across central and northern Europe. In some regions more fires occur in the cool season, especially spring, such as in the UK, the southeastern Baltic and eastern Europe (Miller et al., 2025) when drier, dormant vegetation is more likely to reach low fuel moistures (Nikonovas et al., 2024). In contrast, the Mediterranean, Türkiye and Iberia are characterised by a strong summer fire season where frequent and large fires are most common, with large fires especially prevalent in western Iberia, and the Adriatic (Galizia et al., 2021). The five case study regions considered in this analysis span different wildfire regimes and were selected for very high levels of wildfire activity in the 2025 fire season, shown in Fig. 2. From east to west:

https://doi.org/10.5194/egusphere-2026-1193
Preprint. Discussion started: 20 March 2026

1. Northwestern Iberia experienced a widespread wildfire outbreak, peaking from 15-19th August, 2025. Extreme heat and winds drove large wildfires – leading to Spain's highest burned area on record (393,000 ha) and Portugal's second highest fire year (279,000 ha) after the catastrophic fires of 2017 (Keeping et al., 2025b, Sánchez-Hernández et al. 2025).
2. Western and northern Britain was subject to record breaking burned area in 2025 (48,000 ha over the entire UK), with wildfire activity peaking from 2-8th April, when two large wildfires simultaneously occurred in Galloway Forest Park, Scotland, and Ystrad Fflur, Wales (Poynting and Rivault, 2025).
3. Occitania, southwestern France, experienced an extreme wildfire from 5-8th August in Aude, rapidly spreading to become the largest French fire (17,000 ha, Copernicus, 2025) to be recorded in 80 years (Bruneau, 2025). Whilst wildfire activity was otherwise not particularly extreme across France, the Aude wildfire contributed to nearly half of France's total burned area, pushing 2025 to France's 3rd most extreme year after 2022 and 2019.
4. Eastern Adriatic and Ionian also saw extreme wildfires, with two peaks of wildfire activity from 22-27 July and 11-13 August. Albania experienced almost 200 large-scale fires, and Kosovo (per UNSCR 1244) had its highest burned area on record. Whilst Greece has seen considerably worse fire seasons in eastern Greece (e.g. 2007, 2023), the two western regions of Epirus and Western Greece experienced the highest or second highest burned area on record (WWF, 2025).
5. Western and northern Türkiye experienced two peaks of wildfire activity from 27th June-3rd July and 20-28th July, leading to Türkiye's second highest wildfire season (154,000 ha) after 2021 (202,000 ha). Despite less burned area than 2021, the impacts were higher, with extreme wildfires at the wildland urban interface (WUI) leading to fatalities and requiring widespread evacuations (Keeping et al., 2025a).

A number of countries also experienced record-breaking wildfire activity, namely Cyprus, Germany and Slovakia. These were not studied due to the small area of the burned area region in Cyprus not being spatially contiguous with the nearby region of northern and western Türkiye, and due to very low burned area in absolute terms in Germany and Slovakia.

2.1 Northwestern Iberia

Northwestern Iberia, which includes central and northern Portugal and northwest of Spain, is the region with highest burned area across the Iberian Peninsula (Calheiros et al. 2020, Rodrigues et al. 2020, Trigo et al. 2016) as was also the case in 2025. Summer meteorological conditions, particularly heat extremes and moisture deficits, explain approximately 70% of the interannual variability of July and August burned area (Sousa et al. 2015). Antecedent wet and mild conditions during late winter and early spring months typically allow the development of live fuels that become highly flammable in the following hot and dry summer (Gouveia et al. 2012, Russo et al. 2017). Typically, large burned areas occur when high-pressure systems develop over the Atlantic (Sousa et al. 2015), generating the necessary hot and dry conditions for the widespread of fire activity. Northwestern Iberia is characterised by relatively high annual precipitation values, fueled by the frequent fronts interacting

https://doi.org/10.5194/egusphere-2026-1193
Preprint. Discussion started: 20 March 2026

with the marked topography leading to considerably wetter conditions than most southern and Mediterranean regions experience. Its natural vegetation is needleleaf or deciduous forest, substituted to a large extent by pastures and secondary forest plantations (e.g. eucalyptus, pinus) that present fire danger throughout the entire year (Trigo et al. 2016).

Despite the importance of the meteorological drivers, human and environmental factors also modulate the burned area variability of the region. While fire weather has increased significantly in the past 40 years (Turco et al., 2019), summer burned area has not shown a comparable long-term increase due to suppression efforts (Sánchez-Hernández et al. 2025) and an approximate 50% decrease of ignitions in Portugal since 2017 (AGIF report, 2025). Most rural regions in northwestern Iberia have suffered widespread abandonment and depopulation since the 1970s, contributing to an increase in fuel availability for the ignition and wildfire spread (Trigo et al., 2016). Nevertheless, while burned area is decreasing and fire weather increasing, the more extreme fires such as those in 2025 are exceeding the suppression capacity.

2.2 Western and Northern Britain

Fire occurrence peaks during spring in northern and western parts of Great Britain (Nikonovas et al. 2024) and the greatest burned area occurs in mountain, bog and heath landscapes – all characterised by low, highly connected vegetation (Forestry Commission, 2023). Southeastern and central regions of England, which is not part of the study area identified for this study, on the other hand are increasingly summer fire dominated, particularly in arable or improved grassland land covers (Nikonovas et al., 2024; Forestry Commission, 2023). The majority of vegetation fire in the UK are small (usually less than 1 ha; Forestry Commission, 2023, Gagkas et al., 2022) though larger and landscape scale fires do occur, especially during droughts and prolonged heatwaves (Ivison et al., 2025; Little et al, 2025).

Nearly all wildfires in the UK are anthropogenic in ignition though there is limited routine investigation of wildfire causes (Belcher et al., 2021). Although the majority of vegetation fires are smaller than other regions in Europe, they can still have significant impacts on communities, infrastructure and ecosystems (Belcher et al, 2021), especially when multiple events at the same time can cause pressure on land managers and emergency services (NFCCa, 2025).

2.3 Occitania

The Occitania region of France shares a similar fire regime to the rest of the French Mediterranean coast. This fire regime is characterized by frequent, but small summer fires which are often wind or drought driven (Castel-Clavera et al, 2023; Pimont et al., 2021). 2003 saw a record-breaking year for fire occurrence in the region, leading to the implementation of strong fire suppression policies, which have limited small to moderately sized fires but not the likelihood of large fires (Castel-Clavera et al., 2023). Fire occurrence and size in the region is influenced by infrastructure networks such as road and urbanisation, as well as crops, which fragment the landscape (Ruffault & Mouillot, 2015; Frejaville & Curt, 2017). Such land cover characteristics can impact ignitions and microclimates, altering baseline fire regimes (Bowring et al., 2024). However, whilst

https://doi.org/10.5194/egusphere-2026-1193
Preprint. Discussion started: 20 March 2026

land use and fire weather have been shown to equally influence wildfire occurrence, fire weather emerges as the key driver in large fires once spread has begun, with significant increases in potential fire activity over the last decades shown to be linked to increases in fire weather occurrence (Castel-Clavera et al., 2023). Since 2010, over 5,500 hectares of vineyards have been removed and abandoned in the region. As a consequence, there has been an increase in the cover of garrigue vegetation, which is a highly flammable and shrubby vegetation type. Historically, vineyards in the valleys of the mountains through which the Aude fire spread may have provided discontinuous and less flammable fuel, preventing wildfire from spreading from one slope to another.

2.4 Eastern Adriatic and Ionian

Western Greece and the Ionian islands are less fire-prone than Eastern Greece, with heat, droughts, and winds generally less intense. Weather conditions conducive to catastrophic wildfires nonetheless occur in the region, particularly in the summer. Given that precipitation is more abundant in western parts of the country (Hatzianastassiou et al., 2008), fuel availability is also higher and constitutes another pronounced hazard factor. Wildfires are primarily human-caused, and typically occur in mosaic shrubland and pine forest ecosystems.

Further north, Albania is illustrative of the highly fire-prone eastern Adriatic summer fire regime. The highest concentrations of fire frequency and burned area are coastal (Jaupaj & Jaupaj, 2025), with rapidly spreading wildfires especially prevalent in the south. Satellite-based analyses using Sentinel imagery, which shows that wildfire impacts during the period 2020–2025 have predominantly affected open and semi-natural vegetation types, including sclerophyllous shrublands, broadleaved forests, and, to a large extent, degraded formations such as garrigue and transitional woodland–shrub. Burned-area statistics for this timeframe indicate that these latter classes account for a substantial share of total fire impact, reflecting long-term land degradation, repeated disturbance, and progressive fuel simplification (Jaupaj, 2025).

The eastern Adriatic and Ionian are largely karstic in geology (Hollingsworth, 2009), meaning rapid drainage and thin soils result in very low soil water volumes. Consequently, vegetation degradation due to disturbance or drought can lead to high dead fuel volumes. This is a key driver of wildfire in the region, with the karstic regions of Albania corresponding most strongly to those that experience the most severe wildfires (Parise et al., 2004; Serjani et al., 2001) – despite fire weather being more moderate in these coastal environments (Jaupaj, 2025).

2.5 Northern and Western Türkiye

The wildfire regime of northwestern Türkiye is a transitional dual system, with the historically humid, low-frequency regime of the Euro-Siberian Black Sea forests increasingly replaced by the frequent, high-intensity fire dynamics of the Mediterranean coast. The high-intensity fires peak in summer, with a late-spring also seeing a pulse of smaller, predominantly human-ignited agricultural fire use in Thrace and southern Marmara. Although usually small, these agricultural fires frequently escape into

https://doi.org/10.5194/egusphere-2026-1193
Preprint. Discussion started: 20 March 2026

forest edges – especially given a dry spell, as observed in the Bursa–Bilecik–Eskişehir fires of early summer 2025. Critical wildfire danger is understood to increase sharply under elevated temperatures, low humidity and delayed autumn precipitation. This condition is now increasingly common during summer heatwaves, as Mediterranean climate characteristics expand northward and formerly humid forests lose their buffering capacity. The region's topography further amplifies fire danger, as interactions between the hot, dry southwesterly Lodos wind and the northeasterly, Black Sea Poyraz wind generate erratic wind fields that complicate fire spread and suppression, particularly in interior Marmara and the Western Black Sea (Biçen et al. 2022).

While rapid urbanization, tourism development, and the expanding WUI elevate ignition probability in Türkiye's most densely populated regions, where almost all fires are human-caused (Ekberzade et al. 2025), concurrent rural depopulation and abandonment of traditional grazing have also led to shrub encroachment and increased fuel continuity in parts. Pinus brutia forests of the northern Aegean are more prone to intense crown fires, whilst the montane forests of mixed *Pinus nigra*, *Abies spp.* and *P. sylvestris* have historically been associated with lower intensity surface fires.

2.6 Research Justification

As detailed in the five sections above, there is detailed knowledge of the regional drivers of extreme wildfire events across European fire regimes – with many changes in these drivers observed across environments. However, partially due to the relatively short observed, satellite-based wildfire record, the causes of historic changes in the fire regime are poorly understood, especially in comparison to the highly detailed understanding of drivers in the most recent decades. To fill this gap, we provide a systematic attribution study of the weather-related drivers of fire, aiming to give a detailed overview of how the likelihood of the different contributing weather conditions to extreme wildfire has changed over time. This quantification of the changing probability of realised extreme fire weather and its resulting wildfires can be a key input to expert and operational planning for future wildfire extremes across Europe.

By assessing five extreme fire seasons across Europe, this research samples a high diversity of meteorological drivers of elevated fire danger (e.g. spring drought in Britain; heat and hydroclimatic whiplash in Iberia; and compound hot, dry and windy conditions in the Eastern Adriatic) across a broad range of fire-prone environments, whilst also accounting for trends in vegetation and land use. In addition to being specifically useful to understanding (1) why the 2025 fire year was so extreme in Europe and (2) how the hazard profile is changing in the five case study regions, this work is also illustrative of the spread of possible extreme fire events and their drivers across Europe and how those are likely to change in the future.

https://doi.org/10.5194/egusphere-2026-1193
Preprint. Discussion started: 20 March 2026

3 Data and Methods

3.1 Meteorological Variables

For each region, we examine the annual maximum of three fire weather variables averaged over a rolling seven-day period: daily maximum VPD, daily maximum wind speed, and the hot-dry-windy index (Srock et al., 2018) – defined here as the product of daily maximum VPD and wind speed. An evaluation of these fire weather variables is provided in Appendix F. We also analyse the meteorological spring maximum (MAM) of these variables for the western and northern Britain region, due to the clear spring peak in wildfire activity in this region. Additionally, we examine the spring (MAM) and summer (JJA) effective precipitation over all study regions – which affects antecedent fuel growth and drought conditions. Effective precipitation is defined at the seasonally accumulated precipitation minus potential evapotranspiration, here calculated according to the Hargreaves formula (Hargreaves and Samani, 1982).

3.2 Data Sources

Observational analysis was conducted using the ERA5-Land reanalysis product (Muñoz-Sabater et al., 2021), which is a land-only rerun of the ERA5 climate reanalysis at a 0.1° spatial resolution using the H-TESSEL land model. Annual fire weather statistics were used from the years 1960 to present.

We synthesise the results of the reanalysis attribution with results from ensemble of global circulation models (CMIP6) and regional climate models (Euro-CORDEX). CMIP6 is a set of simulations from 19 climate models (Eyring et al., 2016), with the period 1850-2014 based on historical simulations and the SSP5-8.5 up to +2.6°C global warming taken for future projections. Euro-CORDEX is part of the Coordinated Regional Climate Downscaling Experiment (CORDEX) of the European domain (Jacob et al., 2014; Vautard et al., 2021). The period up to 2005 was based on historical simulations, and future projection up to +2.6°C was made using the RCP8.5 scenario. Not all variables were available for all models, and models were evaluated per section 3.3 before inclusion in the attribution analysis.

3.3 Attribution Methodology

To investigate the dependence of trends in effective precipitation and selected fire indices on global mean surface temperatures, we use an established probabilistic attribution methodology (Philip et al. 2020, van Oldenborgh et al. 2021). A linear model is fitted to each time series, in which the mean of the distribution is assumed to depend on the global mean surface temperature (GMST), while the variance and (where applicable) shape parameters remain fixed over time, with all parameters estimated using maximum likelihood methods. To remove variability in the GMST due to the El Niño-Southern Oscillation, we use a four-year rolling mean of the annual GMST, centred on the third year. Seasonal effective precipitation is assumed to be normally distributed about the mean, while annual maxima of 7-day fire indices are assumed to follow a nonstationary Generalised Extreme Value (GEV) distribution.

https://doi.org/10.5194/egusphere-2026-1193
Preprint. Discussion started: 20 March 2026

The fitted model is used to calculate the likelihood of observing an event of equal or greater magnitude than the value observed in 2025 (the 'exceedance probability'), in both the current climate and in a 'counterfactual' climate in which the climate is 1.3°C cooler than 2025, representing a preindustrial climate without human-caused warming (1850-1900, based on the Global Warming Index). The exceedance probability of the event in the current climate is expressed as its inverse, the return period, which is the expected number of years between events and is typically easier to interpret than the probabilities themselves, which can be very small. We also use the fitted model to calculate the expected intensity of a similarly extreme event in the 1.3°C cooler counterfactual climate. This allows us to estimate the change in intensity of similarly extreme events, and also the factor change in the likelihood of experiencing events of the observed magnitude (the probability ratio, or PR), associated with 1.3°C of global warming. Uncertainties on all of these quantities are obtained via a bootstrapping procedure, in which whole years are resampled with replacement, the model refitted, and all quantities estimated again for 1000 bootstrap samples.

This process is repeated not only for the ERA5-land reanalysis, but also for a collection of climate models. Following Philip et al (2020) we use two different ensembles of climate models with different framings: global circulation models (GCMs) from the CMIP6 ensemble, and regional climate models from the Euro-CORDEX ensemble (see section 3.2 above). Climate models were first evaluated on their ability to replicate each variable's seasonal and spatial patterns across each study region. For each climate model that passes the first stage of model evaluation, time series of the appropriate index are obtained, and the same statistical model is fitted, using all years of data up to 2025 and the model's own GMST (in the case of the Euro-CORDEX models, the GMST of the parent GCM). If the uncertainty intervals of the parameter estimates do not overlap with those of the observational data, the model is excluded from further analysis, since this implies that the model does not accurately replicate the behaviour of the variable or index. For those models that also pass this stage of the evaluation, we use the statistical model to calculate the magnitude of an event with the same return period in 2025 as the observed event; the return period of an event of that magnitude in a 1.3°C cooler climate; and the change in intensity of such an event associated with 1.3°C of warming. This analysis is then repeated using all years of available data up to 2070, calculating the changes from the present to a 1.3°C warmer future climate (that is, 2.6°C warmer than the preindustrial era). This level was chosen for the future scenario as this is an optimistic estimate of our current emissions trajectory if existing NDCs are implemented (UNEP, 2024). Confidence intervals are again obtained by bootstrapping.

The results from the analysis of the climate models are finally combined into a single estimate (with associated uncertainty) of the change in intensity / probability ratio simulated by the climate models by using a precision-weighting algorithm in which more confident estimates (those with lower uncertainty) are given more weight. This estimate is then combined with the estimate from ERA5-land, again in a precision-weighted average, to obtain a final synthesised estimate of the attributable change in intensity and likelihood of similar events. For more details of this procedure, see Otto et al. (2024).

https://doi.org/10.5194/egusphere-2026-1193
Preprint. Discussion started: 20 March 2026

3.4 Fire Radiative Power as a Metric of Wildfire Activity

Fire radiative power (FRP) is a measure of the rate of energy release by active wildfires according to satellite-sensed infrared light bands, which we use here as a measure of the intensity of wildfire activity within a region. It directly relates to the total calorific value of consumed fuel, and consequently strongly relates to the intensity of the fire front and the area of the grid cell concurrently burning at the point of observation. FRP products can miss short duration wildfires (MODIS overpasses approximately twice daily), wildfires on overcast days (generally of lower intensity due to weather conditions), and can aggregate multiple wildfires per grid cell at coarser resolutions as used in this study. Nonetheless, FRP is a useful metric for the intensity of large-scale, extreme wildfire events – which may encompass multiple individual wildfires (Bowman et al., 2017, Cunningham et al., 2024).

3.5 Leaf Area Index as a Metric of Fuel Availability

LAI is a dimensionless measure that primarily represents the amount of living and photosynthetically active vegetation, used here as a metric for vegetation/fuel availability in a landscape. Instantaneous vegetation greenness tends to reduce wildfire occurrence and spread due to increased vegetation moisture content, whereas accumulated antecedent vegetation can increase wildfire activity due to vegetation build-up and the availability of dead biomass (Kuhn-Régnier et al., 2022). As such, mean spring (MAM) LAI can be used as a proxy for the amount of vegetation which may become available to burn during the subsequent summer season. Mean summer (JJA) LAI could act both as a potential barrier to wildfires (through live vegetation) but also as potential fuel if this vegetation were to dry out quickly. We analysed the trends in leaf area index (LAI) from two LAI products: the MODIS 500m LAI product (Myneni et al., 2021) and the corrected Seoul National University (SNU) LAI product at a 0.1° resolution (Jeong et al., 2024). The SNU LAI data was available from 1982 to 2021 and the MODIS LAI data was available from 2001-2024, providing a time-series covering the last 42 years (1982-2024) with a 20-year overlap (2001-2021). We conducted a spatial aggregation to 0.5° resolution and computed the significant pixel-wise trends in annual spring (MAM: March, April, May) and summer (JJA: June, July, August) LAI using a Mann-Kendall test and significance threshold of 0.05. The magnitude of significant trends were estimated using a Theil-Sen estimator to fit a linear slope. Spatially averaged trends were also computed for each of the study regions by taking the mean spring (MAM) and summer (JJA) LAI over the study regions and fitting a linear trend following the same trend methodology.

3.6 Managed Land Fraction as a Measure of Land Reclamation or Abandonment

We analysed changes in cultivated versus natural lands in Europe using the HILDA+ land-cover dataset (Winkler et.al., 2021) for the years 1990 and 2019 for Europe, (-12° to 45°E, 34° to 72°N), to inform on the changing extent to which vegetation is managed within each region. We consider all croplands and the pastures as human managed lands, while as all forest land cover types, grass/shrubland, and sparsely vegetated are considered as natural, not cultivated lands. Then, we estimate the fraction of the area that was converted from natural to managed land, as well as the fraction of the land that was converted

https://doi.org/10.5194/egusphere-2026-1193
Preprint. Discussion started: 20 March 2026

from managed to natural land, between years 1990 and 2019. We further extract trend in the fraction of managed land relative to natural and managed land over time since 1960, for each of five case study regions. This does not capture trends in the wildland and rural urban interfaces, which contribute strongly to both ignitions (Badia et al., 2011) and impacts (Radeloff et al., 2018) of wildfires, with the focus being on the effect of overall vegetation management intensity in a landscape.

4 Results

4.1 Europe-wide Drivers

In this section we discuss observed anomalies in fire weather relevant variables, including fire radiative power (FRP), VDP, wind maxima and SPEI in summer (JJA) as well as spring (MAM) in 2025. The long term trends in leaf area index (LAI) and land management were also assessed.

Overall burned area in 2025 in Europe was highest since 2006 when recording began (European Commission, 2026). The large wildfires in northwestern Iberia dominate remotely sensed fire radiative power (Sánchez-Hernández et al., 2025), with high intensity hot spots also detected in northern Türkiye, both Ionian coasts, the northern Aegean coast, and Scotland (Fig. 3a, Appendix Fig. 7.4.1). The FRP signal is also strong in Ukraine, for example in the Danube delta bordering Romania; however, as these wildfires were driven by intense military activity, they were not considered as a case study region. Fig. 3b shows the ranking of FRP values across Europe. At a resolution of 0.5°, 455 000 km2 (6.5%) of Europe experienced the highest ranking year of total FRP, with 1 155 000 km2 (16.6%) experiencing a year in the top three for fire activity (percentages given relative to the area with non-zero FRP from 2003-2025). These areas are substantially greater than the baseline area for a 23 year period, with total FRP similar to – though slightly lower than – the hot summers of 2003 and 2006.

The highest 7-day average period of maximum daily VPD and its anomaly relative to 1990-2019 show high values across Europe (Fig. 3c, 3d), with the exception of some Baltic regions and Belarus. Extreme VPD values strongly relate to wildfire danger, with high values relating to extreme evaporative demand and very low fine fuel moistures (Rodrigues et al., 2024). VPD is highest in southern Europe due to its strong relationship with temperature, which also results in a strong sensitivity to climate change – contributing to the widespread high extremes observed in 2025 (Swain et al., 2025). Anomalies are much less strong in wind speed, with small positive anomalies corresponding to upticks in wildfire activity in northwestern Iberia, the eastern Adriatic and Ionian coast, and northern and western Türkiye (Fig. 3e, 3f). Weekly extremes in the product of daily maximum wind speed and vapour pressure deficit (HDWI) also show a strong positive anomaly across most of Europe (Fig. 3g, 3h) with the strongest relative anomalies in northwestern Spain, the Pyrenees, and northern Türkiye.

Spring saw severe drought conditions in Britain and much of northern Europe (Fig. 3i). A moist spring across most of southern Europe was followed by a whiplash into very dry summer conditions (Fig. 3j), which on average will have resulted in higher

https://doi.org/10.5194/egusphere-2026-1193
Preprint. Discussion started: 20 March 2026

than average vegetation and lower than average fuel moisture and elevated wildfire likelihood (Swain et al., 2025). The large exception to the 2025 southern European wet spring was moderately dry conditions in Türkiye. Summer drought was most intense in Iberia and western France as well as in the Balkan peninsula and Türkiye.

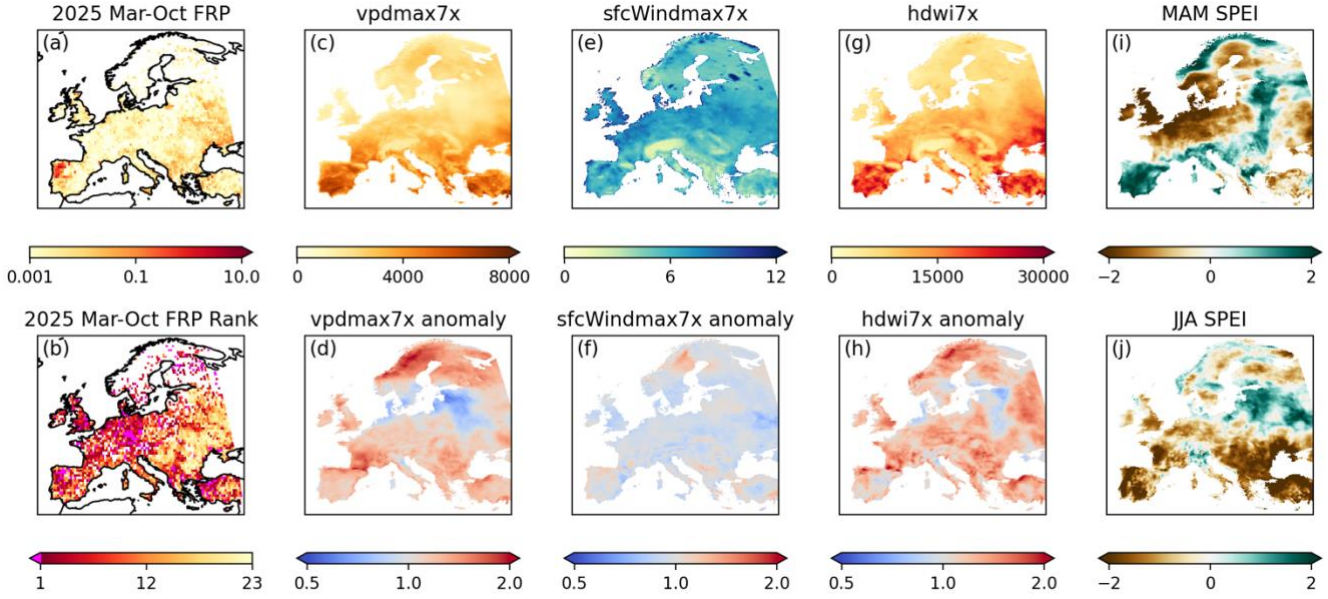

Figure 3: (a), the average FRP over the period March to October, 2025, according to the MODIS active fire product, and (b), the rank of 2025 MODIS FRP from Mar-Oct compared to other years since 2003. (c), The maximum annual 7-day rolling average of maximum daily vapour pressure deficit (vpdmax7x) according to ERA5-Land for each grid-cell, and (d), the anomaly of vpdmax7x in 2025 relative to the climatology from 1990-2019. (e) the maximum annual 7-day rolling average of maximum daily windspeed (sfcWindmax7x) according to ERA5-Land for each grid-cell, and (f), the anomaly of sfcWindmax7x in 2025 relative to the climatology from 1990-2019. (g) the maximum annual 7-day rolling average of the hot-dry-windy index – the product of maximum daily vapour pressure deficit and maximum daily windspeed (hdwi7x) – according to ERA5-Land for each grid-cell, and (h), the anomaly of hdwi7x in 2025 relative to the climatology from 1990-2019. (i), the standardised precipitation evapotranspiration index (SPEI) for spring (March-May) in 2025, calculated relative to 1990-2019. (j), the SPEI for summer (June-August) in 2025, calculated relative to 1990-2019.

There is a strong and widespread positive trend in LAI over spring, particularly in central and western Europe, extending to Türkiye (Fig. 4). This increase in spring greening may result in an increase in the amount of live vegetation available to burn in the summer fire season. The positive spring LAI trend is less pronounced or decreasing in northern Europe, including the British Isles and Scandinavia. Perhaps counterintuitively, this may also have an increasing effect on wildfire danger in some environments, as wildfire activity can peak in these cooler regions before the growing season starts – with drought conditions exacerbating low fuel moisture and likely fire intensity (Nikonovas et al., 2024; Sjöström et al., 2023; Eisfelder et al., 2025).

https://doi.org/10.5194/egusphere-2026-1193
Preprint. Discussion started: 20 March 2026

The summer LAI trends are more spatially heterogeneous (Fig. 4). Significant decreasing trends are observed in northern and central France, inland Spain and inland Türkiye. There are areas with strong greening trends, including the Alpine regions, much of Italy and southern Balkans. As a general trend, the combination of stronger spring greening trends relative to summer would suggest an overall increase in the amount of biomass available to burn in the summer fire season. Nevertheless, there are significant spatial variations. Western and northern Britain, northwestern Iberia and Türkiye show homogenous spatial patterns in terms of LAI trends. Both Occitania and the eastern Adriatic and Ionian regions show differences in spatial patterns, with the positive summer LAI trend being much stronger in the southern region of the Occitania case study and in the southern region Adriatic and Ionian case study.

In Fig. 5, we show the Naturalisation Fraction (Fig. 5), representing the conversion of managed lands - specifically croplands and pastures - to natural vegetation such as forests and shrublands. As noted above, all forests here are taken as unmanaged, which is in many countries not always the case, thus the metric is to be taken as indicative. This process is largely driven by rural land abandonment, a phenomenon particularly prevalent in northwestern Iberia, Eastern Europe and mountainous regions. Conversely, the lower right panel depicts the trend of Agricultural Intensification, where natural or unmanaged lands are converted into human-managed systems. The transition from managed to unmanaged land significantly alters both the volume and spatial arrangement of biomass available for combustion. As traditional agricultural and grazing practices decline, former pastures and open woodlands undergo vegetation succession, becoming overgrown with shrubs and dense successional vegetation. This process increases the total fuel load in these regions. Furthermore, managed landscapes historically provided fuel breaks through land-use diversification that tend to be lost as naturalization progresses. The resulting landscape becomes more spatially contiguous, allowing wildfires to propagate across larger areas with fewer obstacles to the wildfire spread.

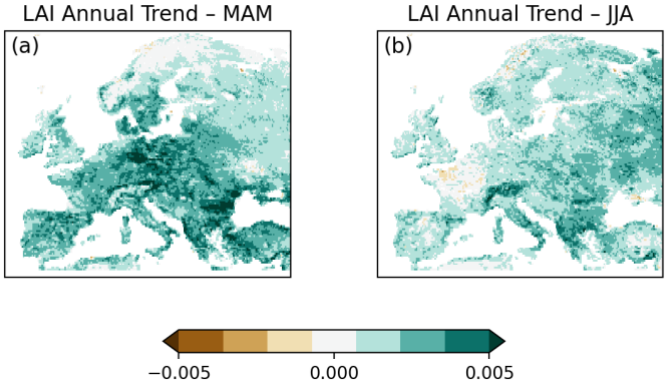

Figure 4: summary of the annual trend (yr^{-1}) at 0.5° aggregated grid cells in (a) spring (March-May) and (b) summer (June-August) leaf area index (LAI) per a Theil-Sen estimator of the linear slope – using corrected LAI data from Ryu et al. (2018): 1982 to 2024.

https://doi.org/10.5194/egusphere-2026-1193
Preprint. Discussion started: 20 March 2026

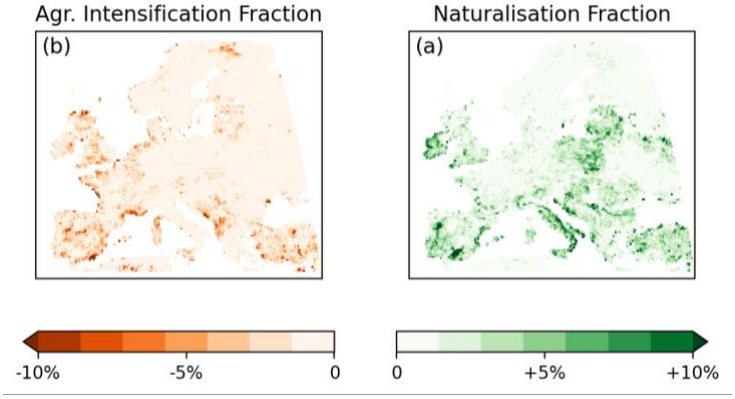

Figure 5: the fraction of land converted from (a) managed (all croplands and pastures) to unmanaged (forest, grassland, shrubland, and sparsely vegetated) and (b) unmanaged to managed per HILDA (Winkler et.al., 2021) from 1990 to 2019.

As the effects of these European wide trends can be very different, depending on the fire regime, we now present observed trends and attribution of meteorological variables to climate change for the five study regions. Reanalysis and climate model based attribution results were separately undertaken in this analysis (see Appendix Section 7.1 for a complete overview), with the synthesis of both reported in the results section per Philip et al. (2020) unless otherwise stated.

4.2 Northwestern Iberia

As discussed above, the wildfire activity in northwestern Iberia was the primary European signal in 2025 for both FRP and emissions (Parrington and McNorton, 2025, Fig. 3). An extreme 10-day peak in FRP in mid-August preceded by persistent high temperatures and VPD and concurrent with an uptick in winds (Fig. 6a). The event occurred in a dry summer (Fig. 6c), following a wet spring (Fig. 6b). Therefore, favourable conditions for fuel accumulation were followed by an anomalously intense (Fig. 6c) drying period – creating high, dry fuel loads most conducive to intense summer wildfires. The lush spring and dry summer is also substantiated by high spring and relatively low summer LAI (Fig. 6d).

https://doi.org/10.5194/egusphere-2026-1193
Preprint. Discussion started: 20 March 2026

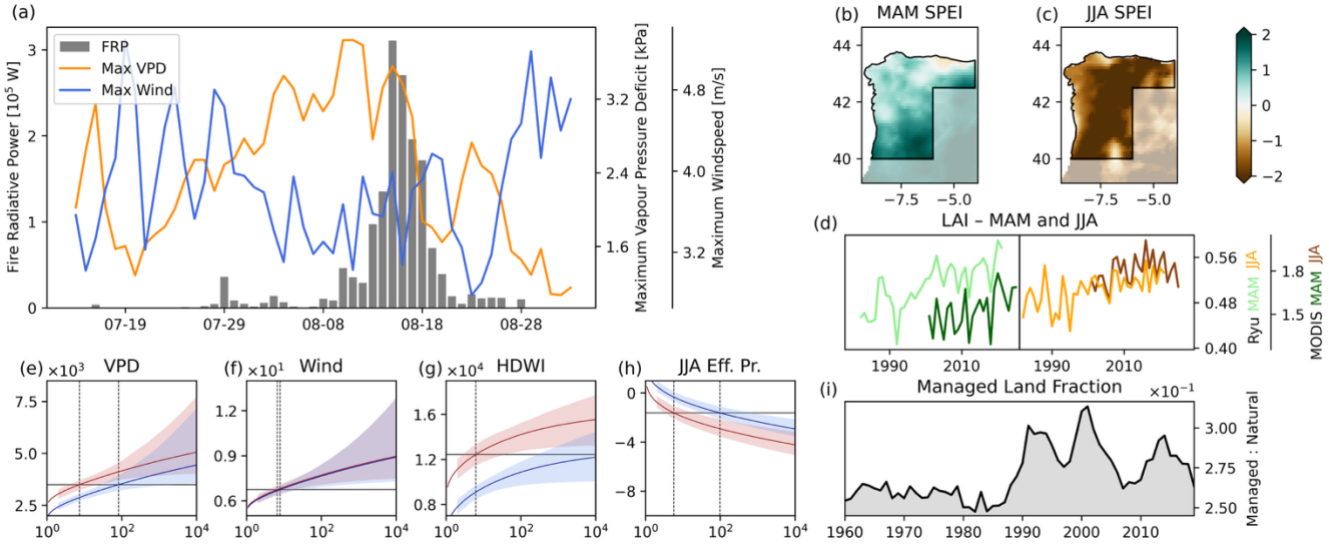

Figure 6: Northwestern Iberia summary of event conditions and regional trends. (a), time series of daily maximum wind speed and daily maximum VPD averaged over the study region, overlaid with remotely sensed fire radiative power. (b), spring (MAM) 3-month standardised precipitation-evapotranspiration index. (c), summer (JJA) 3-month standardised precipitation-evapotranspiration index. (d), Trends in spring (MAM) and summer (JJA) leaf area index (LAI) according to bias corrected data per Ryu et al. (2018) and raw data from MODIS. (e), the GEV fit of spring maximum 7-day smoothed daily maximum vapour pressure deficit (vpdmax7x) in the present climate (red) and preindustrial climate (blue). (f), the GEV fit of spring maximum 7-day daily maximum surface wind speed (sfcWindmax7x) in the present climate (red) and smoothed preindustrial climate (blue). (g), the GEV fit of spring maximum 7-day smoothed hot-dry-windy index (HDWI, the product of vpdmax and sfcWindmax) in the present climate (red) and preindustrial climate (blue). (h), the GEV fit of JJA effective precipitation (precipitation less evapotranspiration) in the present climate (red) and preindustrial climate (blue). (i), the fraction of managed land relative to natural and managed land over time, per HILDA.

Whilst trends in reanalysis data are higher, the synthesis of observations and models (Philip et al., 2020) finds a more conservative increase in the probability of the 7-day VPD conditions of 3.5 times, and an increase of 400 Pa in the intensity of a similar return-period event, due to climate change. A further 2.5 times increase in likelihood is predicted by climate models under +1.3°C further climate change. The confidence interval on the change in weekly extreme wind speed encompasses both positive and negative effects, with the central estimate being a 15% increase in likelihood or small 0.07 m/s increase in magnitude. The HDWI value was approximately 3 times as likely or 20% more intense compared to in the preindustrial climate. However, considering only observed data, the hot, dry, windy event was extremely unlikely before human-caused climate change, and is near infinitely more likely today. Future climate projections also find a strong increase in these conditions,

https://doi.org/10.5194/egusphere-2026-1193
Preprint. Discussion started: 20 March 2026

480 indicating that the sensitivity of VPD to temperatures is not projected to accompany a substantial decrease in windy conditions on hot, dry days (Table 1).

Low summer effective precipitation was approximately five times more likely due to climate change, and about 50% drier in comparison to preindustrial for an event of similar return period. This drying trend is projected to continue with future climate
485 change, with a further 2.5 probability ratio or 40% further decrease in effective precipitation for what is currently a one in five year dry event. The spring moisture trend is not emergent from variability (Table A5), meaning that lush springs followed by very dry summers remain likely in the future. Indeed, the remotely sensed LAI shows a greening trend in both spring and summer, with the trend strongest in spring and appearing to have recently plateaued or decreased in summer (Fig. 6d). The region has seen significant variation in the managed land fraction since the 1990s, with natural vegetation having increased
490 overall (Fig. 6i), however strong simultaneous abandonment and naturalisation trends are apparent in the region (Fig. 5).

Table 1: the change in probability (with 95% confidence interval) of the conditions seen in northwestern Iberia in 2025. The maximum annual 7-day average of maximum daily VPD, maximum daily surface wind speed, and the product of those (HDWI) was assumed to follow a GEV distribution in which the location parameter varies with GMST. The
495 **likelihood of low effective precipitation and spring (MAM) and summer (JJA) were assumed to follow a Gaussian distribution with the location parameter again varying with GMST. The synthesis of climate models and observations is undertaken according to Philip et al. (2020). Statistically significant effects are given in bold. The present climate is assumed to be +1.3°C higher than the preindustrial average, with the future scenario defined as +2.6°C above preindustrial. A full breakdown of the attributed probability ratio and intensity delta are provided in Appendix A.**

2025 Extreme Event	Future Probability / Present Probability		Future Probability / Present Probability
	ERA5-Land	Synthesis with CMIP6 and CORDEX models	CMIP6 and CORDEX models
7-day HDWI	**8740 (36.2, inf)**	**2.86 (1.26, 29.3)**	**2.61 (1.41, 4.87)**
7-day VPDx	**11.1 (2.69, 455)**	**3.58 (1.07, 48.7)**	**2.48 (1.38, 4.48)**
7-day sfcWindx	1.18 (0.352, 4.85)	1.154 (0.358, 5.91)	1.07 (0.558, 2.13)
MAM Effective Precipitation	1.2 (0.84, 1.6)	1.1 (0.79, 1.6)	**1.1 (1, 1.2)**
JJA Effective Precipitation	**14 (3, 93)**	**5.4 (1.3, 34)**	**2.5 (1.7, 3.8)**

500

https://doi.org/10.5194/egusphere-2026-1193
Preprint. Discussion started: 20 March 2026

4.3 Western and Northern Britain

Early April 2025 saw a distinct FRP peak in western and northern areas of Britain, coinciding with a short period where maximum daily VPD exceeded 600 Pa, and conditions were still reasonably windy (Fig. 7a). This was accompanied by a very strong drought anomaly (Fig. 7b) which was likely a chief contributor to 2025's record-breaking burned area in the region.

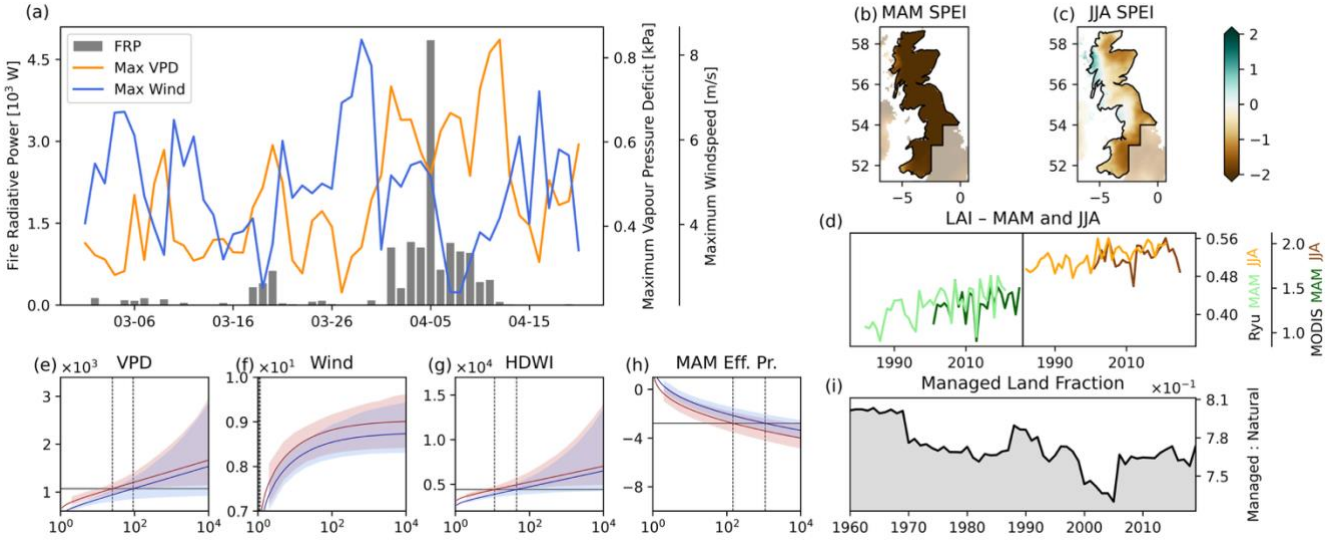

Figure 7: Western and northern Britain summary of event conditions and regional trends. (a), time series of daily maximum wind speed and daily maximum VPD averaged over the study region, overlaid with remotely sensed fire radiative power. (b), spring (MAM) 3-month standardised precipitation-evapotranspiration index. (c), summer (JJA) 3-month standardised precipitation-evapotranspiration index. (d), Trends in spring (MAM) and summer (JJA) leaf area index (LAI) according to bias corrected data per Ryu et al. (2018) and raw data from MODIS. (e), the GEV fit of annual maximum 7-day smoothed daily maximum vapour pressure deficit (vpdmax7x) in the present climate (red) and preindustrial climate (blue). (f), the GEV fit of annual maximum 7-day daily maximum surface wind speed (sfcWindmax7x) in the present climate (red) and smoothed preindustrial climate (blue). (g), the GEV fit of annual maximum 7-day smoothed hot-dry-windy index (HDWI, the product of vpdmax and sfcWindmax) in the present climate (red) and preindustrial climate (blue). (h), the GEV fit of JJA effective precipitation (precipitation less evapotranspiration) in the present climate (red) and preindustrial climate (blue). (i), the fraction of managed land relative to natural and managed land over time, per HILDA.

In western and northern Britain, there are no significant trends in weekly VPD, wind speed or hot-dry-windy extremes to the 95% confidence threshold. There are no clear trends in wind speed or HDWI, with a best estimate of a 68% increase in the likelihood of similar VPD conditions. Reanalysis data does show a statistically significant increase in the likelihood of similar VPD and HDWI conditions. Whilst the emergence of a fire weather driven summer fire season is possible with future warming (Perry et al., 2022), the spring peak of fire activity in 2025 was drought driven. The statistical model fit to spring effective

https://doi.org/10.5194/egusphere-2026-1193
Preprint. Discussion started: 20 March 2026

precipitation found a return period of one in 140 years (with a 95% CI of 23-8300 years) to the MAM precipitation deficit, with a strong observed central estimate of the increase in the likelihood of such an event of approximately 6.6 times. Whilst high in magnitude this trend is not reproduced in climate models that find no trend in spring drought since preindustrial (Table 2). Spring LAI shows a minor increasing trend in this region (Fig. 7d), possibly due to an earlier spring onset (Li et al., 2022), and the fraction of managed land in Britain is comparatively stable (Fig. 7i).

Table 2: the change in probability (with 95% confidence interval) of the conditions seen in western and northern Britain in 2025. The maximum annual 7-day average of maximum spring (MAM) daily VPD, maximum spring daily surface wind speed, and the product of those (spring maximum HDWI) was assumed to follow a GEV distribution in which the location parameter varies with GMST. Effective precipitation and spring (MAM) and summer (JJA) were assumed to follow a Gaussian distribution with the location parameter again varying with GMST. The synthesis of climate models and observations is undertaken according to Philip et al. (2020). Statistically significant effects are given in bold. The present climate is assumed to be +1.3°C higher than the preindustrial average, with the future scenario defined as +2.6°C above preindustrial. A full breakdown of the attributed probability ratio and intensity delta are provided in Appendix B.

2025 Extreme Event	Future Probability / Present Probability		Future Probability / Present Probability
	ERA5-Land	Synthesis with CMIP6 and CORDEX models	CMIP6 and CORDEX models
7-day MAM HDWI	**3.92 (1.61, 56.9)**	1.10 (0.561, 3.44)	0.997 (0.609, 1.66)
7-day MAM VPDx	**3.67 (1.32, 78.3)**	1.68 (0.489, 14.0)	1.31 (0.612, 2.73)
7-day MAM sfcWindx	1.07 (0.894, 1.28)	1.02 (0.865, 1.23)	0.912 (0.575, 1.44)
MAM Effective Precipitation	6.6 (0.19, 170)	1.5 (0.079, 30)	1.1 (0.34, 3.2)
JJA Effective Precipitation	0.37 (0.08, 1)	0.52 (0.097, 2.2)	1.7 (0.79, 3.7)

4.4 Occitania

A single wildfire event in Aude, on 5th August, generated an extremely strong spike in FRP. Up until the event, wind and VPD had been inversely related, with 5th August corresponding to the first summer overlap of higher wind and VPD conditions (Fig. 8a). Leading up to the event, spring moisture had been typical in the region (Fig. 8b), followed by a moderately dry summer anomaly, most intense over the region where the Aude wildfire occurred. This drought resulted in a low 2025 summer LAI, which likely resulted in a higher proportion of dead or stressed vegetation – more vulnerable to wildfire spread.

https://doi.org/10.5194/egusphere-2026-1193
Preprint. Discussion started: 20 March 2026

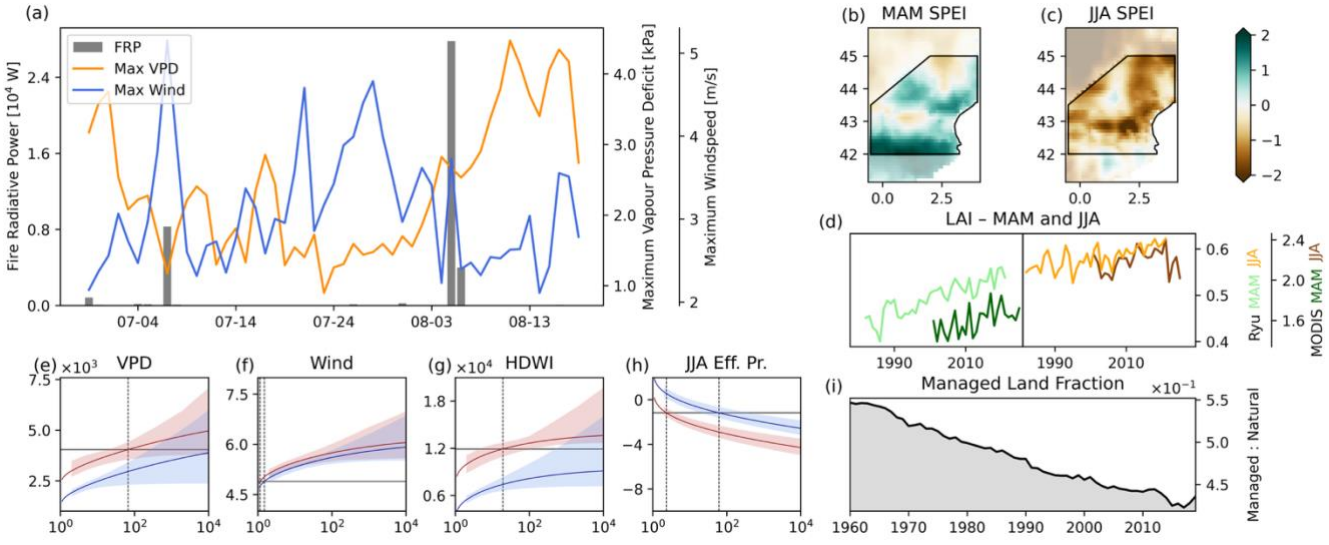

Figure 8: Occitania summary of event conditions and regional trends. (a), time series of daily maximum wind speed and daily maximum VPD averaged over the study region, overlaid with remotely sensed fire radiative power. (b), spring (MAM) 3-month standardised precipitation-evapotranspiration index. (c), summer (JJA) 3-month standardised precipitation-evapotranspiration index. (d), Trends in spring (MAM) and summer (JJA) leaf area index (LAI) according to bias corrected data per Ryu et al. (2018) and raw data from MODIS. (e), the GEV fit of annual maximum 7-day smoothed daily maximum vapour pressure deficit (vpdmax7x) in the present climate (red) and preindustrial climate (blue). (f), the GEV fit of annual maximum 7-day daily maximum surface wind speed (sfcWindmax7x) in the present climate (red) and smoothed preindustrial climate (blue). (g), the GEV fit of annual maximum 7-day smoothed hot-dry-windy index (HDWI, the product of vpdmax and sfcWindmax) in the present climate (red) and preindustrial climate (blue). (h), the GEV fit of JJA effective precipitation (precipitation less evapotranspiration) in the present climate (red) and preindustrial climate (blue). (i), the fraction of managed land relative to natural and managed land over time, per HILDA.

The likelihood of hot and dry conditions at least as extreme as those observed in 2025 showed an extremely strong increasing trend in the reanalysis data. This was tempered by a much more moderate (but still predominantly increasing) effect across climate models – with the central estimate being that 2025's VPD conditions have been made over 4 times more likely to do past climate change. As in other regions, the trend in hot, dry and windy conditions is temperature driven, with climate change having had little positive or negative effect on the likelihood of widespread high wind events. Additionally, there is a strong summer drying effect in the region, with 2025's moderately dry conditions made over three times as likely with a 70% increase in the moisture deficit arising from human-caused climate change (Table 3).

https://doi.org/10.5194/egusphere-2026-1193
Preprint. Discussion started: 20 March 2026

There is a strong spring greening trend in the region (Fig. 8d), with the increase in dry summer events resulting in an increased likelihood of high fuel-load, high fuel curing conditions most conducive to extreme wildfire events. This increase in fuel availability is mirrored by a decrease in the managed land fraction over the study area, with land abandonment in the area likely resulting in heightened fire danger over more dense and continuous vegetation.

Table 3: the change in probability (with 95% confidence interval) of the conditions seen in Occitania in 2025. The maximum annual 7-day average of maximum daily VPD, maximum daily surface wind speed, and the product of those (HDWI) was assumed to follow a GEV distribution in which the location parameter varies with GMST. Effective precipitation and spring (MAM) and summer (JJA) were assumed to follow a Gaussian distribution with the location parameter again varying with GMST. The synthesis of climate models and observations is undertaken according to Philip et al. (2020). Statistically significant effects are given in bold. The present climate is assumed to be +1.3°C higher than the preindustrial average, with the future scenario defined as +2.6°C above preindustrial. A dash is given where observations and climate models are unsynthesisable due to infinite values. A full breakdown of the attributed probability ratio and intensity delta are provided in Appendix C.

2025 Extreme Event	Future Probability / Present Probability		Future Probability / Present Probability
	ERA5-Land	Synthesis with CMIP6 and CORDEX models	CMIP6 and CORDEX models
7-day HDWI	**∞ (21.2, ∞)**	-	1.96 (0.561, 7.04)
7-day VPDx	**461 (5.61, ∞)**	4.45 (0.23, 1930)	2.54 (0.714, 10.4)
7-day sfcWindx	1.29 (0.886, 2.06)	1.09 (0.870, 1.58)	0.973 (0.864, 1.10)
MAM Effective Precipitation	1.5 (0.9, 2.5)	1.1 (0.79, 1.6)	1.1 (0.98, 1.2)
JJA Effective Precipitation	**20 (6, 140)**	**3.3 (1.2, 15)**	**1.4 (1.1, 1.8)**

4.5 Eastern Adriatic and Ionian

The eastern Adriatic and Ionian coast saw two distinct periods of high wildfire activity in summer of 2025 – both corresponding to simultaneous highs in VPD and wind speed (Fig. 9a). The majority of the study regions saw moist conditions – with the exception of a dry anomaly on the Greek and southern Albanian coasts (Fig. 9b). This was followed by summer drought conditions (Fig. 9c) – meaning that overall conditions were generally favourable for fuel growth and subsequent senescence

https://doi.org/10.5194/egusphere-2026-1193
Preprint. Discussion started: 20 March 2026

585 and drying (curing). Supporting this, spring LAI was normal, with a low summer LAI possibly related to an increase in vegetation stress.

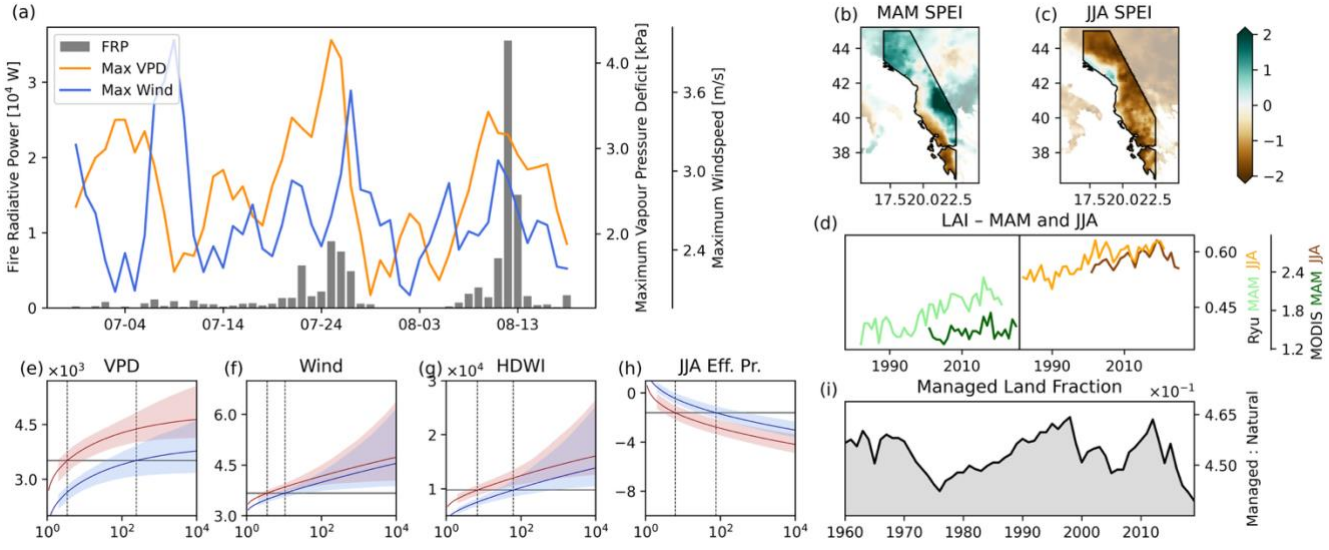

Figure 9: Eastern Adriatic and Ionian summary of event conditions and regional trends. (a), time series of daily maximum wind speed and daily maximum VPD averaged over the study region, overlaid with remotely sensed fire 590 **radiative power. (b), spring (MAM) 3-month standardised precipitation-evapotranspiration index. (c), summer (JJA) 3-month standardised precipitation-evapotranspiration index. (d), Trends in spring (MAM) and summer (JJA) leaf area index (LAI) according to bias corrected data per Ryu et al. (2018) and raw data from MODIS. (e), the GEV fit of annual maximum 7-day smoothed daily maximum vapour pressure deficit (vpdmax7x) in the present climate (red) and preindustrial climate (blue). (f), the GEV fit of annual maximum 7-day daily maximum surface wind speed** 595 **(sfcWindmax7x) in the present climate (red) and smoothed preindustrial climate (blue). (g), the GEV fit of annual maximum 7-day smoothed hot-dry-windy index (HDWI, the product of vpdmax and sfcWindmax) in the present climate (red) and preindustrial climate (blue). (h), the GEV fit of JJA effective precipitation (precipitation less evapotranspiration) in the present climate (red) and preindustrial climate (blue). (i), the fraction of managed land relative to natural and managed land over time, per HILDA.**

600 The hot, dry and windy conditions that drove both major wildfire events in summer, 2025 (Fig. 9a) have strongly increased as a consequence of human caused climate change. The most extreme 7 days of VPD conditions are estimated to have increased in likelihood by approximately nine times, and weekly extreme winds are found to have a probability ratio of approximately 80% – whilst both of these central estimates show a high magnitude of change in likelihood, neither is statistically significant to the 95% confidence interval. The 7-day HDWI extreme observed in 2025 is statistically significant, with conditions about 605 four times more likely compared to in the preindustrial climate, with an event of a similar return period (about 7 years) to today about 20% more intense. Whilst spring effective precipitation shows an unclear signal in response to climate change, summer

https://doi.org/10.5194/egusphere-2026-1193
Preprint. Discussion started: 20 March 2026

effective precipitation displays a strong increase in likelihood and intensity of dry spells – especially according to observations – with 2025's dry conditions about 3.5 times more likely (Table 4).

There also appears to be a spring greening trend, in the region – especially clear in the corrected time series developed from Ryu et al. (2018). There has also been an historic greening trend in summer – though this appears to have plateaued in recent years. This trend likely reflects high fuel loads and an increasingly connected landscape since 1980 – which can have a corresponding increasing effect on the likelihood of large and intense wildfire events. The region has been characterised by periods of net land reclamation and abandonment, however in recent years there has been a period of relatively rapid land abandonment – which can also exacerbate wildfire behaviour.

Table 4: the change in probability (with 95% confidence interval) of the conditions seen in eastern Adriatic and Ionian in 2025. The maximum annual 7-day average of maximum daily VPD, maximum daily surface wind speed, and the product of those (HDWI) was assumed to follow a GEV distribution in which the location parameter varies with GMST. Effective precipitation and spring (MAM) and summer (JJA) were assumed to follow a Gaussian distribution with the location parameter again varying with GMST. The synthesis of climate models and observations is undertaken according to Philip et al. (2020). Statistically significant effects are given in bold. The present climate is assumed to be +1.3°C higher than the preindustrial average, with the future scenario defined as +2.6°C above preindustrial. A full breakdown of the attributed probability ratio and intensity delta are provided in Appendix D.

2025 Extreme Event	**Future Probability / Present Probability**		**Future Probability / Present Probability**
	ERA5-Land	**Synthesis with CMIP6 and CORDEX models**	**CMIP6 and CORDEX models**
7-day HDWI	**8.99 (2.13, 133)**	**3.97 (1.01, 38.0)**	**2.35 (1.33, 4.20)**
7-day VPDx	**70.2 (5.78, 125000)**	9.11 (0.711, 1310)	**2.37 (1.54, 3.59)**
7-day sfcWindx	**3.00 (1.28, 12.9)**	1.83 (0.613, 7.88)	0.802 (0.437, 1.51)
MAM Effective Precipitation	1.4 (0.91, 2.3)	1.4 (0.78, 2.7)	1.3 (0.97, 1.6)
JJA Effective Precipitation	**11 (1.7, 95)**	3.6 (0.75, 22)	2 (0.96, 4.1)

https://doi.org/10.5194/egusphere-2026-1193
Preprint. Discussion started: 20 March 2026

4.6 Northern and Western Türkiye

The 2025 fire season in northern and western Türkiye was defined by extreme meteorological and hydrological conditions that drove two distinct peaks in wildfire activity. The initial surge began in mid-June, driven by an earlier-than-usual period of very high VPD – indicating exceptionally dry air. This period briefly overlapped with, and was followed by, a phase of high wind speeds on June 27, creating conditions conducive to rapid fire spread before a notable break later in the month. The more intense late July fires occurred amid even higher VPD coincident with several days of strong winds (Fig. 10a).

Preconditioning these active fire periods, northwestern Türkiye experienced a significant hydrological deficit, especially throughout the spring and summer months. Mild moisture stress in spring (MAM, Fig. 10b) intensified into severe drought conditions by the summer (JJA, Fig. 10c). This aridity likely limited the biomass accumulation of annual plants, and possibly caused increased stress and mortality amongst longer-lived vegetation – evidenced by the moderately low spring and very low summer LAI values (Fig. 10d). Moisture-stressed and deceased shrubs and trees can strongly enhance landscape flammability.

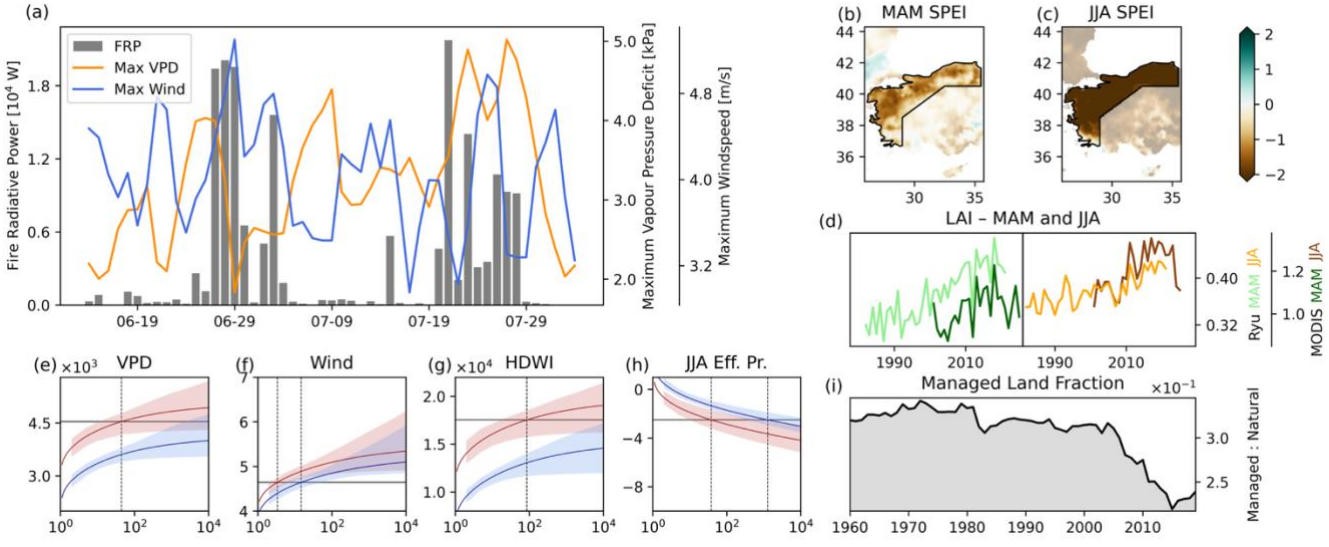

Figure 10: Northern and Western Türkiye summary of event conditions and regional trends. (a), time series of daily maximum wind speed and daily maximum VPD averaged over the study region, overlaid with remotely sensed fire radiative power. (b), spring (MAM) 3-month standardised precipitation-evapotranspiration index. (c), summer (JJA) 3-month standardised precipitation-evapotranspiration index. (d), Trends in spring (MAM) and summer (JJA) leaf area index (LAI) according to bias corrected data per Ryu et al. (2018) and raw data from MODIS. (e), the GEV fit of annual maximum 7-day smoothed daily maximum vapour pressure deficit (vpdmax7x) in the present climate (red) and preindustrial climate (blue). (f), the GEV fit of annual maximum 7-day daily maximum surface wind speed (sfcWindmax7x) in the present climate (red) and smoothed preindustrial climate (blue). (g), the GEV fit of annual maximum 7-day smoothed hot-dry-windy index (HDWI, the product of vpdmax and sfcWindmax) in the present

https://doi.org/10.5194/egusphere-2026-1193
Preprint. Discussion started: 20 March 2026

climate (red) and preindustrial climate (blue). (h), the GEV fit of JJA effective precipitation (precipitation less evapotranspiration) in the present climate (red) and preindustrial climate (blue). (i), the fraction of managed land relative to natural and managed land over time, per HILDA.

In reanalysis data we find a near infinite increase in the probability of extreme 7-day periods of VPD and HDWI over northern and western Türkiye, with the intensity of a similarly rare event observed to have increased by approximately 900 Pa (VPD) or 35% (HDWI) since the preindustrial. Whilst climate models were not synthesisable with observed trends due to infinite values, they also showed a high magnitude of change with warming (Appendix E), with climate models finding a 13 times increase in the likelihood of equivalently intense VPD conditions due to climate change. Windy conditions were also estimated to have increased in likelihood due to climate change (Table 5).

Climate change has had a strong effect on summer drought increasing the likelihood of dry conditions such as those seen in 2025 by approximately 20 times. Historically increasing spring and summer LAI have been followed by recent very low years, which could be associated with the increased instance of extreme drought in the region. Over past decades there has been a strong trend towards the conversion of managed to natural land-use classes, this likely relates to increasing land abandonment and a consequent heightening of the wildfire hazard.

Table 5: the change in probability (with 95% confidence interval) of the conditions seen in northern and western Türkiye in 2025. The maximum annual 7-day average of maximum daily VPD, maximum daily surface wind speed, and the product of those (HDWI) was assumed to follow a GEV distribution in which the location parameter varies with GMST. Effective precipitation and spring (MAM) and summer (JJA) were assumed to follow a Gaussian distribution with the location parameter again varying with GMST. The synthesis of climate models and observations is undertaken according to Philip et al. (2020). Statistically significant effects are given in bold. The present climate is assumed to be +1.3°C higher than the preindustrial average, with the future scenario defined as +2.6°C above preindustrial. A dash is given where observations and climate models are unsynthesisable due to infinite values. A full breakdown of the attributed probability ratio and intensity delta are provided in Appendix E.

2025 Extreme Event	Future Probability / Present Probability		Future Probability / Present Probability
	ERA5-Land	Synthesis with CMIP6 and CORDEX models	CMIP6 and CORDEX models
7-day HDWI	**inf (134, inf)**	-	**5.98 (1.42, 28.3)**
7-day VPDx	**inf (92.8, inf)**	-	**7.15 (2.35, 22.5)**
7-day sfcWindx	**4.38 (1.08, 16.4)**	1.56 (0.753, 3.81)	1.08 (0.767, 1.49)

https://doi.org/10.5194/egusphere-2026-1193
Preprint. Discussion started: 20 March 2026

MAM Effective Precipitation	**6.2 (1.3, 40)**	3.3 (0.68, 21)	1.4 (0.97, 2)
JJA Effective Precipitation	**31 (3.2, 310)**	**20 (1.4, 330)**	**5 (2.1, 12)**

5 Discussion

Increasingly intense heatwaves in Europe have been linked to the occurrence of the continent's largest wildfires (Costa-Saura et al., 2025). This is primarily due to the exponential response of VPD to temperature (Swain et al., 2025), which through extremes in atmospheric moisture demand can drive very low dead fuel moistures and consequently high wildfire danger (Resco de Dios et al., 2022). Given the minor and uncertain responses of wind speed to global mean surface temperature, major increases in hot and dry conditions will drive increasingly frequent hot, dry and windy compound events. The four southern European events studied in this analysis all saw extreme VPD values concurrent to, or preceding, the wildfire outbreaks, and in all four regions the highest 7-day average of maximum daily VPD (hereafter VPDx7x) has greatly increased with global average temperatures. For example in Occitania, VPDx7x was over 4,000 Pa with a current return period of about 70 years – contributing to by far the largest wildfire event in the region in over 50 years. In northwestern Iberia, maximum VPD was near or above 3,000 Pa for 16 days before the wildfires, with VPDx7x not a rare event in today's climate (Appendix A). In all regions, observations showed clear emergence of a strong increase in the likelihood and intensity of VPDx7x beyond natural variability, while the trend in climate models is much weaker but still positive – most notably emergent reanalysis based probability ratios of 70 (eastern Adriatic/Ionian), 460 (Occitania), and near-infinity (western and northern Türkiye) were estimated to be 4.2, 2.2, and 11.2 respectively in climate models. This large difference relates to the underestimation of summer warming over Europe under EURO-CORDEX (Vautard et al., 2020) and CMIP6 (Ribes et al., 2022) models – which has been explained by the underestimation of regional aerosol reduction by climate models (Schumacher et al. 2024). The synthesised attribution of VPDx7x accounting for both reanalysis and climate model data presented here can therefore be taken as a conservative estimate.

Because the study regions were selected for extreme wildfire activity, all regions experienced dry fire-season conditions – a prerequisite for intense and rapid spreading fires. Northwestern Iberia and the eastern Adriatic/Ionian both saw lush springs followed by dry summers, this so-called hydroclimate whiplash (Swain et al., 2025, McNorton et al., 2025) driving favourable growing and then drying conditions for unusual accumulation of dry fuels. In northwestern Iberia, shrublands were more severely burnt than established forests, and in the eastern Adriatic, the semi-arid climate and low total moisture capacity of the thin soil layer means that plants are adapted to grow rapidly when moisture is available (Schwinning and Ehleringer, 2001). In all southern European regions, the summer drying trend in effective precipitation is much stronger than in spring, meaning

https://doi.org/10.5194/egusphere-2026-1193
Preprint. Discussion started: 20 March 2026

that future fire seasons are more likely to be characterised by a highly productive spring followed by summer fuel curing. Türkiye, which also has a summer fire season, experienced a dry spring in contrast to the moist growing season in other regions. Wildfires were most extreme in forested regions of Türkiye, where persistent lows in effective precipitation throughout spring and summer resulted in higher than average vegetation mortality increasing dead fuel loads and surface wildfire intensity (Stephens et al., 2018). The increasingly intense fire regime in northern Türkiye can partially be explained by a substantial spring and emergent summer drying trend (Appendix E) in historically moister forests (Ekberzade et al., 2024). The extremely dry British spring also exacerbated western and northern Britain's existing spring fire season. This spring dry event was extremely rare, and is projected to remain so with future climate change. It is, however, informative on how low live fuel moisture due to pre-growing season vegetation dormancy (Little et al., 2024; Davies et al., 2010) can be compounded by very low effective precipitation. Both spring and summer LAI in all regions show an increasing trend since 1980, regardless of trends in land use, which can likely be explained by CO2 fertilization (Jeong et al., 2026) and an earlier start to the spring growing season (Menzel et al., 2006). Summer LAI shows a rapid, recent browning trend across study regions, which cannot be explained by recent orbital drift in MODIS (Jiang et al., 2017) due to no accompanying trend in spring. This could be the result of the trend towards drier summer conditions over much of Europe (Bakke et al., 2023) and the very strong increase in European extreme summer heat (Arias et al., 2023) which can have a major effect on vegetation stress and mortality (McDowell et al., 2008).

We find a large increase in most of the extreme heat, compound hot-dry-windy, and seasonal dryness meteorological drivers of the severe wildfires across the five case study regions. With the emergence of these novel extremes in wildfire, there also emerge important changes to wildfire-related risks and their management. In the highly fire-prone eastern Adriatic/Ionian and northwestern Iberian regions the hot, dry and windy conditions that drove 2025's wildfires are now commonplace, but have been very rare in the past, when considering only reanalysis data. Regardless of whether this is the result of an underestimation of the trend in the climate models, as suggested by several studies discussed above, or random undersampling of possible but unrealised extreme conditions in the past, both regions are now fire regimes in which these historically rare conditions can be expected once or twice a decade. In Türkiye and Occitania, 2025's fire weather conditions were still unlikely, but rapidly becoming more common, with reanalysis-only attribution finding near infinite increases in the likelihood of weekly HDWI conditions. In northern Türkiye, recent drying and large fires in the Black Sea Forests could be the first signs of a transformation towards a more Mediterranean fire regime (Ekberzade et al., 2024). In Occitania, the Aude wildfire was an archetypical extreme wildfire event, driven by extreme heat and winds, which are increasing globally (Abatzoglou et al., 2025) and regionally (Barbero et al., 2020) with climate change – and may offer insight into future extremes in the region. In Britain, the emergence of a higher intensity summer fire season (Arnell et al., 2021; Perry et al., 2022) is of increasing importance to risk managers (NFCCb, 2025), though this effect is less pronounced in the northern and western British region studied here. The emergence of novel fire regimes pose major challenges from a management perspective. Although European policymakers are aware of the emergence of new wildfire extremes (von der Leyen, 2025), with a new pan-European fire fighting force signalled

https://doi.org/10.5194/egusphere-2026-1193
Preprint. Discussion started: 20 March 2026

(Bassler, 2026), land ownership and management practices are fragmented - with adaptations often made in response to past, realised impacts as opposed to the present or future risk of as yet unrealised events (Travis, 2014).

Foremost amongst these impacts of extreme wildfires are those on health, structures and ecology. Whilst less visible than ecological or property destruction, millions of global excess deaths are estimated due to wildfire smoke annually (Chen et al., 2021). The wildfire emissions in 2025 were the highest on record since 2003, primarily contributed to by the Iberian wildfires from 10-20th August which resulted in multiple days of poor air quality (McNorton and Parrington, 2025). Given that large, rapid-spreading wildfires are increasing in the region due to climate change (Section 4.2, Senande-Rivera et al., 2025) this impact is likely of increasing pertinence. Whilst increasing extreme fire likelihood is important, the coincidence of this with the expansion of the WUI poses the most risk to structures. In Türkiye, there has been a large expansion in the WUI in recent decades, with a large number of structures destroyed and over 50,000 people evacuated this year (Keeping et al., 2025a). Guo et al. (2024) find the greatest expansion of the WUI in Europe to have been over Türkiye and Portugal, where rural land abandonment and increasingly extreme fire weather are causing conditions favourable to large, fast spreading wildfires. This expansion of the WUI is also associated with a substantial increase in ignition pressure (Badia et al., 2011), further amplifying risk due to a greater number of wildfire events. In addition to financial losses from property destruction, wildfires can pose a major risk to Mediterranean viticulture as fire smoke can spoil grape harvests (Madhusoodanan, 2021). Whilst wildfires are an integral part of the ecosystem for many fire adapted Mediterranean species – especially shrublands (Keeley and Pausas, 2022) – extremely intense and large wildfires can be very harmful. Frequent intense crown fires, such as those seen in Türkiye, the eastern Adriatic/Ionian and Occitania, can drive irreversible shifts towards open woodland or shrubland states (Diaz-Delgado et al., 2003; Baudena et al., 2019) – which has been projected under regional climate scenarios (Ekberzade et al., 2024).

This study relies on a constrained set of meteorological, vegetation and land-use predictors to characterise trends in their contribution to wildfire danger. These variables characterise the key driving effects of instantaneous fire weather (VPD, wind speed and HDWI), antecedent moisture conditions (seasonal effective precipitation and SPEI), seasonal in live vegetation cover (LAI), and land management (managed or unmanaged land). However, some limitations do apply. First, wind speed as parameterised in reanalysis products does not correspond well to actual observed wind speed, where these observations exist. Wind varies substantially at fine temporal and spatial scales, whilst reanalysis products estimate mean flow at a much coarser spatial and temporal resolution – which could be argued to differ from the scale at which winds drive wildfire events. Furthermore, IFS based models ERA5 and ERA5-Land have been found to underestimate mean wind flow generally (Sheridan et al., 2022, Arregoces et al., 2024) and over Europe (Murcia et al., 2022, Patra et al., 2025). Nonetheless, reanalysis products are well correlated (Brune et al., 2021; Murcia et al., 2022) with observations over Europe, allowing monotonic predictive relationships to be made with observations to predict actual wind values (Weekes and Tomlin, 2014; Basse et al., 2021). We therefore deem the reanalysis and climate model characterisations of mean wind speed as closely related to the effect of winds

https://doi.org/10.5194/egusphere-2026-1193
Preprint. Discussion started: 20 March 2026

on wildfire, with high values in one closely related to high values in the other. Second, LAI provides a good representation of the area covered by photosynthetically active vegetation, but does not directly represent total fuel load, including dead fuels. Whilst a comprehensive fuel model, able to distinguish live and dead fuels, would be very useful, seasonal and total LAI in combination with moisture stress (SPEI) is sufficient to describe the basic trends in fuel moisture and abundance covered here. Third, the land management fraction used to describe land management here is of variable utility in different regions. For example, in the UK the great majority of forests are managed in some way, but nonetheless vulnerable to fires (e.g. Swinley Forest in 2011 or Galloway Forest Park in 2025), whilst agriculturally managed land is much less so. Whilst trends in land management should thus perhaps be ignored over Britain, in other more fire-prone regions it provides a useful heuristic for changes in land use and vegetation management.

6 Conclusion

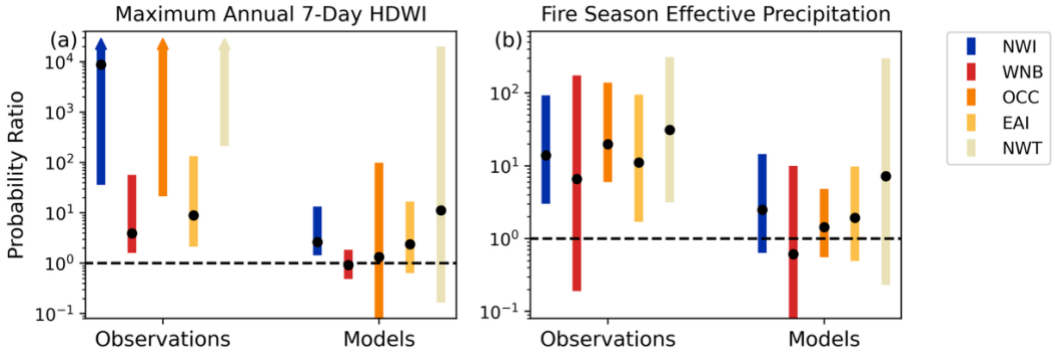

Figure 11: Probability ratios for change in likelihood of (a) annual/seasonal maximum 7-day HDWI (HDWI7x), and (b) summer effective precipitation. Bars represent the 95% confidence interval, black dots the central estimate, and upwards arrows show where the central estimate and/or upper bound were near infinite. Ratios are taken as between the likelihood of the event for each study region in the preindustrial climate (0°C) and present climate (+1.3°C). The region codes are NWI, northwestern Iberia; WNB, western and northern Britain; OCC, Occitania; EAI, Eastern Adriatic and Ionian; NWT, northern and western Türkiye. The fire season considered was meteorological summer for NWI, OCC, EAI and NWT and meteorological spring for WNB, for WNB HDWI7x was only calculated over the meteorological spring, as opposed to the full year.

This study offers a comprehensive overview and attribution of the key weather drivers of five extreme wildfire events over Europe in 2025. These events spanned a broad range of weather drivers and extremity of event. In northwestern Iberia, persistent heat followed by moderate winds, in combination with a moist spring and dry summer, contributed to the largest Spanish burned area on record. On the eastern Adriatic and Ionian coast, simultaneous elevated winds and VPD occurred in combination with similar wet spring, dry summer conditions. In both cases, all meteorological drivers were more common than 10-year events. In western and northern Britain, an extremely rare 140-year spring drought and 25-year spring VPD event

https://doi.org/10.5194/egusphere-2026-1193
Preprint. Discussion started: 20 March 2026

contributed to the highest UK burned area on record. In Occitania, summer and spring moisture were not extraordinary, but a 70-year VPD event contributed to France's largest record wildfire in 80 years. In northern and western Türkiye, a moderately dry spring was followed by a 30-year dry summer event which, in combination with rare VPD and HDWI conditions, drove extremely damaging wildfires throughout the region. The case study regions also spanned distinct fire regimes, including the European region most prone to large fires in northwestern Iberia, an historically small fire dominated region in Occitania, and western and northern Britain where wildfires predominantly occur in the spring. These regimes are also changing rapidly, with large wildfires increasing in Iberia and southwestern France, the emergence of a summer fire season in Britain, and the transition of historically humid northern Turkish forest to a drier, more fire prone environment. Across all of these diverse drivers and different fire regimes, a straightforward increase in the likelihood and intensity was found across many key weather drivers of wildfire. Strong trends towards drier summers were found across the southern European regions, with emergence from natural variability in northwestern Iberia, Occitania and northern and western Türkiye (Fig. 11b). Extreme weekly VPD was also found to have increased in frequency across all study region fire seasons, with extremes emergent in the reanalysis data across all regions, with the synthesised trend especially strong over Türkiye. Despite minor to nonexistent trends in high winds, these shifts in VPD resulted in emergence from natural variability in the hot, dry, windy compound index (HDWI) across the synthesis of reanalysis and climate models in northwestern Iberia, the eastern Adriatic/Ionian, and northern and western Türkiye, and in the reanalysis only for western and northern Britain, and Occitania (Fig. 11a).

7 Appendices

7.1 Appendix A – Synthesis of Attribution Results Northwestern Iberia

Table A1: Event magnitudes and return periods (per ERA5-Land) for the Northwestern Iberia case-study region.

	Event Magnitude	Return Period
HDWI7x	12400	6.25 (2.93, 33.1)
VPDmax7x	3500	7.44 (3.51, 20.1)
sfcWind7x	6.74	6.71 (3.42, 20.0)
effPr MAM	117.42	1.17 (1.03, 1.6)
effPr JJA	-349.46	5.42 (2.84, 17.57)

Table A2: HDWI7x attribution summary.

https://doi.org/10.5194/egusphere-2026-1193
Preprint. Discussion started: 20 March 2026

Data	HDWI7x		
		Probability ratio (95% CI)	Intensity change (%) (95% CI)
Observations	Past- Present	8740 (36.2, inf)	36.7 (20.7, 58.6)
Models		2.63 (1.43, 13.4)	13.1 (4.58, 23.5)
Synthesis		2.86 (1.26, 29.3)	19.1 (8.48, 32.6)
Weighted Model-Only Synthesis	Present- Future	2.61 (1.41, 4.87)	10.4 (4.90, 16.1)

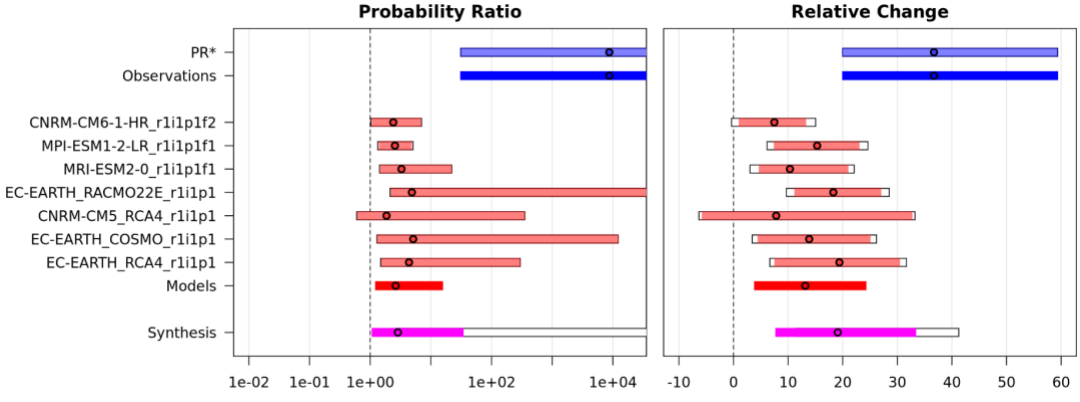

Figure A1: HDWI synthesis from pre-industrial to present day (+1.3°C)

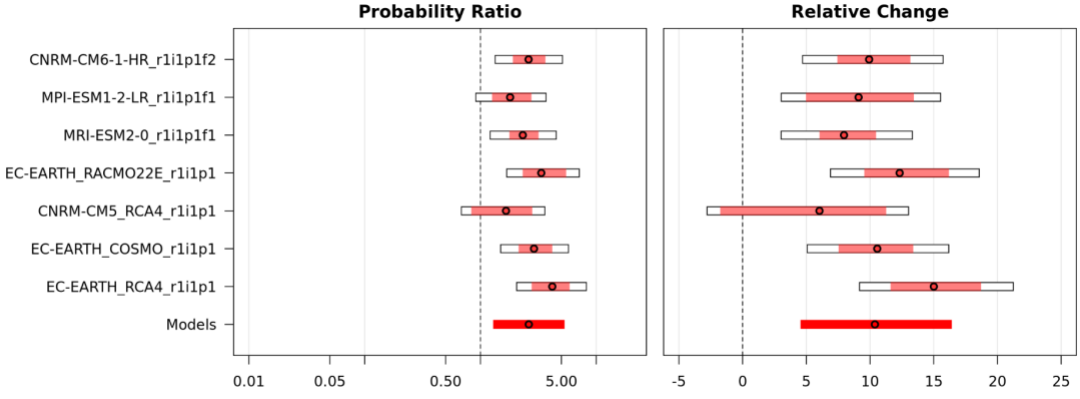

Figure A2: HDWI synthesis from present day (+1.3°C) to +2.6°C

https://doi.org/10.5194/egusphere-2026-1193
Preprint. Discussion started: 20 March 2026

Table A3: VPD7x attribution summary

Data	VPDmax7x		
		Probability ratio (95% CI)	Intensity change (Pa) (95% CI)
Observations	Past- Present	11.1 (2.69, 455)	618 (300, 926)
Models		2.34 (0.764, 17.9)	269 (60.7, 497)
Synthesis		3.58 (1.07, 48.7)	383 (134, 640)
Weighted Model-Only Synthesis	Present- Future	2.48 (1.38, 4.48)	295 (184, 419)

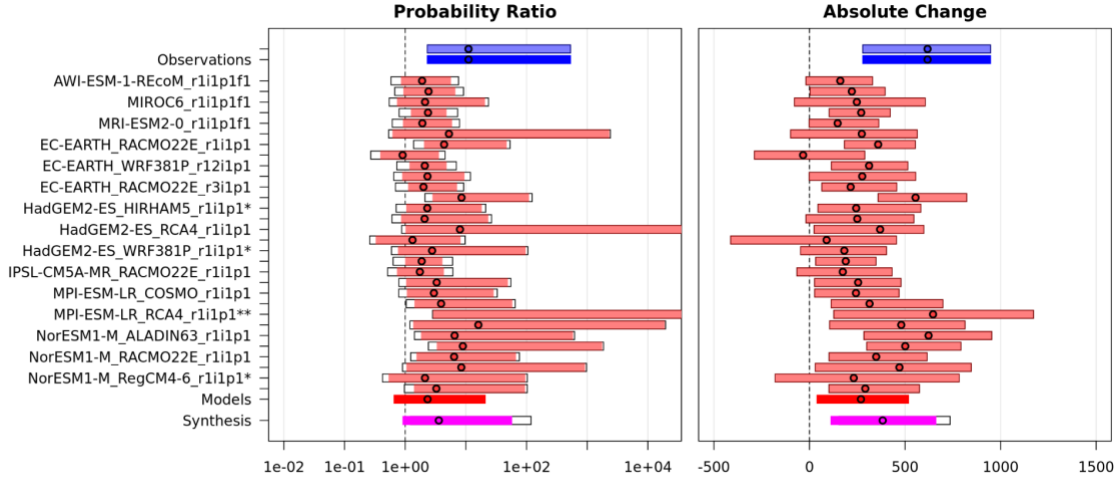

Figure A3: Maximum 7-day VPD synthesis from pre-industrial to present day (+1.3°C)

https://doi.org/10.5194/egusphere-2026-1193
Preprint. Discussion started: 20 March 2026

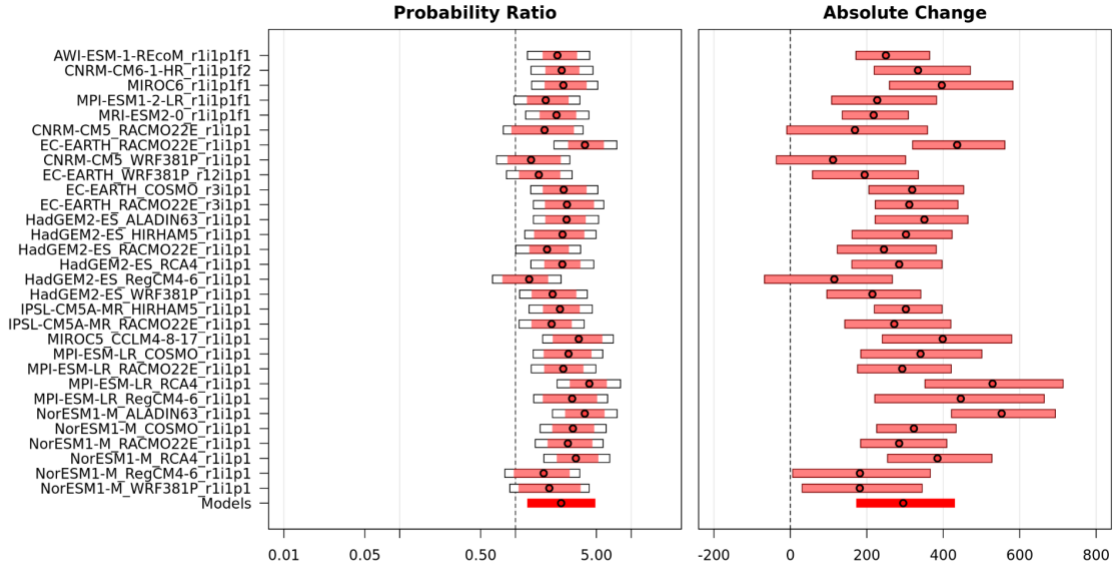

Figure A4: Maximum 7-day VPD synthesis from present day (+1.3°C) to +2.6°C

Table A4: sfcWind7x attribution summary

Data	sfcWindmax7x		
		Probability ratio (95% CI)	Intensity change (m/s) (95% CI)
Observations	Past- Present	1.18 (0.352, 4.85)	0.0694 (-0.393, 0.479)
Models		1.11 (0.367, 7.34)	0.0723 (-0.306, 0.521)
Synthesis		1.154 (0.358, 5.91)	0.0709 (-0.349, 0.501)
Weighted Model-Only Synthesis	Present- Future	1.07 (0.558, 2.13)	0.0254 (-0.236, 0.303)

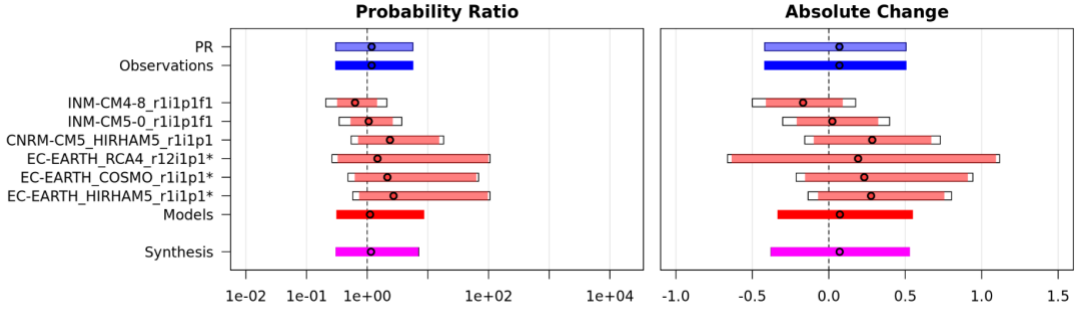

https://doi.org/10.5194/egusphere-2026-1193
Preprint. Discussion started: 20 March 2026

Figure A5: Maximum 7-day wind speed synthesis from pre-industrial to present day (+1.3°C)

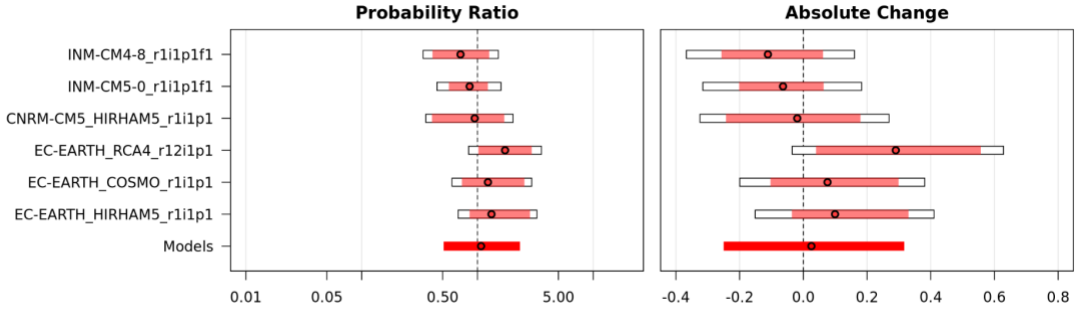

Figure A6: Maximum 7-day wind speed synthesis from present day (+1.3°C) to +2.6°C

Table A5: MAM effective precipitation attribution summary

Data	MAM Effective Precipitation		
		Probability ratio (95% CI)	Intensity change (%) (95% CI)
Observations	Past- Present	1.2 (0.84, 1.6)	-49 (-130, 31)
Models		0.99 (0.74, 1.5)	-2.3 (-61, 60)
Synthesis		1.1 (0.79, 1.6)	-19 (-86, 50)
Weighted Model-Only Synthesis	Present- Future	1.1 (1, 1.2)	-30 (-54, -6)

https://doi.org/10.5194/egusphere-2026-1193
Preprint. Discussion started: 20 March 2026

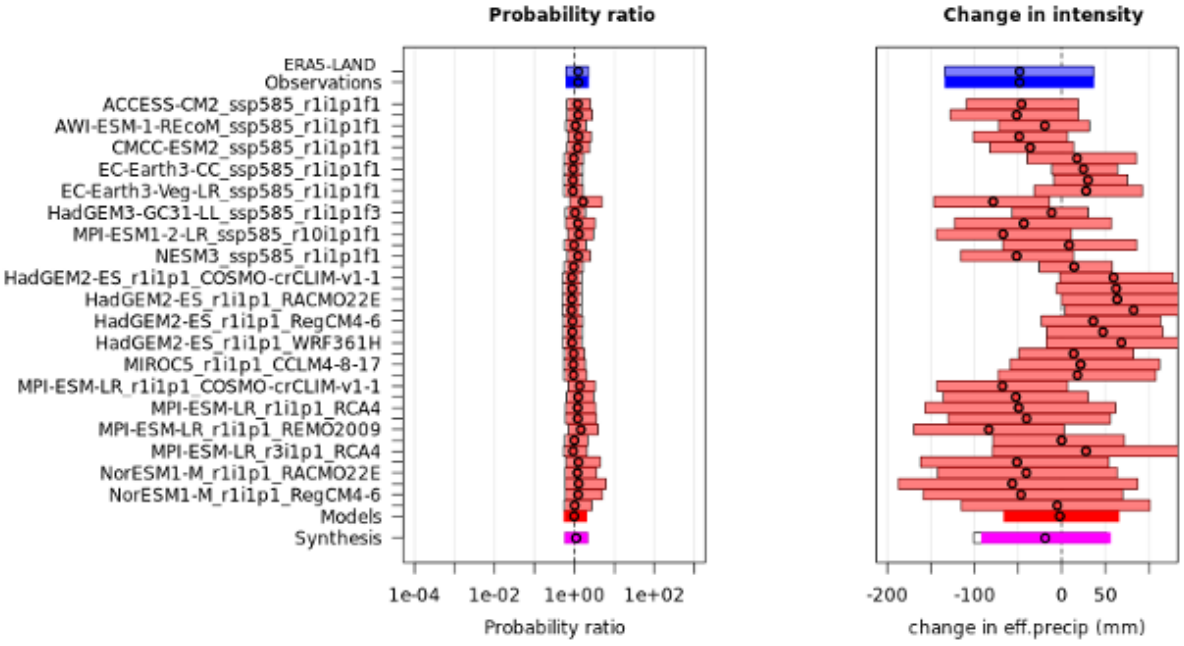

Figure A7: MAM eff precip synthesis from pre-industrial to present day (+1.3°C)

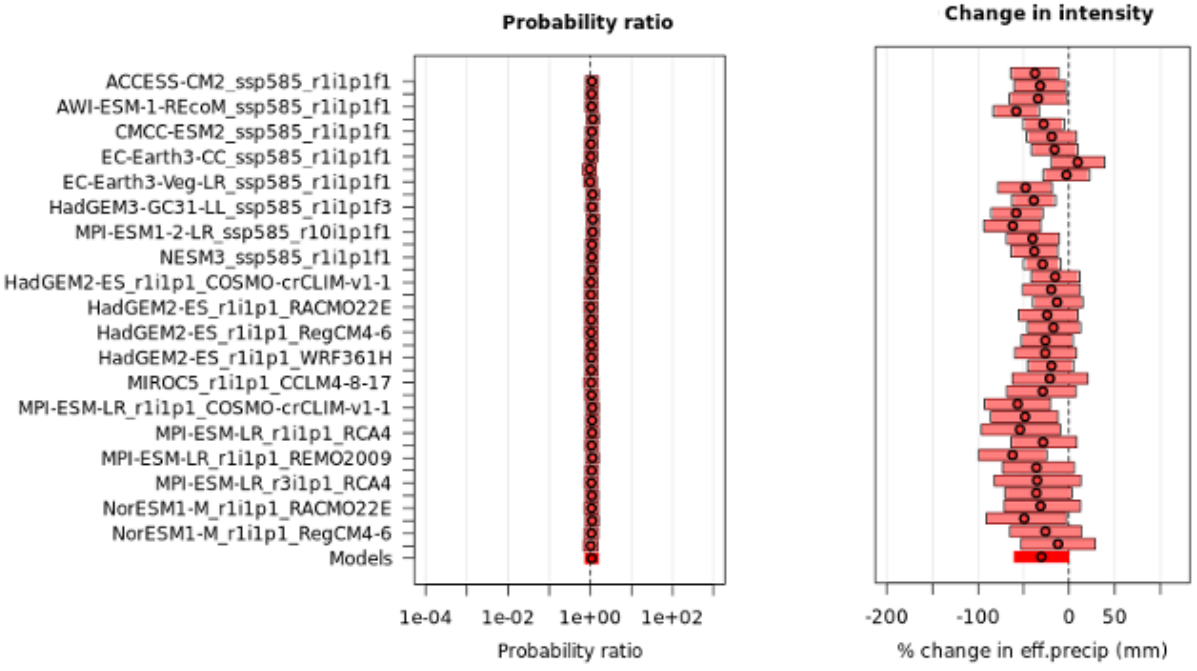

Figure A8: MAM eff precip synthesis from present day (+1.3°C) to +2.6°C

https://doi.org/10.5194/egusphere-2026-1193
Preprint. Discussion started: 20 March 2026

Table A6: JJA effective precipitation attribution summary

Data	JJA Effective Precipitation		
		Probability ratio (95% CI)	Intensity change (%) (95% CI)
Observations	Past- Present	14 (3, 93)	-75 (-120, -28)
Models		2.5 (0.63, 14)	-32 (-67, 3.4)
Synthesis		5.4 (1.3, 34)	-47 (-87, -7)
Weighted Model-Only Synthesis	Present- Future	2.5 (1.7, 3.8)	-43 (-59, -27)

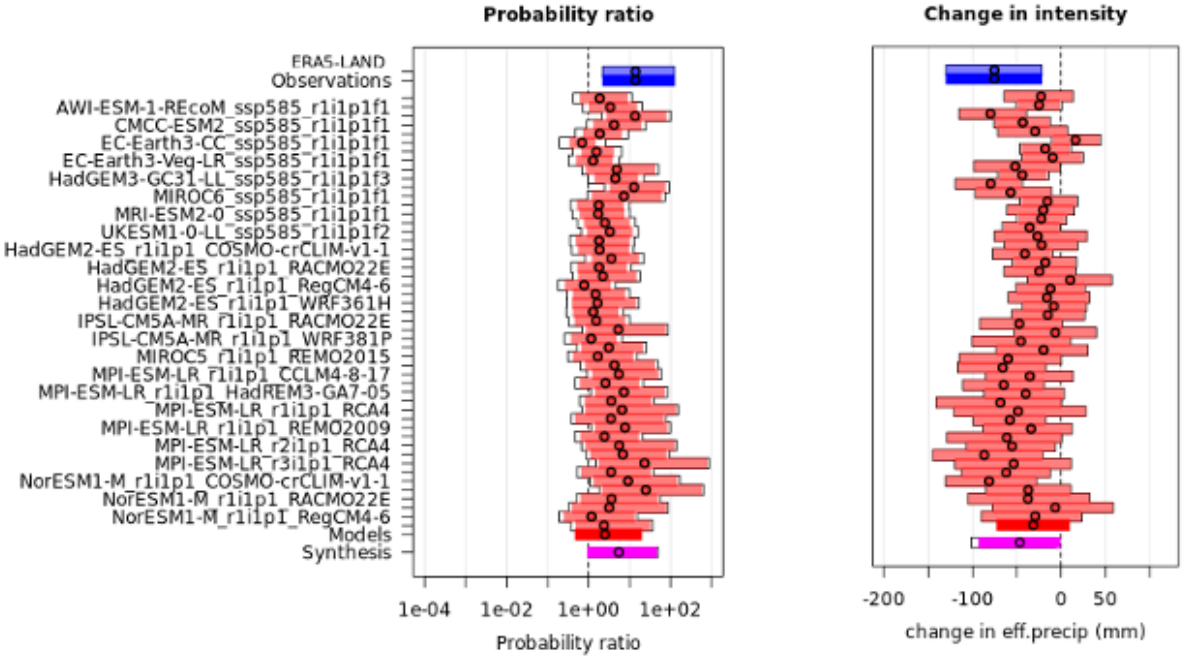

Figure A9: JJA eff precip synthesis from pre-industrial to present day (+1.3°C)

https://doi.org/10.5194/egusphere-2026-1193
Preprint. Discussion started: 20 March 2026

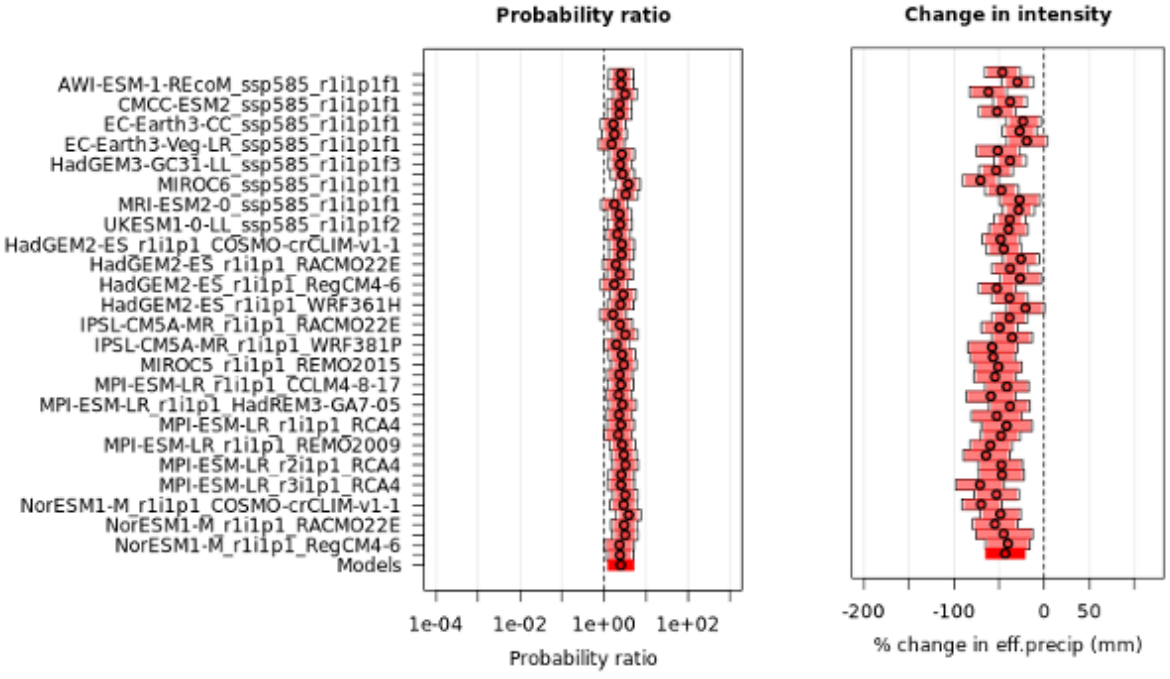

Figure A10: JJA eff precip synthesis from present day (+1.3°C) to +2.6°C

7.2 Appendix B – Synthesis of Attribution Results Western and Northern Britain (March to May)

Table B1: Event magnitudes and return periods (per ERA5-Land) for the Western and Northern Britain case-study region.

	Event Magnitude	Return Period
HDWI7x (MAM)	4410	11.5 (5.81, 36.1)
VPDmax7x (MAM)	1070	25.3 (9.98, 215)
sfcWind7x (MAM)	6.53	1.08 (1.02, 1.23)
effPrMAM	-38.1	141.49 (23.47, 8328.5)
effPrJJA	-1.42	6.8 (3.09, 28.17)

Table B2: HDWI7x attribution summary

https://doi.org/10.5194/egusphere-2026-1193
Preprint. Discussion started: 20 March 2026

Data	HDWI7x (MAM)		
		Probability ratio (95% CI)	Intensity change (%) (95% CI)
Observations	Past- Present	3.92 (1.61, 56.9)	13.6 (4.95, 27.9)
Models		0.922 (0.488, 1.85)	-0.867 (-9.19, 8.58)
Synthesis		1.10 (0.561, 3.44)	5.39 (-3.08, 17.0)
Weighted Model-Only Synthesis	Present- Future	0.997 (0.609, 1.66)	0.195 (-6.36, 6.82)

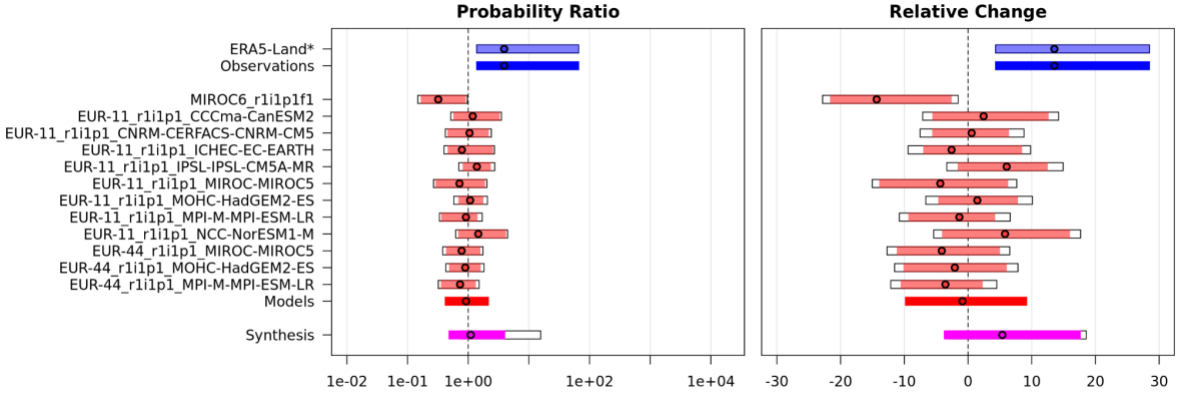

Figure B1: HDWI synthesis from pre-industrial to present day (+1.3°C)

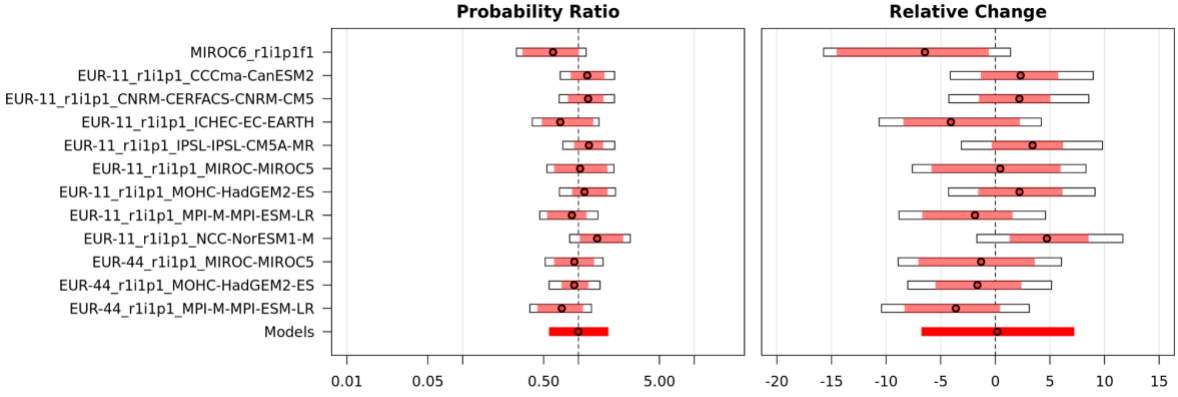

Figure B2: HDWI synthesis from present day (+1.3°C) to +2.6°C

Table B3: VPD7x attribution summary

https://doi.org/10.5194/egusphere-2026-1193
Preprint. Discussion started: 20 March 2026

Data	VPDmax7x (MAM)		
		Probability ratio (95% CI)	Intensity change (Pa) (95% CI)
Observations	Past- Present	3.67 (1.32, 78.3)	130 (40.5, 288)
Models		1.17 (0.310, 5.10)	21.6 (-45.7, 91.8)
Synthesis		1.68 (0.489, 14.0)	47.1 (-26.0, 145)
Weighted Model-Only Synthesis	Present- Future	1.31 (0.612, 2.73)	20.1 (-20.8, 59.7)

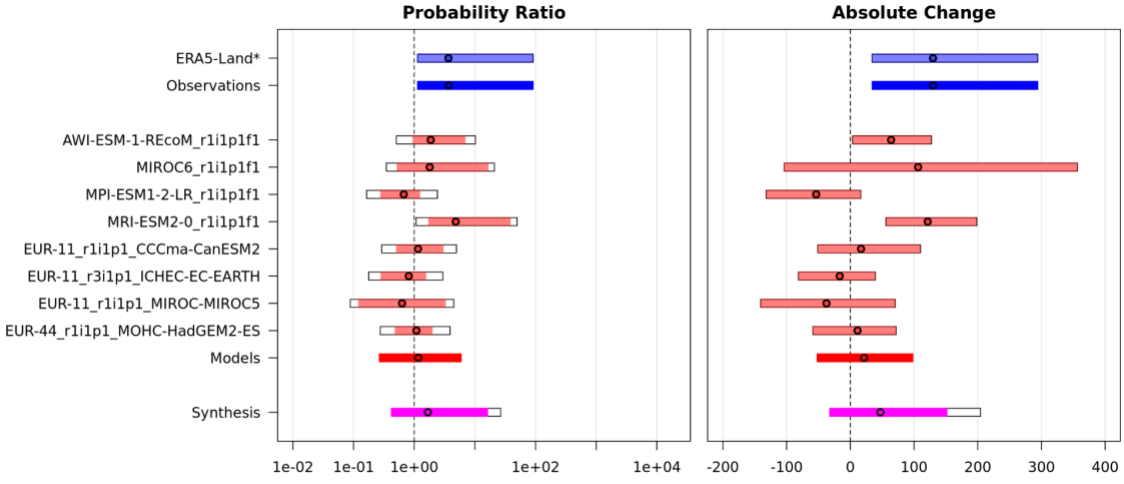

865

Figure B3: Maximum 7-day VPD synthesis from pre-industrial to present day (+1.3°C)

https://doi.org/10.5194/egusphere-2026-1193
Preprint. Discussion started: 20 March 2026

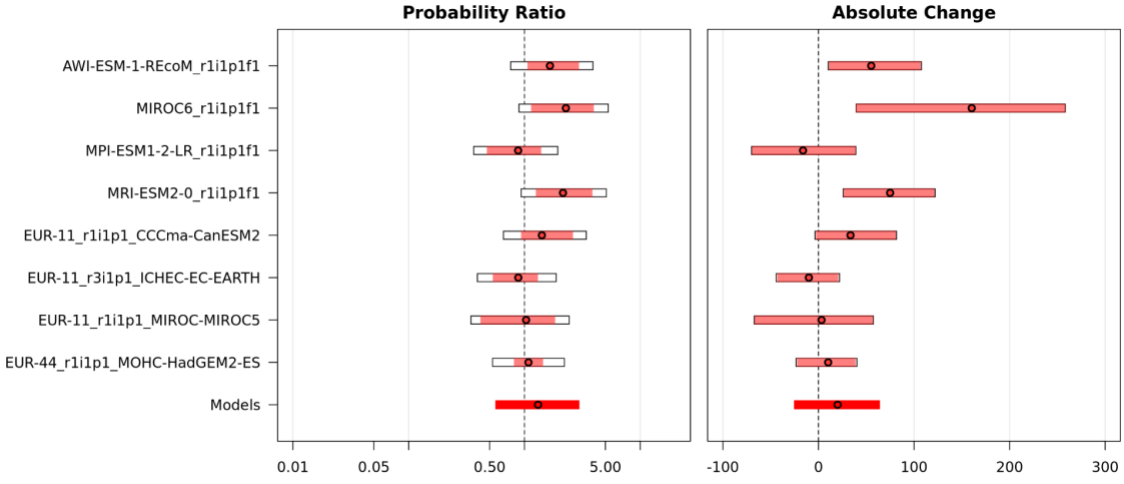

Figure B4: Maximum 7-day VPD synthesis from present day (+1.3°C) to +2.6°C

870

Table B4: sfcWind7x attribution summary

Data	sfcWindmax7x (MAM)		
		Probability ratio (95% CI)	Intensity change (m/s) (95% CI)
Observations	Past- Present	1.07 (0.894, 1.28)	0.275 (-0.415, 0.951)
Models		0.972 (0.840, 1.19)	-0.208 (-1.42, 1.02)
Synthesis		1.02 (0.865, 1.23)	0.160 (-0.685, 1.00)
Weighted Model-Only Synthesis	Present- Future	0.912 (0.575, 1.44)	-0.209 (-1.14, 0.721)

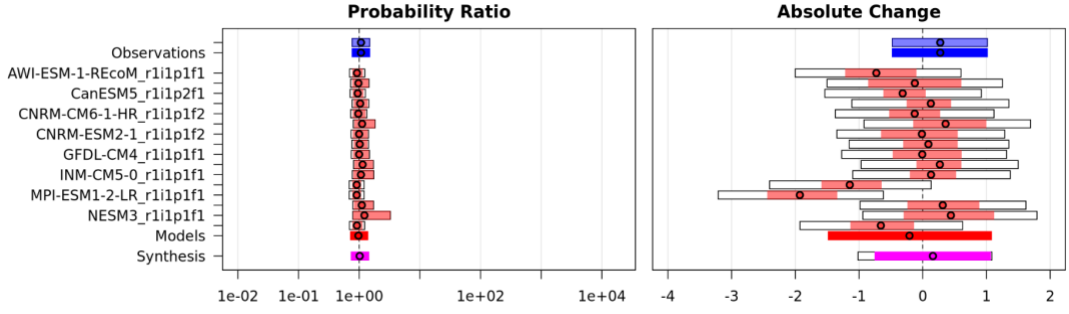

Figure B5: Maximum 7-day wind speed synthesis from pre-industrial to present day (+1.3°C)

875

https://doi.org/10.5194/egusphere-2026-1193
Preprint. Discussion started: 20 March 2026

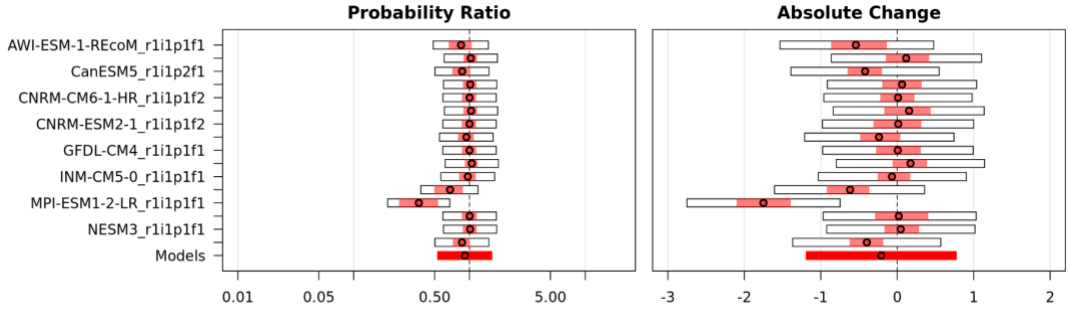

Figure B6: Maximum 7-day wind speed synthesis from present day (+1.3°C) to +2.6°C

Table B5: MAM effective precipitation attribution summary

Data	MAM Effective Precipitation		
		Probability ratio (95% CI)	Intensity change (%) (95% CI)
Observations	Past- Present	6.6 (0.19, 170)	-30 (-81, 20)
Models		0.61 (0.049, 9.9)	7.2 (-23, 38)
Synthesis		1.5 (0.079, 30)	-2.7 (-40, 34)
Weighted Model-Only Synthesis	Present- Future	1.1 (0.34, 3.2)	-1.1 (-16, 14)

880

https://doi.org/10.5194/egusphere-2026-1193
Preprint. Discussion started: 20 March 2026

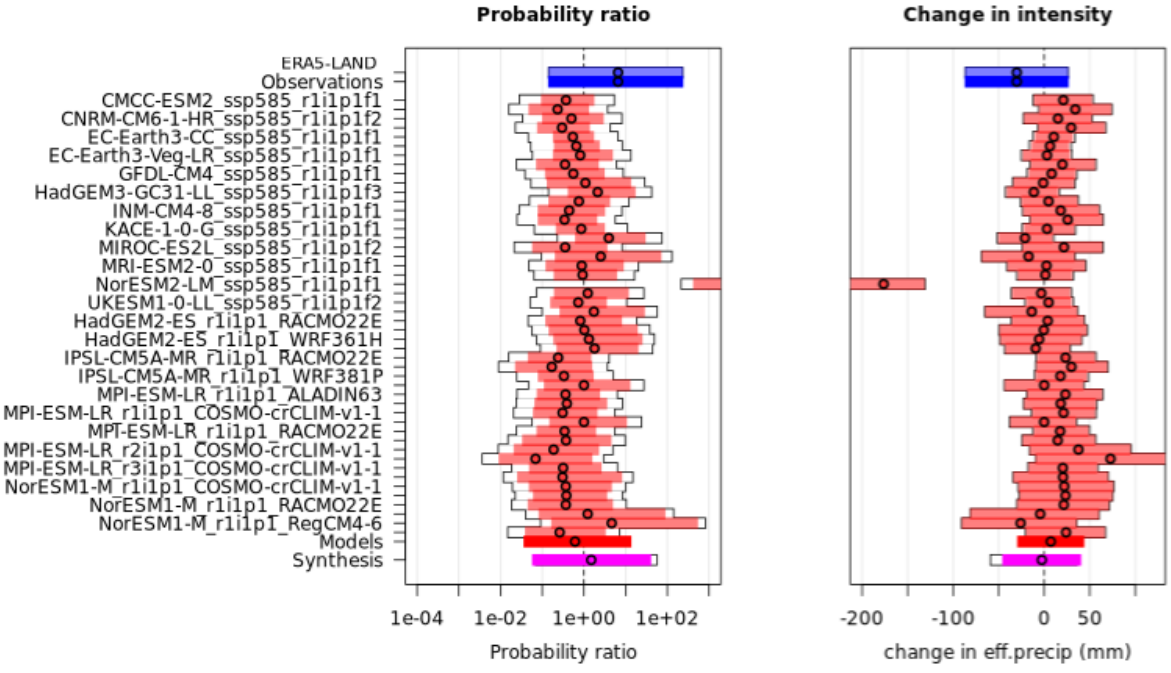

Figure B7: MAM eff precip synthesis from pre-industrial to present day (+1.3°C)

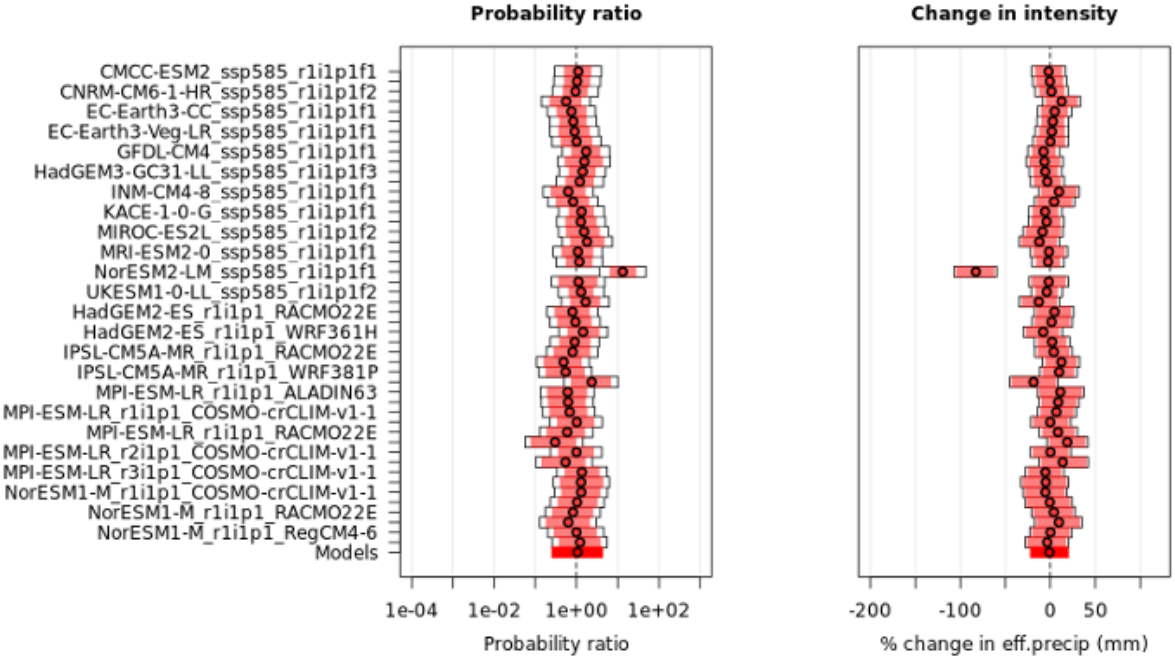

885

https://doi.org/10.5194/egusphere-2026-1193
Preprint. Discussion started: 20 March 2026

Figure B8: MAM eff precip synthesis from (+1.3°C) to +2.6°C

Table B6: JJA effective precipitation attribution summary

Data	JJA Effective Precipitation		
		Probability ratio (95% CI)	**Intensity change (%) (95% CI)**
Observations	**Past- Present**	0.37 (0.08, 1)	56 (0.12, 120)
Models		1.5 (0.19, 15)	-13 (-48, 24)
Synthesis		0.52 (0.097, 2.2)	5.4 (-36, 50)
Weighted Model-Only Synthesis	**Present- Future**	1.7 (0.79, 3.7)	-24 (-40, -7.5)

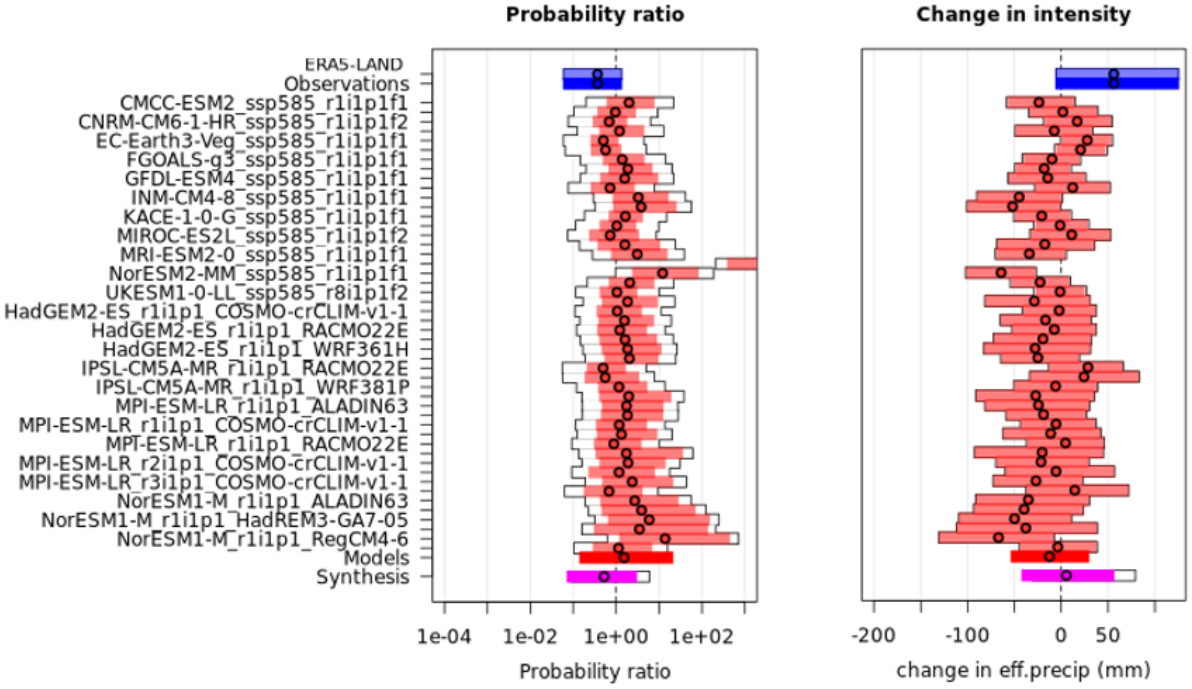

Figure B9: JJA eff precip synthesis from pre-industrial to present day (+1.3°C)

https://doi.org/10.5194/egusphere-2026-1193
Preprint. Discussion started: 20 March 2026

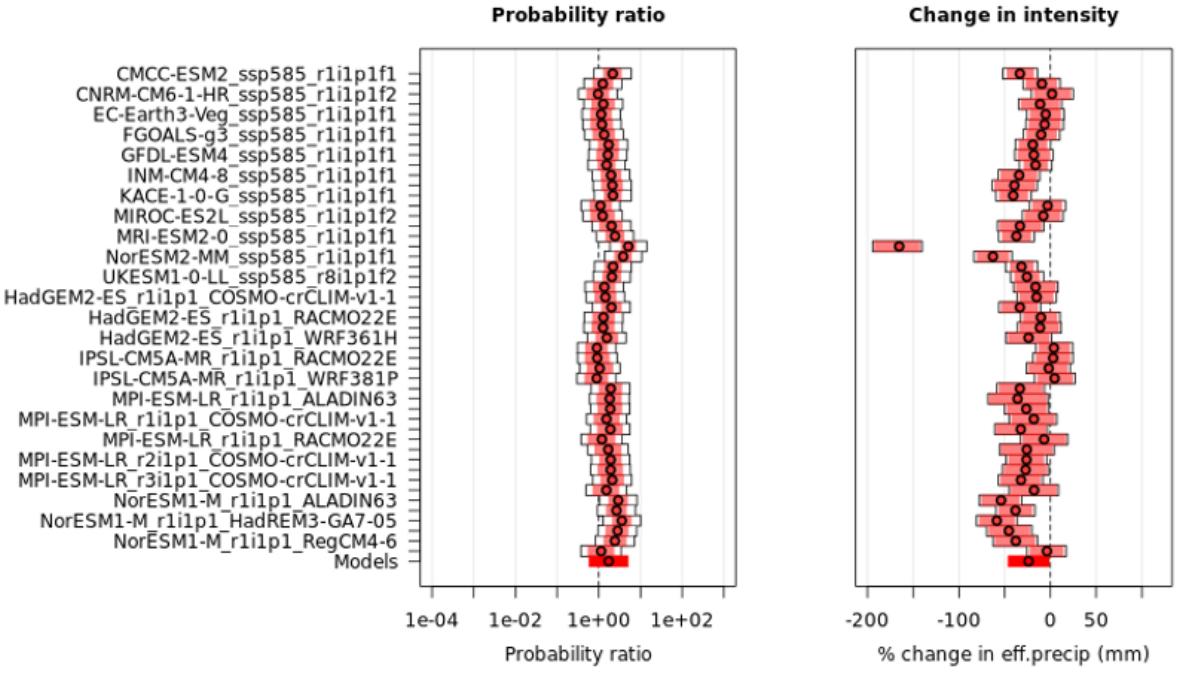

Figure B10: JJA eff precip synthesis from (+1.3°C) to +2.6°C

7.3 Appendix C – Synthesis of Attribution Results Occitania

Table C1: Event magnitudes and return periods (per ERA5-Land) for the Occitania case-study region.

	Event Magnitude	Return Period
HDWI7x	11900	19.4 (4.40, 94.0)
VPDmax7x	4040	67.7 (19.4, Inf)
sfcWind7x	4.89	1.16 (1.02, 1.41)
effPr MAM	88.24	1.29 (1.06, 1.82)
effPr JJA	-206.19	2.22 (1.57, 3.71)

Table C2: HDWI7x attribution summary

https://doi.org/10.5194/egusphere-2026-1193
Preprint. Discussion started: 20 March 2026

Data	HDWI7x		
		Probability ratio (95% CI)	Intensity change (%) (95% CI)
Observations	Past- Present	NA (21.2, NA)	60.9 (35.9, 97.6)
Models		1.33 (0.0430, 98.9)	5.40 (-20.8, 40.8)
Synthesis		NA (NA, NA)	40.8 (13.6, 79.6)
Weighted Model-Only Synthesis	Present- Future	1.96 (0.561, 7.04)	6.54 (-2.72, 16.6)

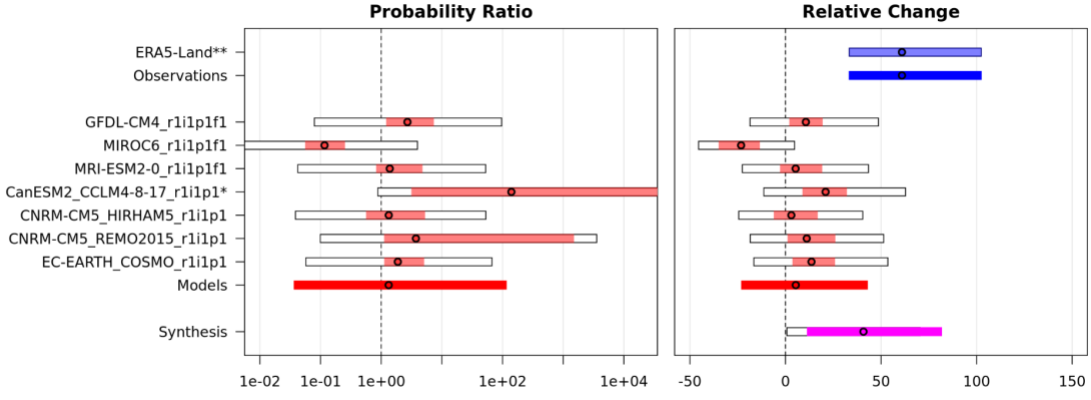

Figure C1: HDWI synthesis from pre-industrial to present day (+1.3°C)

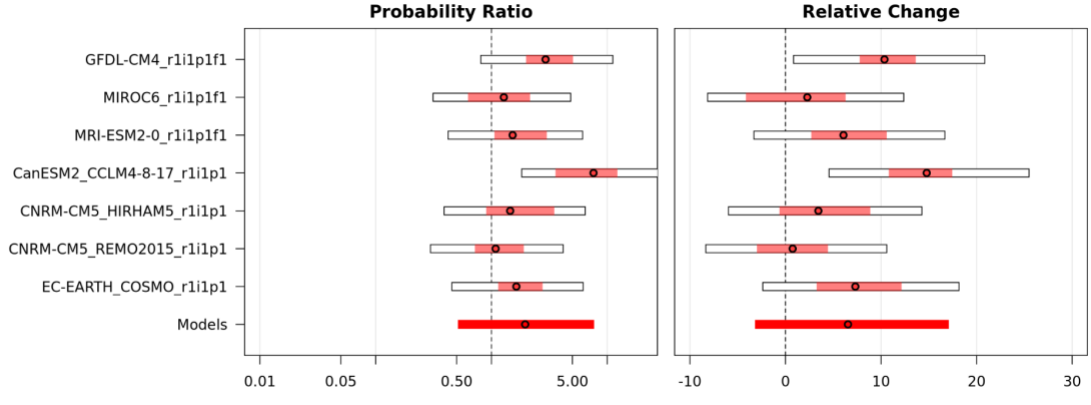

Figure C2: HDWI synthesis from present day (+1.3°C) to +2.6°C

https://doi.org/10.5194/egusphere-2026-1193
Preprint. Discussion started: 20 March 2026

Table C3: VPD7x attribution summary

Data	VPDmax7x		
		Probability ratio (95% CI)	Intensity change (Pa) (95% CI)
Observations	Past- Present	461 (5.61, 257000000)	1080 (697, 1750)
Models		2.25 (0.15, 132)	255 (26.0, 515)
Synthesis		4.45 (0.23, 1930)	403 (139, 769)
Weighted Model-Only Synthesis	Present- Future	2.54 (0.714, 10.4)	250 (126, 394)

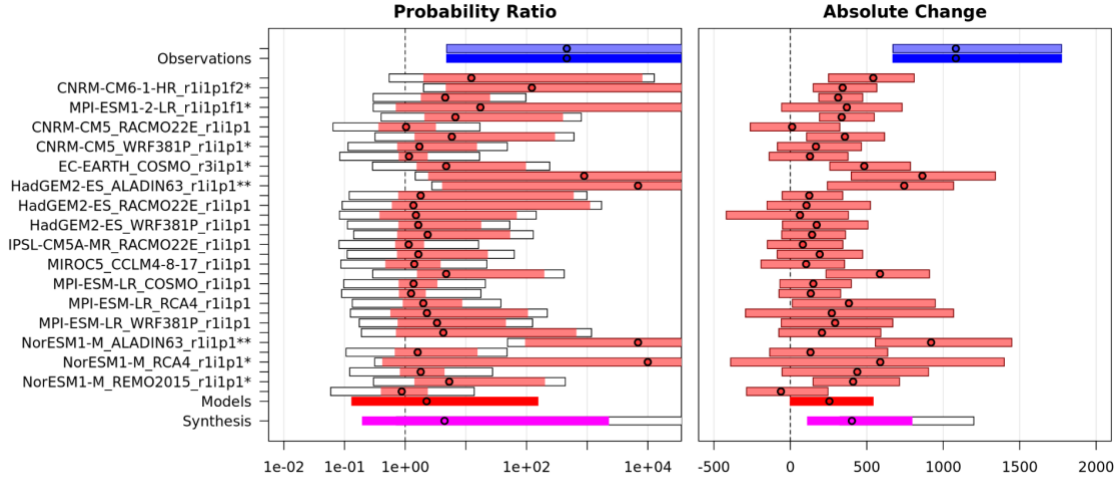

Figure C3: Maximum 7-day VPD synthesis from pre-industrial to present day (+1.3°C)

910

https://doi.org/10.5194/egusphere-2026-1193
Preprint. Discussion started: 20 March 2026

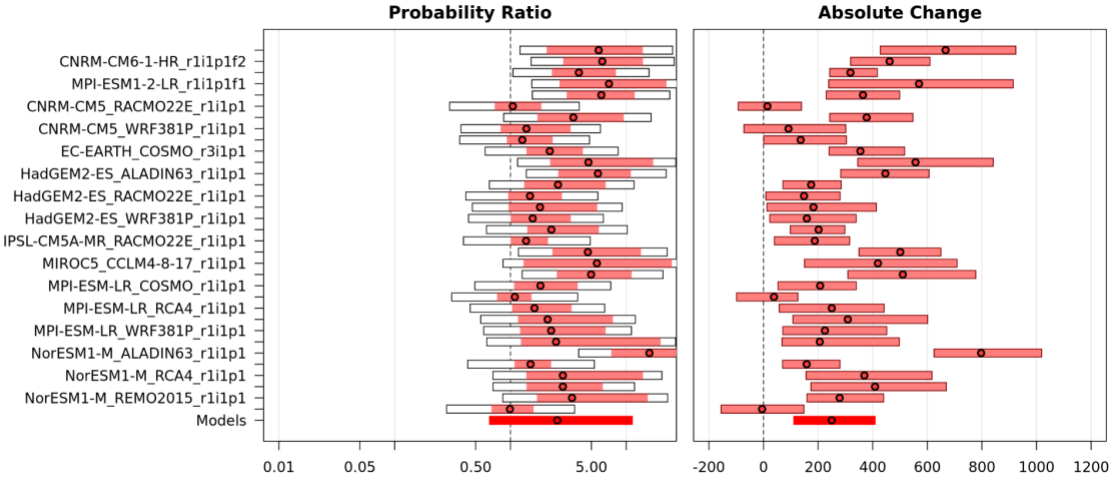

Figure C4: Maximum 7-day VPD synthesis from present day (+1.3°C) to +2.6°C

Table C4: sfcWind7x attribution summary

Data	sfcWindmax7x		
		Probability ratio (95% CI)	Intensity change (m/s) (95% CI)
Observations	Past- Present	1.29 (0.886, 2.06)	0.138 (-0.0733, 0.364)
Models		1.03 (0.894, 1.45)	0.0259 (-0.123, 0.210)
Synthesis		1.09 (0.870, 1.58)	0.0672 (-0.108, 0.267)
Weighted Model-Only Synthesis	Present- Future	0.973 (0.864, 1.10)	-0.0260 (-0.105, 0.0724)

915

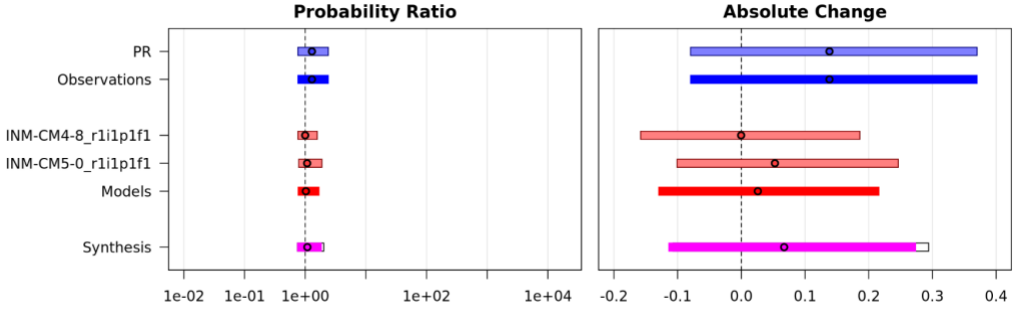

Figure C5: Maximum 7-day wind speed synthesis from pre-industrial to present day (+1.3°C)

https://doi.org/10.5194/egusphere-2026-1193
Preprint. Discussion started: 20 March 2026

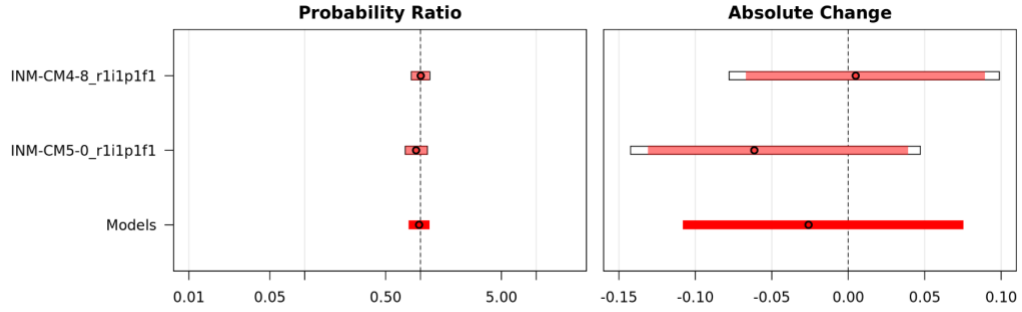

Figure C6: Maximum 7-day wind speed synthesis from present day (+1.3°C) to +2.6°C

Table C5: MAM effective precipitation attribution

Data	MAM Effective Precipitation		
		Probability ratio (95% CI)	Intensity change (%) (95% CI)
Observations	Past- Present	1.5 (0.9, 2.5)	-50 (-110, 11)
Models		0.98 (0.8, 1.4)	-3.8 (-51, 44)
Synthesis		1.1 (0.79, 1.6)	-21 (-74, 32)
Weighted Model-Only Synthesis	Present- Future	1.1 (0.98, 1.2)	-16 (-35, 4.1)

https://doi.org/10.5194/egusphere-2026-1193
Preprint. Discussion started: 20 March 2026

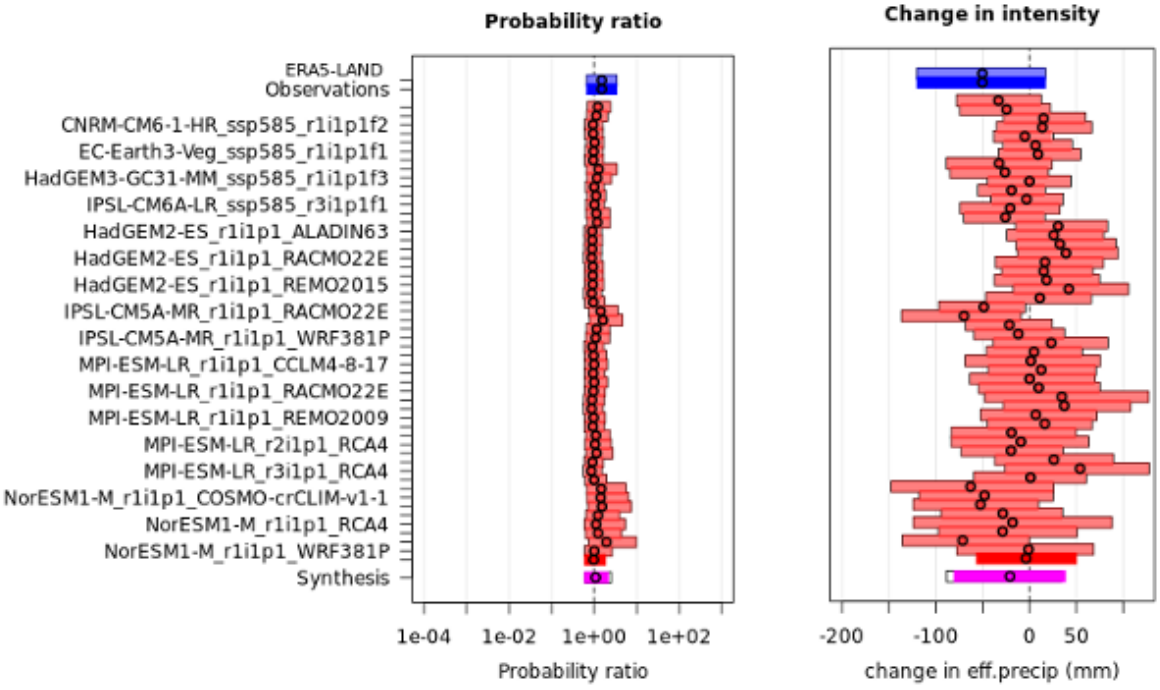

925

Figure C7: MAM eff precip synthesis from pre-industrial to present day (+1.3°C)

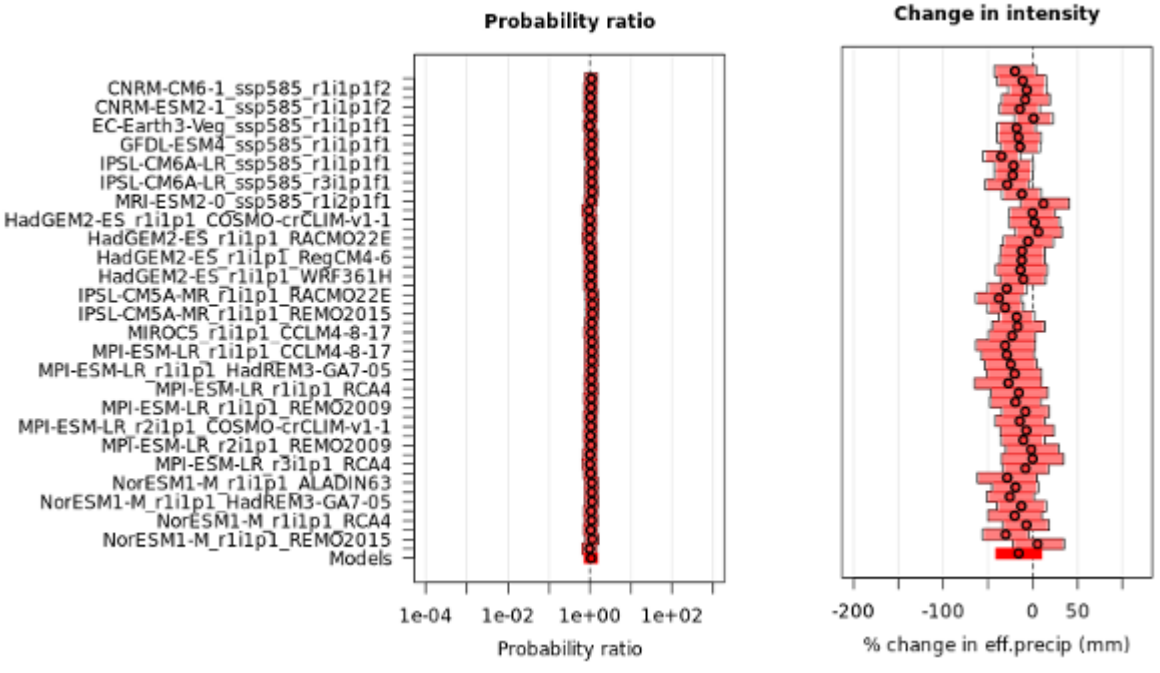

Figure C8: MAM eff precip synthesis from present day (+1.3°C) to +2.6°C

https://doi.org/10.5194/egusphere-2026-1193
Preprint. Discussion started: 20 March 2026

Table C6: JJA effective precipitation attribution

Data	JJA Effective Precipitation		
		Probability ratio (95% CI)	Intensity change (%) (95% CI)
Observations	Past- Present	20 (6, 140)	-120 (-170, -71)
Models		1.4 (0.55, 4.8)	-29 (-74, 16)
Synthesis		3.3 (1.2, 15)	-70 (-120, -23)
Weighted Model-Only Synthesis	Present- Future	1.4 (1.1, 1.8)	-43 (-62, -24)

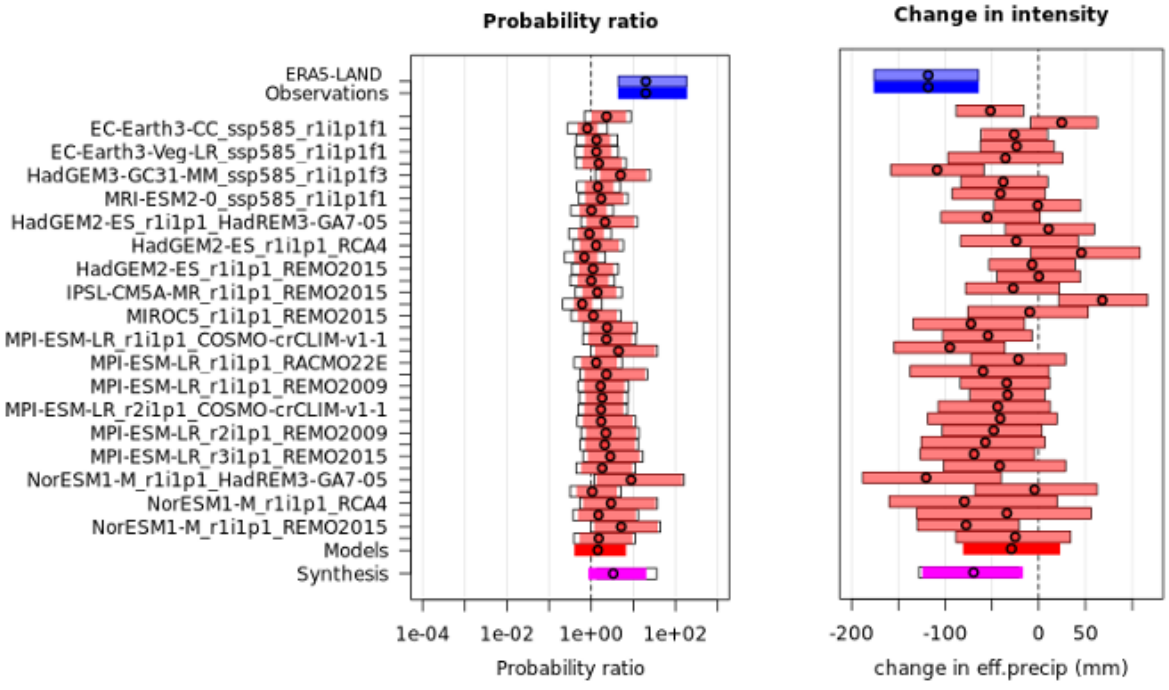

Figure C9: JJA eff precip synthesis from pre-industrial to present day (+1.3°C)

https://doi.org/10.5194/egusphere-2026-1193
Preprint. Discussion started: 20 March 2026

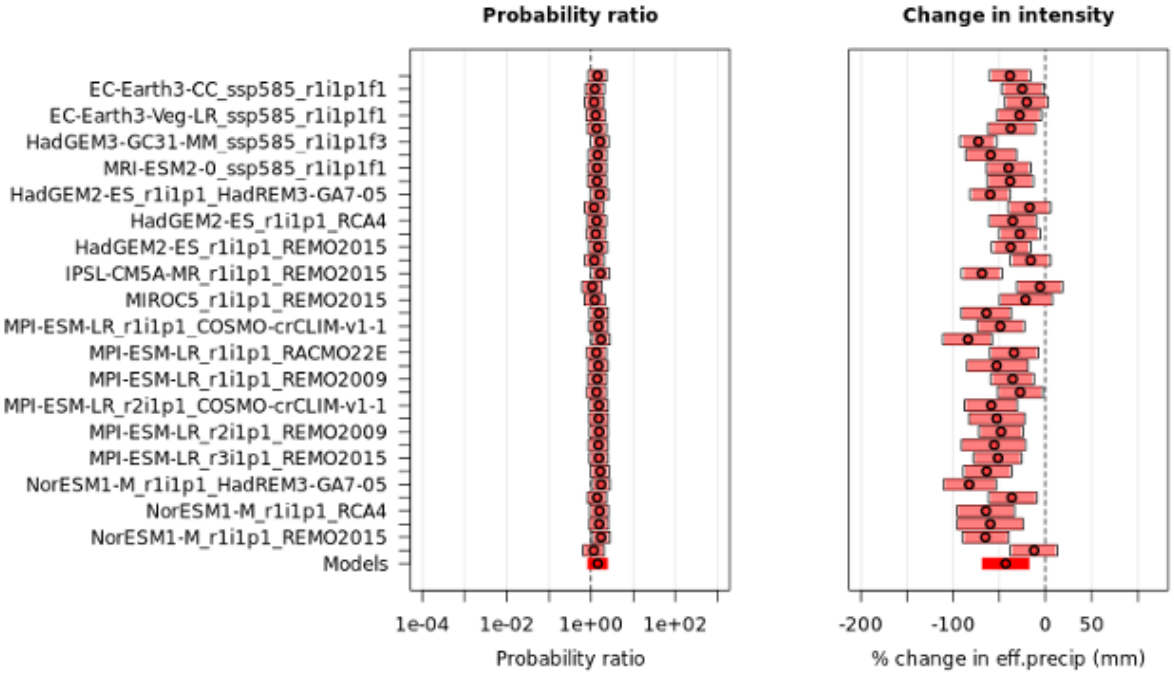

Figure C10: JJA eff precip synthesis from present day (+1.3°C) to +2.6°C

7.4 Appendix D – Synthesis of Attribution Results Eastern Adriatic and Ionian

Table D1: Event magnitudes and return periods (per ERA5-Land) for the Eastern Adriatic/Ionian case-study region.

	Event Magnitude	Return Period
HDWI7x	9760	6.90 (3.39, 18.7)
VPDmax7x	3510	3.49 (1.90, 9.41)
sfcWind7x	3.67	3.57 (2.17, 6.50)
effPr MAM	81.48	1.29 (1.07, 1.71)
effPr JJA	-325.9	5.66 (2.58, 20.82)

Table D2: HDWI7x attribution summary

https://doi.org/10.5194/egusphere-2026-1193
Preprint. Discussion started: 20 March 2026

Data	HDWI7x		
		Probability ratio (95% CI)	Intensity change (%) (95% CI)
Observations	Past- Present	8.99 (2.13, 133)	29.6 (10.8, 55.7)
Models		2.38 (0.635, 16.6)	13.1 (-0.345, 29.7)
Synthesis		3.97 (1.01, 38.0)	19.1 (3.64, 39.1)
Weighted Model-Only Synthesis	Present- Future	2.35 (1.33, 4.20)	9.78 (4.36, 15.4)

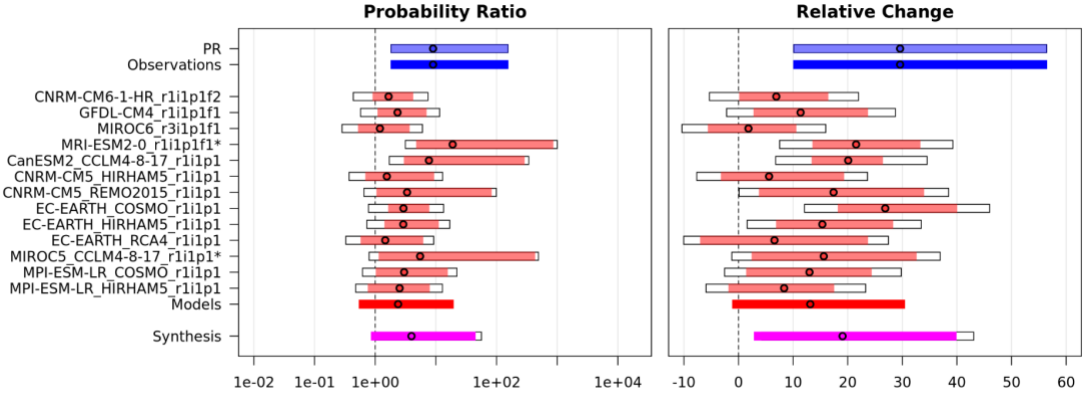

945 **Figure D1: HDWI synthesis from pre-industrial to present day (+1.3°C)**

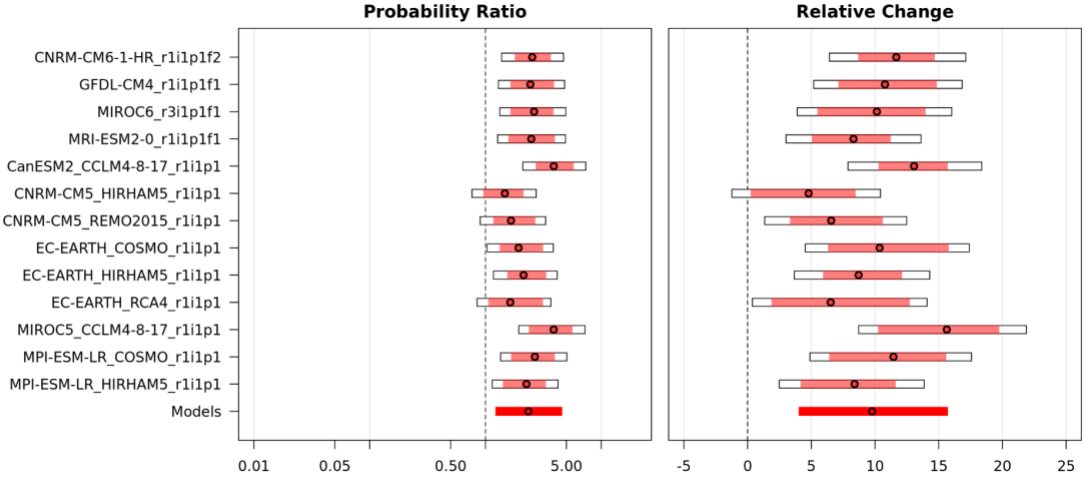

https://doi.org/10.5194/egusphere-2026-1193
Preprint. Discussion started: 20 March 2026

Figure D2: HDWI synthesis from present day (+1.3°C) to +2.6°C

Table D3: VPD7x attribution summary

Data	VPDmax7x		
		Probability ratio (95% CI)	**Intensity change (Pa) (95% CI)**
Observations	**Past- Present**	70.2 (5.78, 125000)	865 (441, 1290)
Models		4.20 (0.321, 150)	496 (197, 796)
Synthesis		9.11 (0.711, 1310)	618 (273, 966)
Weighted Model-Only Synthesis	**Present- Future**	2.37 (1.54, 3.59)	495 (328, 670)

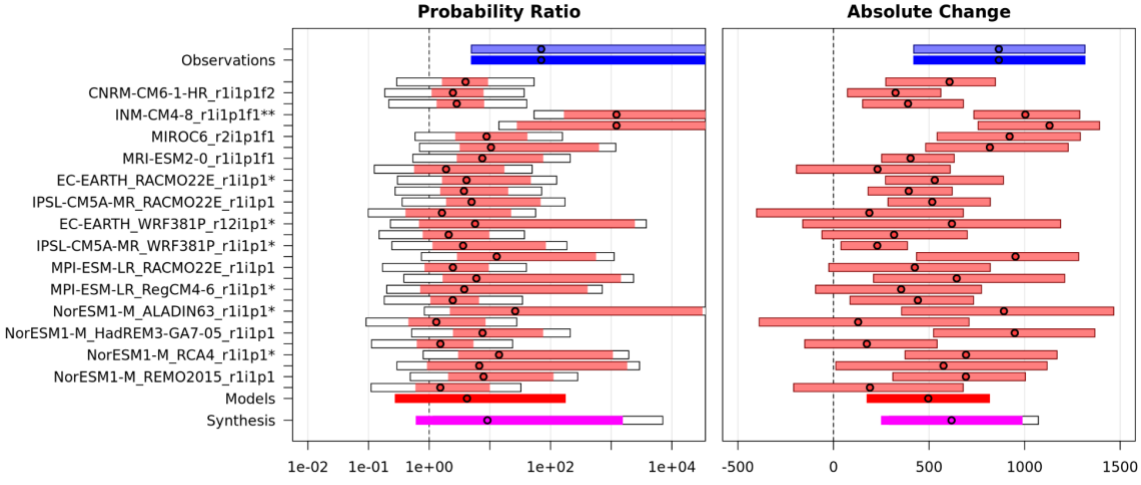

Figure D3: Maximum 7-day VPD synthesis from pre-industrial to present day (+1.3°C)

https://doi.org/10.5194/egusphere-2026-1193
Preprint. Discussion started: 20 March 2026

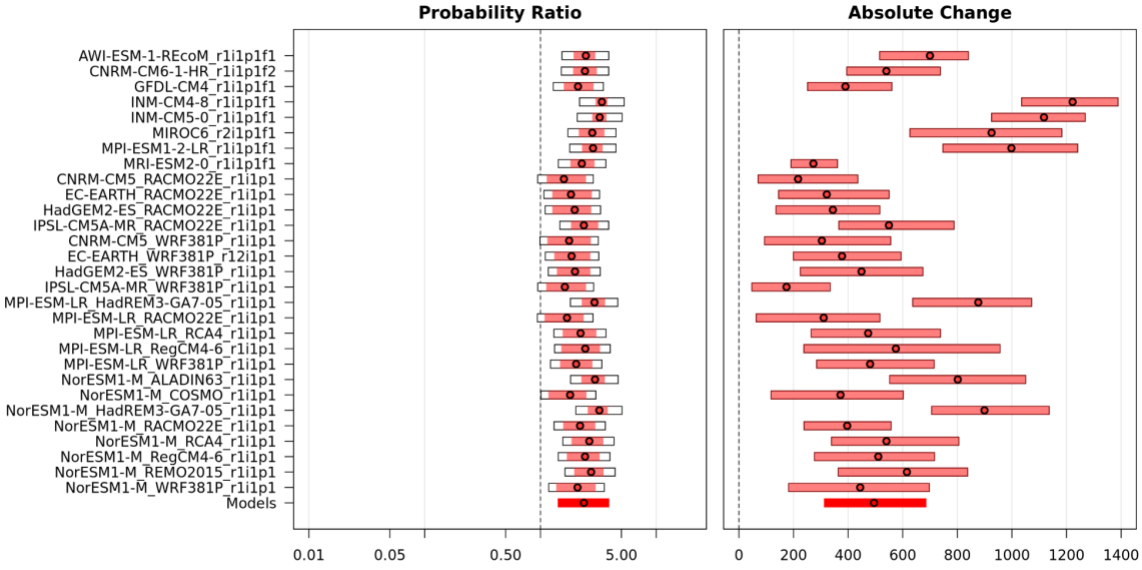

Figure D4: Maximum 7-day VPD synthesis from present day (+1.3°C) to +2.6°C

Table D4: sfcWind7x attribution summary

Data	sfcWindmax7x		
		Probability ratio (95% CI)	Intensity change (m/s) (95% CI)
Observations	Past- Present	3.00 (1.28, 12.9)	0.182 (0.0417, 0.325)
Models		0.868 (0.217, 3.74)	-0.0389 (-0.369, 0.294)
Synthesis		1.83 (0.613, 7.88)	0.148 (-0.0348, 0.333)
Weighted Model-Only Synthesis	Present- Future	0.802 (0.437, 1.51)	-0.0539 (-0.199, 0.0999)

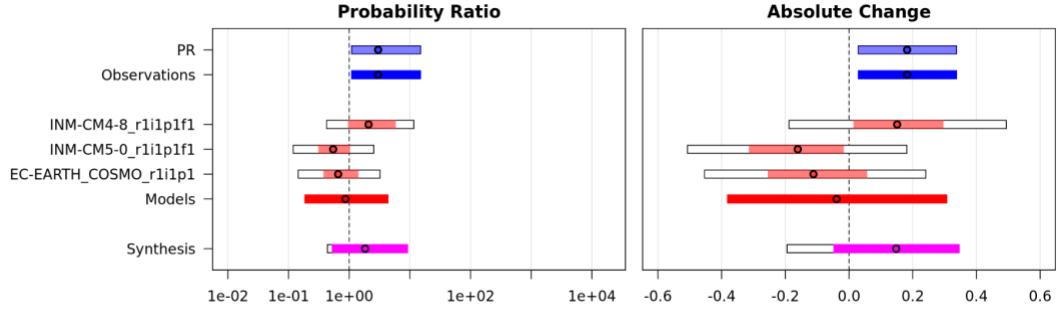

https://doi.org/10.5194/egusphere-2026-1193
Preprint. Discussion started: 20 March 2026

Figure D5: Maximum 7-day wind speed synthesis from pre-industrial to present day (+1.3°C)

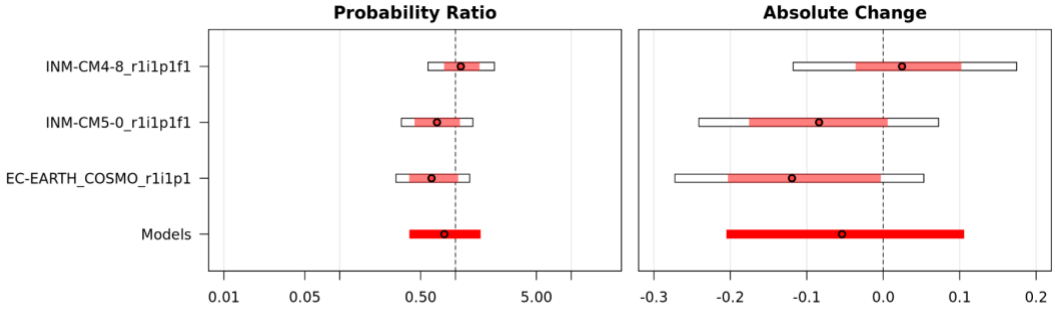

Figure D6: Maximum 7-day wind speed synthesis from present day (+1.3°C) to +2.6°C

965 **Table D5: MAM effective precipitation attribution summary**

Data	MAM Effective Precipitation		
		Probability ratio (95% CI)	Intensity change (%) (95% CI)
Observations	Past- Present	1.4 (0.91, 2.3)	-35 (-85, 8.7)
Models		1.4 (0.32, 6.6)	-22 (-61, 17)
Synthesis		1.4 (0.78, 2.7)	-28 (-71, 14)
Weighted Model-Only Synthesis	Present- Future	1.3 (0.97, 1.6)	-22 (-39, -5.4)

https://doi.org/10.5194/egusphere-2026-1193
Preprint. Discussion started: 20 March 2026

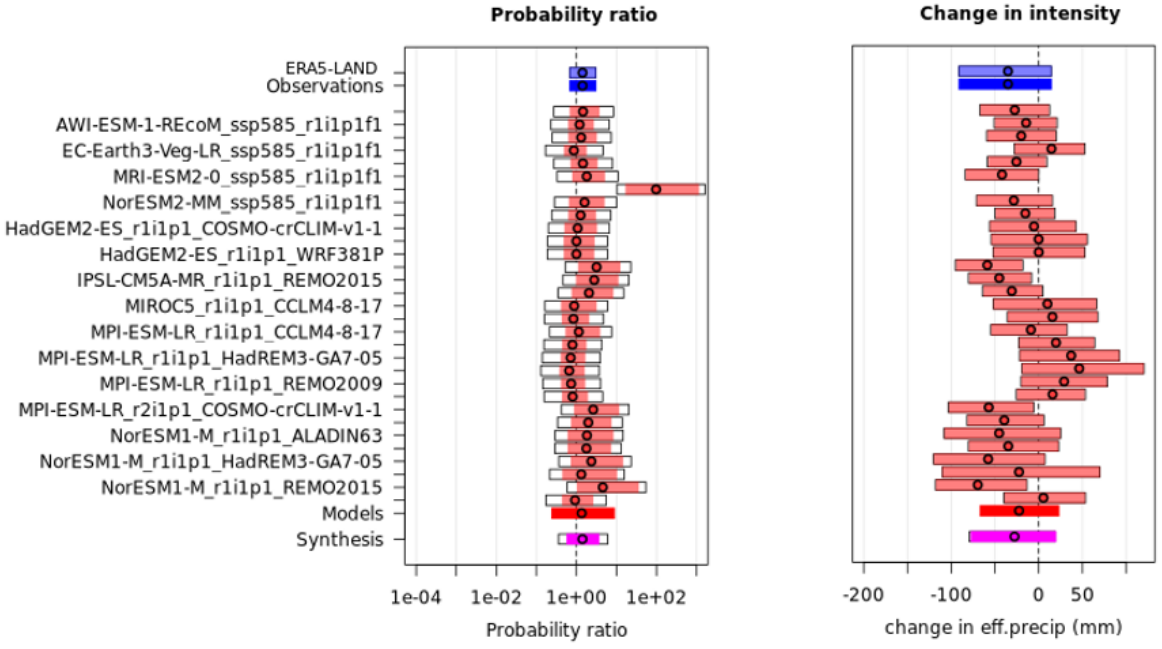

Figure D7: MAM eff precip synthesis from pre-industrial to present day (+1.3°C)

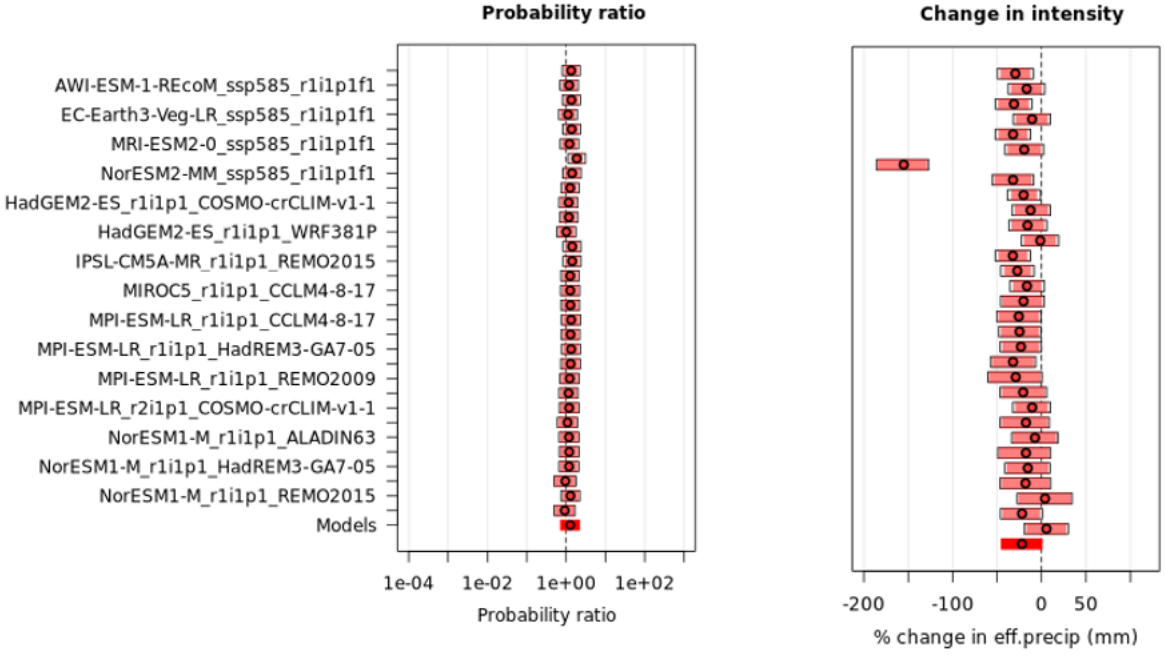

Figure D8: MAM eff precip synthesis from present day (+1.3°C) to +2.6°C

https://doi.org/10.5194/egusphere-2026-1193
Preprint. Discussion started: 20 March 2026

Table D6: JJA effective precipitation attribution summary

Data	JJA Effective Precipitation		
		Probability ratio (95% CI)	Intensity change (%) (95% CI)
Observations	Past- Present	11 (1.7, 95)	-78 (-140, -16)
Models		1.9 (0.5, 9.7)	-25 (-55, 6)
Synthesis		3.6 (0.75, 22)	-35 (-73, 3.6)
Weighted Model-Only Synthesis	Present- Future	2 (0.96, 4.1)	-32 (-47, -17)

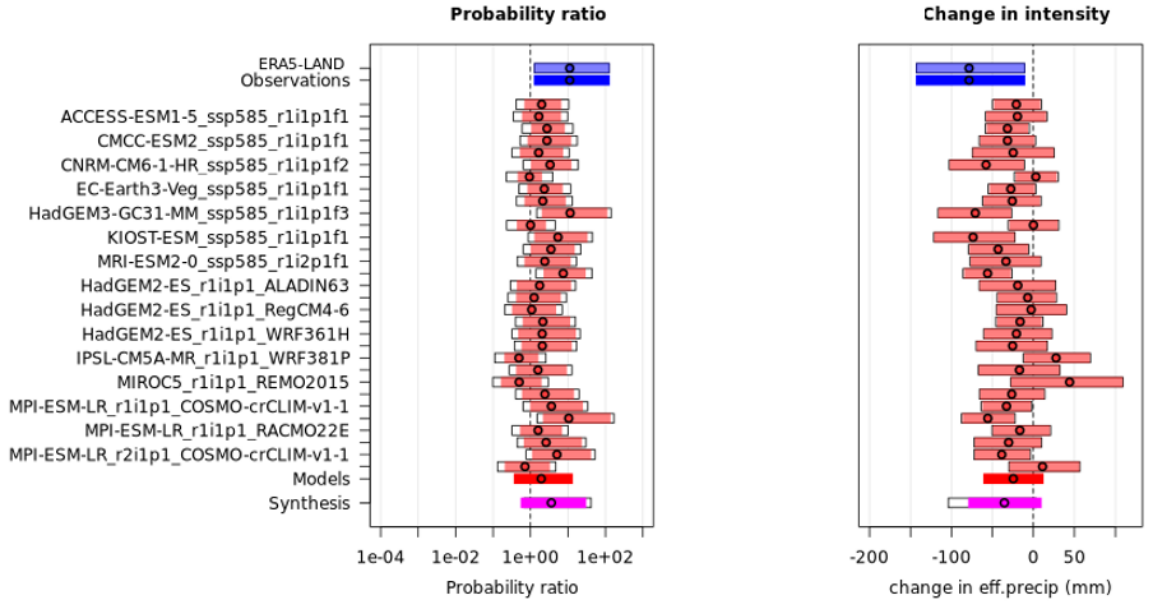

Figure D9: JJA eff precip synthesis from pre-industrial to present day (+1.3°C)

https://doi.org/10.5194/egusphere-2026-1193
Preprint. Discussion started: 20 March 2026

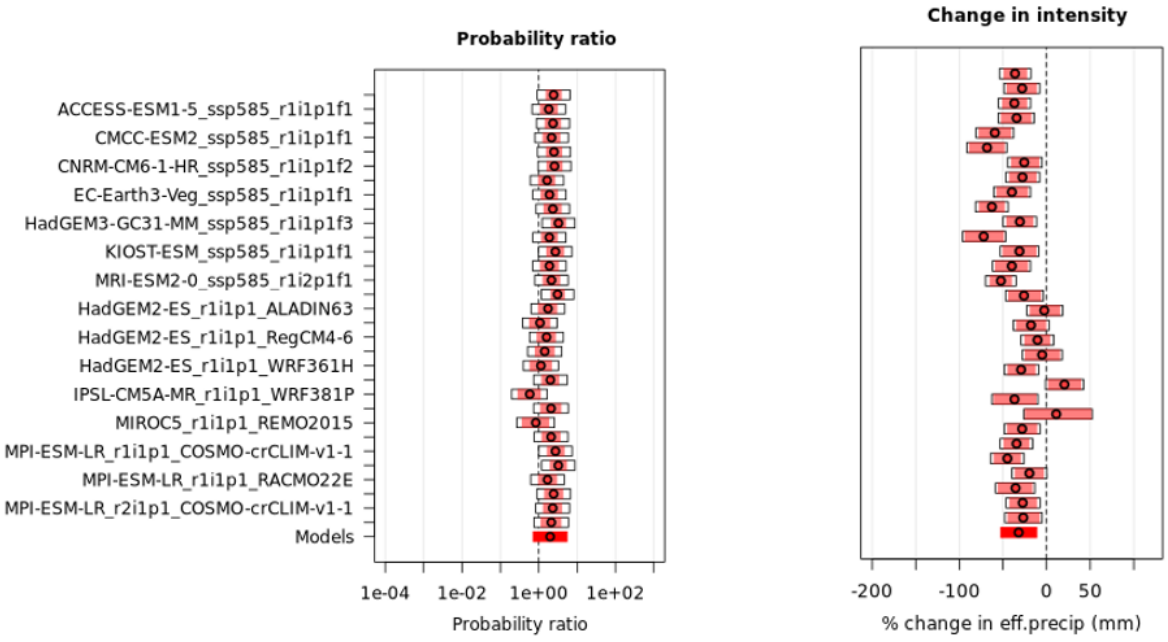

Figure D10: JJA eff precip synthesis from present day (+1.3°C) to +2.6°C

7.5 Appendix E – Synthesis of Attribution Results Northern and Western Türkiye

Table E1: Event magnitudes and return periods (per ERA5-Land) for the Northern and Western Türkiye case-study region.

	Event Magnitude	Return Period
HDWI7x	17500	85.8 (17.1, Inf)
VPDmax7x	4540	44.9 (11.6, Inf)
sfcWind7x	4.64	3.38 (2.05, 7.14)
effPr MAM	-98.98	2.88 (1.69, 6.7)
effPr JJA	-454.38	33 (7.44, 745.58)

Table E2: HDWI7x attribution summary

https://doi.org/10.5194/egusphere-2026-1193
Preprint. Discussion started: 20 March 2026

Data	HDWI7x		
		Probability ratio (95% CI)	Intensity change (%) (95% CI)
Observations	Past- Present	inf (134, inf)	34.4 (20.2, 54.5)
Models		11.2 (0.165, 13400)	10.6 (4.20, 18.4)
Synthesis		Not synthesisable	15.1 (7.00, 25.7)
Weighted Model-Only Synthesis	Present- Future	5.98 (1.42, 28.3)	8.80 (4.45, 13.5)

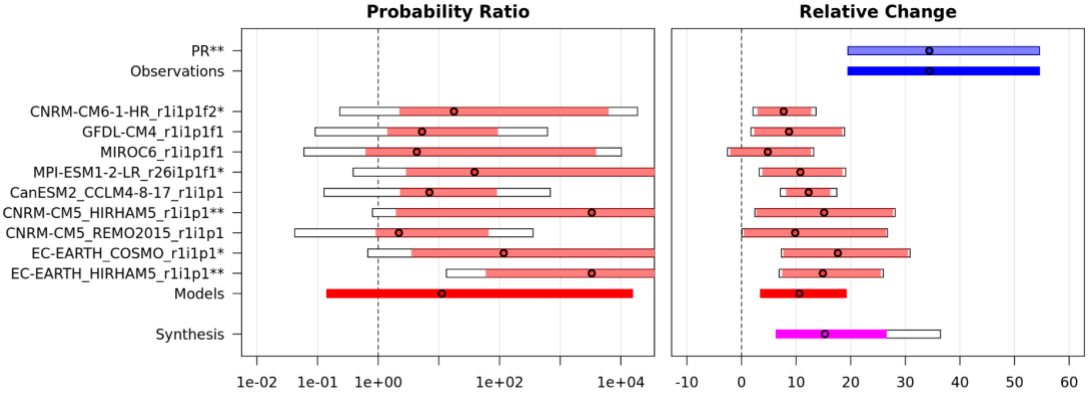

985

Figure E1: HDWI synthesis from pre-industrial to present day (+1.3°C)

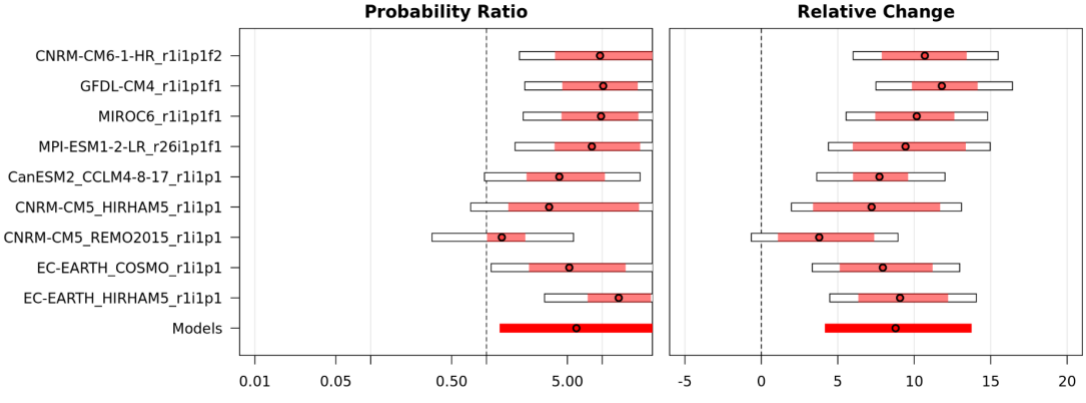

Figure E2: HDWI synthesis from present day (+1.3°C) to +2.6°C

990

Table E3: VPD7x attribution summary

https://doi.org/10.5194/egusphere-2026-1193
Preprint. Discussion started: 20 March 2026

Data	VPDmax7x		
		Probability ratio (95% CI)	Intensity change (Pa) (95% CI)
Observations	Past- Present	inf (92.8, inf)	935 (605, 1270)
Models		13.4 (0.0478, 248000)	436 (162, 709)
Synthesis		Not synthesisable	645 (348, 944)
Weighted Model-Only Synthesis	Present- Future	7.15 (2.35, 22.5)	464 (322, 606)

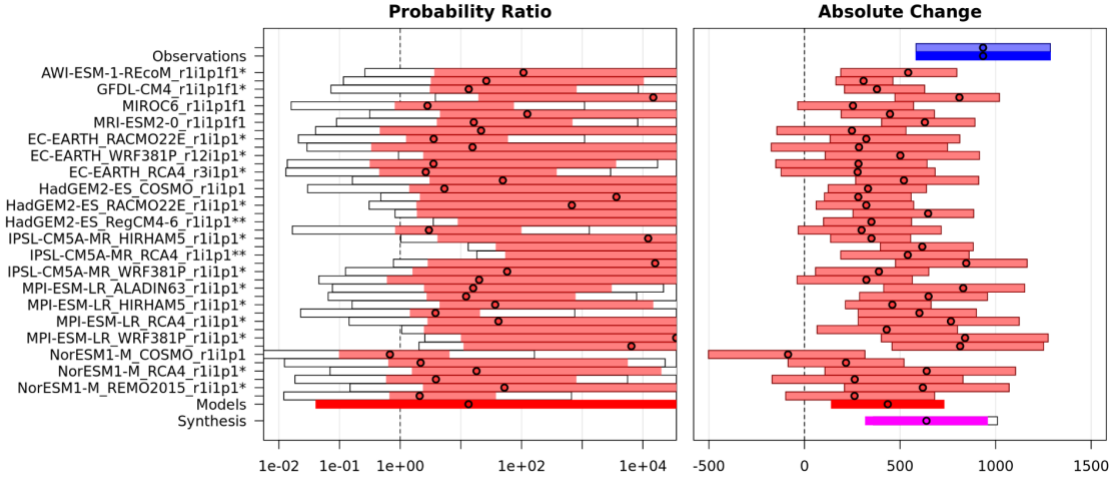

Figure E3: Maximum 7-day VPD synthesis from pre-industrial to present day (+1.3°C)

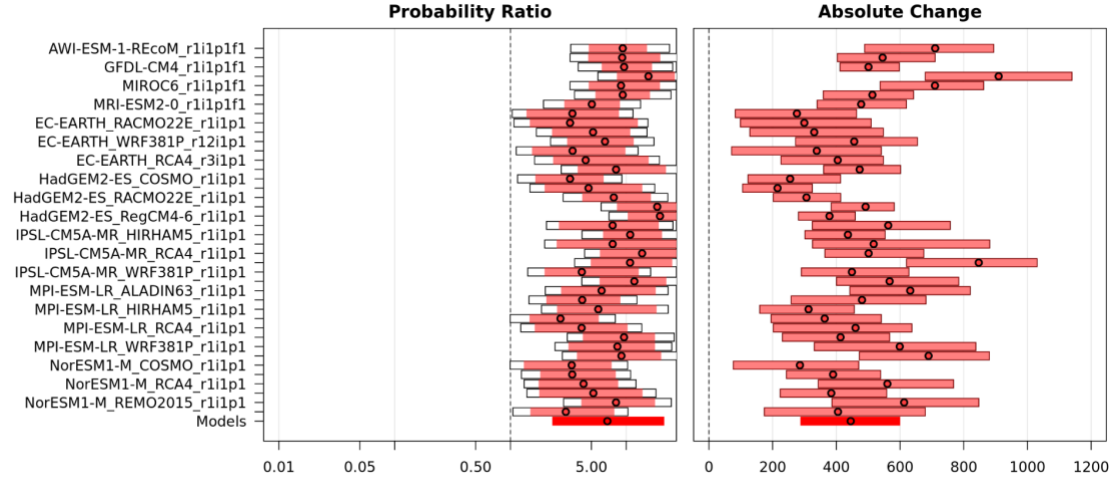

995

https://doi.org/10.5194/egusphere-2026-1193
Preprint. Discussion started: 20 March 2026

Figure E4: Maximum 7-day VPD synthesis from present day (+1.3°C) to +2.6°C

Table E4: sfcWind7x attribution summary

Data	sfcWindmax7x		
		Probability ratio (95% CI)	Intensity change (m/s) (95% CI)
Observations	Past- Present	4.38 (1.08, 16.4)	0.245 (0.00990, 0.440)
Models		1.26 (0.777, 2.72)	0.0806 (-0.0843, 0.255)
Synthesis		1.56 (0.753, 3.81)	0.144 (-0.0512, 0.326)
Weighted Model-Only Synthesis	Present- Future	1.08 (0.767, 1.49)	0.0230 (-0.0793, 0.127)

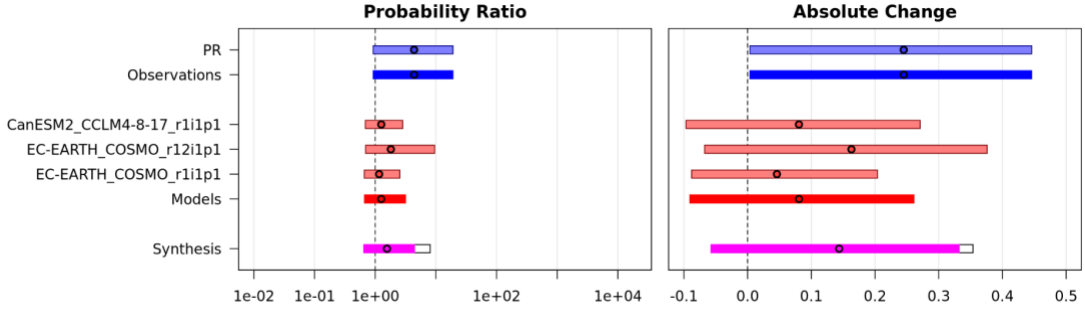

Figure E5: Maximum 7-day wind speed synthesis from pre-industrial to present day (+1.3°C)

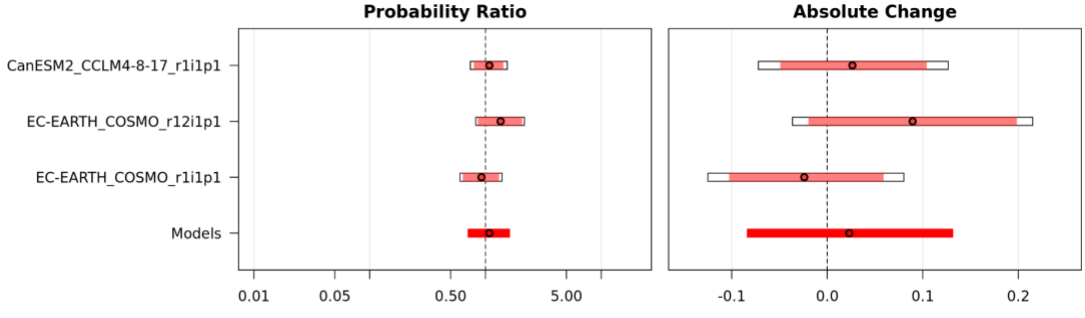

Figure E6: Maximum 7-day wind speed synthesis from present day (+1.3°C) to +2.6°C

Table E5: MAM effective precipitation attribution

https://doi.org/10.5194/egusphere-2026-1193
Preprint. Discussion started: 20 March 2026

Data	MAM Effective Precipitation		
		Probability ratio (95% CI)	Intensity change (%) (95% CI)
Observations	Past- Present	6.2 (1.3, 40)	-63 (-110, -9.6)
Models		1.7 (0.35, 11)	-25 (-61, 11)
Synthesis		3.3 (0.68, 21)	-38 (-78, 4.5)
Weighted Model-Only Synthesis	Present- Future	1.4 (0.97, 2)	-23 (-39, -6.6)

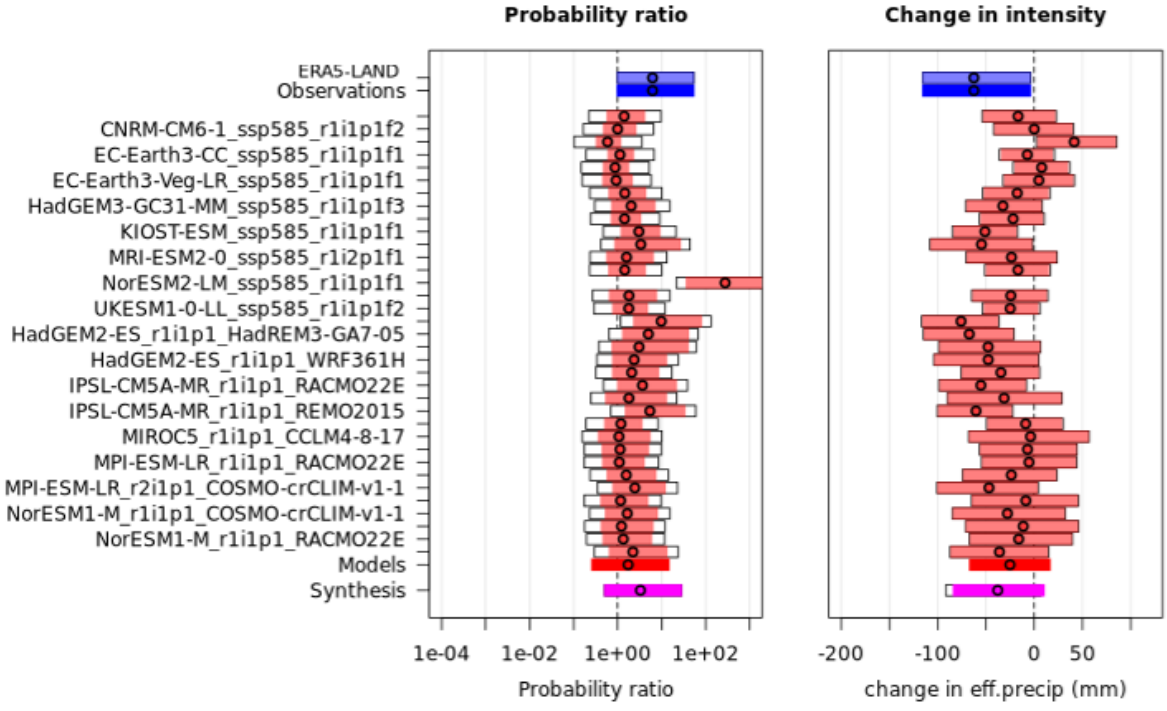

Figure E7: MAM eff precip synthesis from pre-industrial to present day (+1.3°C)

https://doi.org/10.5194/egusphere-2026-1193
Preprint. Discussion started: 20 March 2026

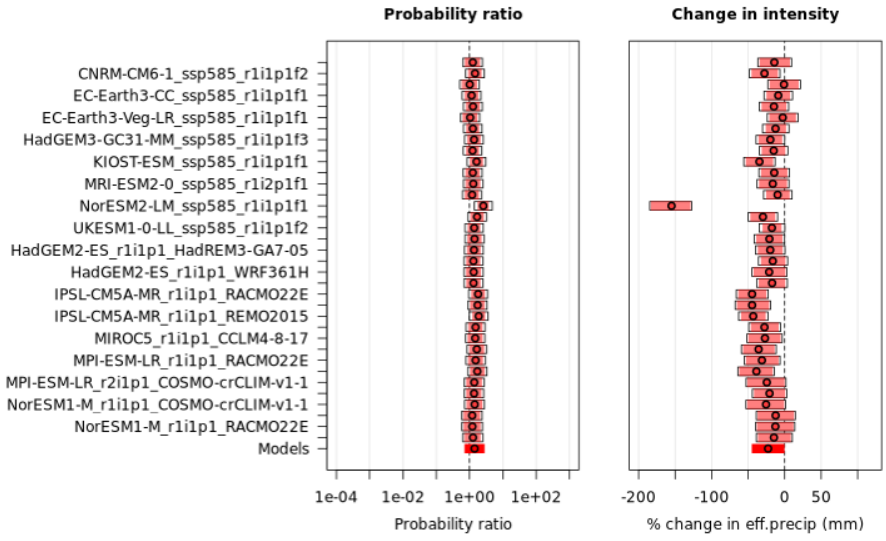

Figure E8: MAM eff precip synthesis from present day (+1.3°C) to +2.6°C

Table E6: JJA effective precipitation attribution

Data	JJA Effective Precipitation		
		Probability ratio (95% CI)	Intensity change (%) (95% CI)
Observations	Past- Present	31 (3.2, 310)	-59 (-110, -16)
Models		7.2 (0.23, 300)	-36 (-66, -5.7)
Synthesis		20 (1.4, 330)	-43 (-79, -8.4)
Weighted Model-Only Synthesis	Present- Future	5 (2.1, 12)	-41 (-55, -26

https://doi.org/10.5194/egusphere-2026-1193
Preprint. Discussion started: 20 March 2026

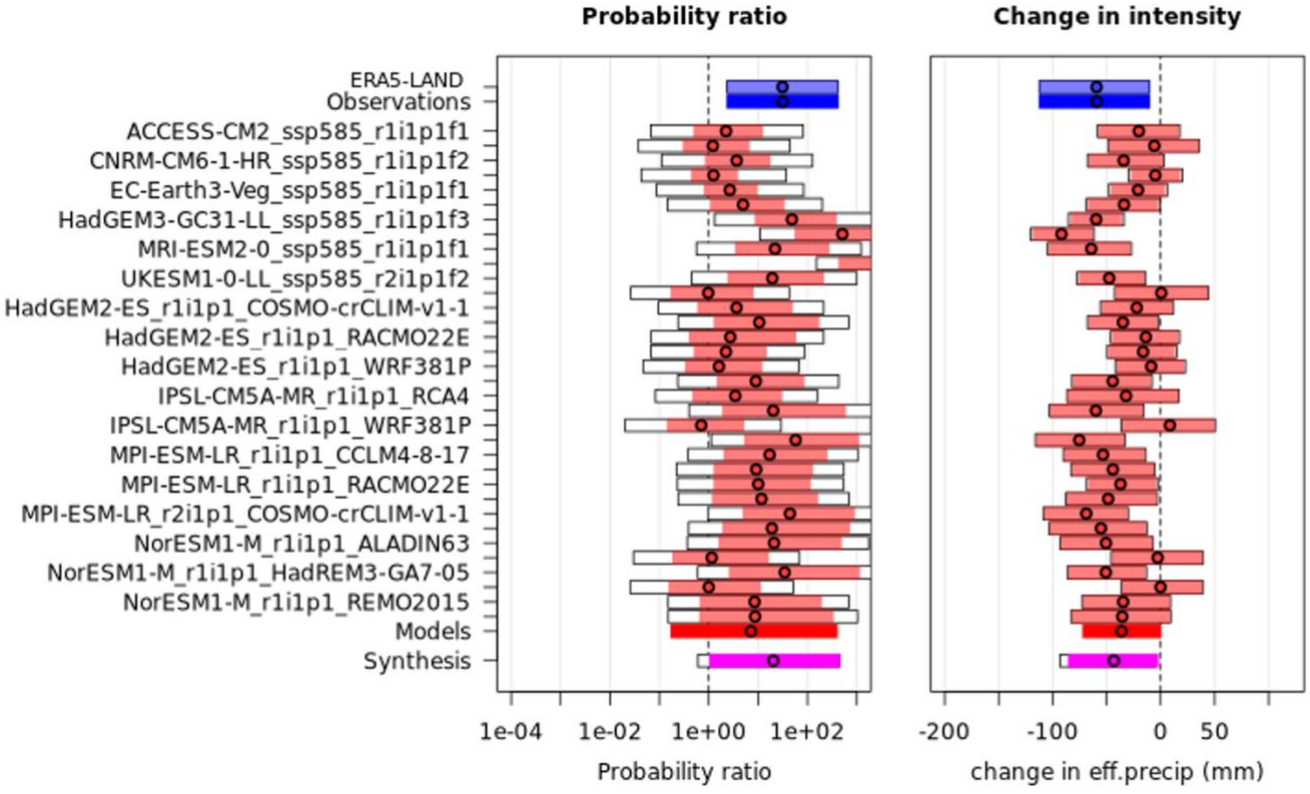

Figure E9: JJA eff precip synthesis from pre-industrial to present day (+1.3°C)

https://doi.org/10.5194/egusphere-2026-1193
Preprint. Discussion started: 20 March 2026

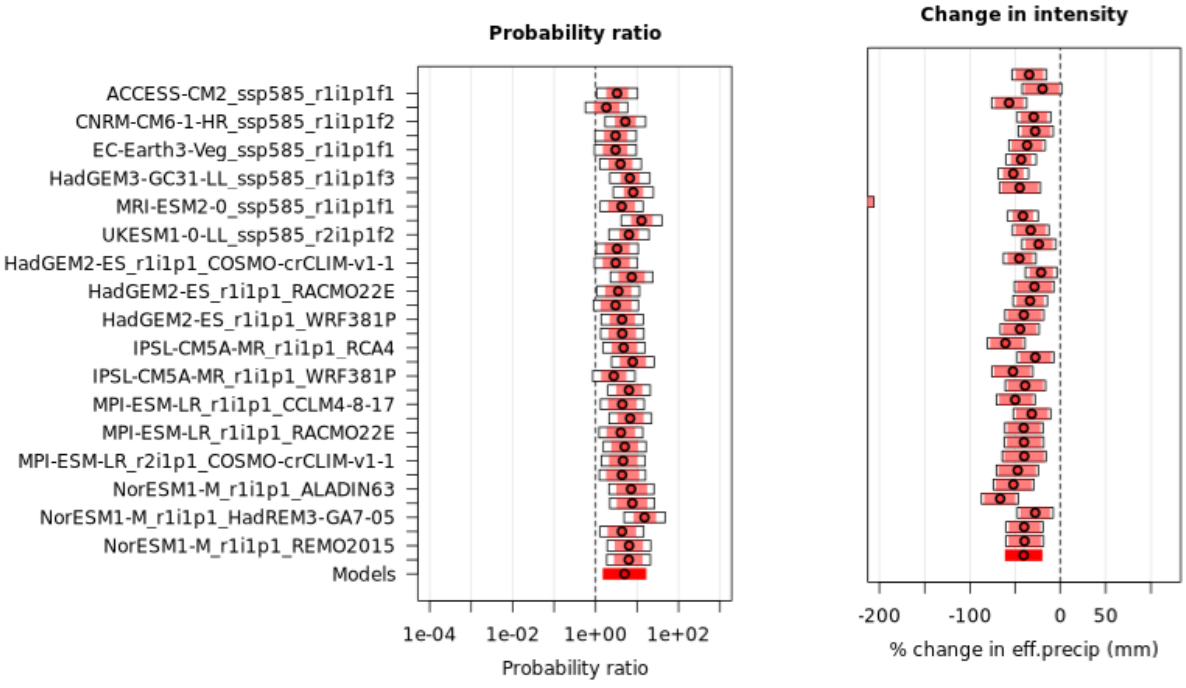

Figure E10: JJA eff precip synthesis from present day (+1.3°C) to +2.6°C

7.6 Appendix F – FWI and HDWI comparison

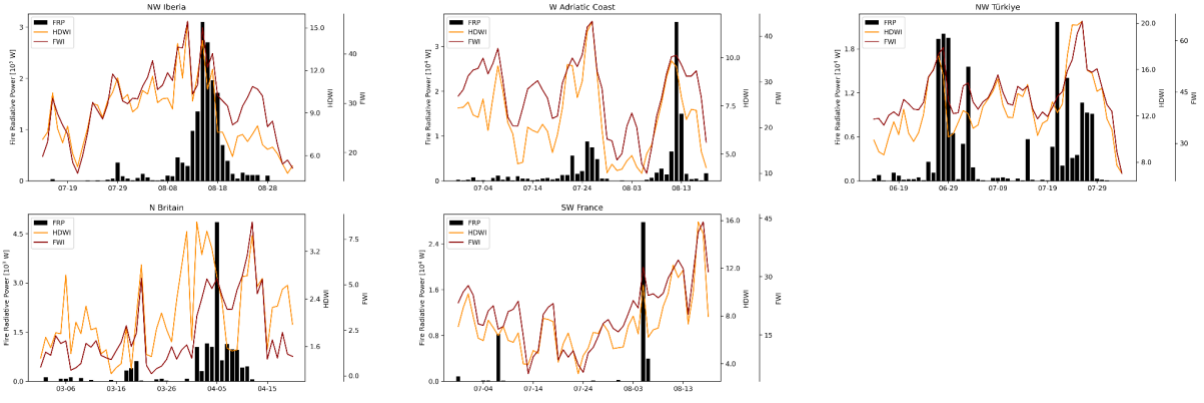

Figure F1: 50-day comparison of the FWI and HDWI indices over each study region with FRP overlaid.

https://doi.org/10.5194/egusphere-2026-1193
Preprint. Discussion started: 20 March 2026

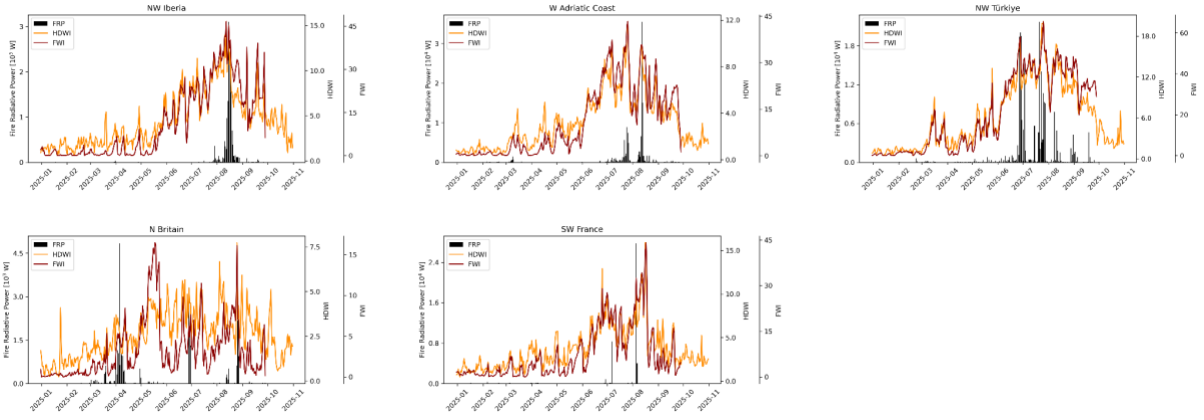

Figure F2: 2025 comparison of the FWI and HDWI indices over each study region with FRP overlaid. Note that the association is very close, though least associated in the cooler N Britain region, where drought effects play a stronger role in comparison to extreme heat and wind.

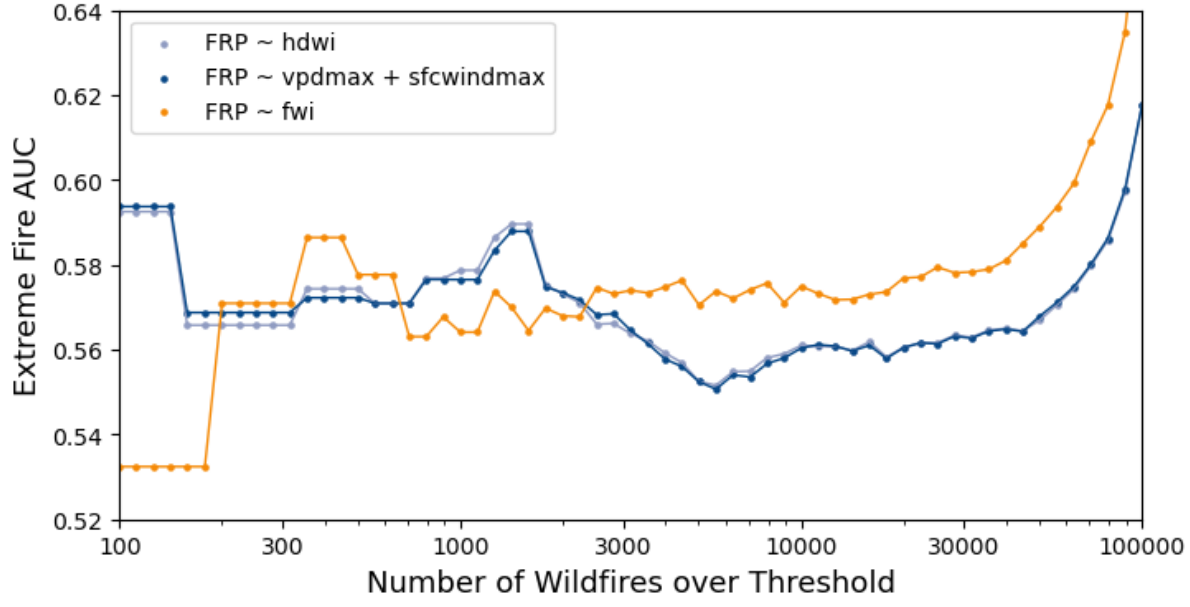

Figure F3: the predictive power of different variable sets in a Gamma distribution GLM with log-link function for classifying the N most extreme wildfires by FRP according to the area under the receiver operating curve statistic (AUC). A single variable HDWI model performs extremely similarly to a model with VPDmax and sfcWindmax accounted for separately. HDWI performs best at capturing the rarest and most extreme wildfires, similarly for the next most extreme wildfires (from the top 3000 to 300 FRP events) and worse for more moderate wildfire events (below the top 3000 class).

https://doi.org/10.5194/egusphere-2026-1193
Preprint. Discussion started: 20 March 2026

7.6 Appendix G – Burned Area Rankings

Table G1: The top 3 ranking severe fire years per EFFIS burned area, for all EFFIS countries where more than half of years exhibit non-zero burned area. 2025 is shown in bold.

Rank	ALB	BGR	BIH	CYP	DEU	ESP	FRA	GBR	GRC	HRV	HUN	IRL
1	2007	2007	2020	**2025**	**2025**	**2025**	2022	**2025**	2007	2017	2022	2011
2	**2025**	2024	2012	2021	2022	2022	2019	2019	2023	2012	2015	2013
3	2011	**2025**	2017	2020	2018	2012	**2025**	2022	2021	2022	2024	2017

Rank	ITA	MKD	MNE	NOR	PRT	ROU	SRB	SVN	SWE	TUR	XKO
1	2007	2024	2017	2019	2017	2022	2024	2022	2018	2021	**2025**
2	2021	2007	2021	2014	**2025**	**2025**	**2025**	2006	2014	**2025**	2007
3	2017	**2025**	2020	2008	2016	2020	2007	2016	2008	2016	2024

Code and data availability

Please find data and code used for this analysis at: https://doi.org/10.5281/zenodo.18839225. Code for data processing, attribution, and visualisation can be found in the european_fire_25_notebooks.zip file, with attribution results (both tabular and figures) in the european_fire_25_results.zip files. Model evaluation tables can be found in the model_synthesis.zip file in the zenodo repository. Models were evaluated for their reproduction of the observed statistical distribution of each variable, and their geospatial and seasonal reproduction of observed trends. Model evaluation figures can be found in the model_evaluation_figures.zip files in the zenodo repository.

Author contributions

Conceptualization, Investigation, and Visualisation was carried out by TK. Formal analysis was carried out by TK, MZ, OH and EG. Data curation was carried out by TK, MZ and CB. Structure of the original draft was carried out by TK. Contribution to sections of original draft as well as review and editing was carried out by all authors. Funding was acquired by FO.

Competing interests

At least one of the (co-)authors is a member of the editorial board of Natural Hazards and Earth System Sciences.

https://doi.org/10.5194/egusphere-2026-1193
Preprint. Discussion started: 20 March 2026

Acknowledgements

TK, MZ, CB, and FO acknowledge funding from the Bezos Earth Fund. We acknowledge computational resources and support provided by the Imperial College Research Computing Service https://doi.org/10.14469/hpc/2232.

References

Abatzoglou, J.T., Williams, A.P. and Barbero, R.: Global emergence of anthropogenic climate change in fire weather indices. Geophys. Res. Lett., 46(1), 326-336. https://doi.org/10.1029/2018GL080959, 2019

Abatzoglou, J.T., Kolden, C.A., Cullen, A.C., Sadegh, M., Williams, E.L., Turco, M. and Jones, M.W.: Climate change has increased the odds of extreme regional forest fire years globally. Nat. Commun. 16, 6390. https://doi.org/10.1038/s41467-025-61608-1, 2025

Arias, P.A., Bellouin, N., Coppola, E., Jones, R.G., Krinner, G., Marotzke, J., Naik, V., Palmer, M.D., Plattner, G.K., Rogelj, J. and Rojas, M., et al: Technical Summary. In Climate Change 2021: The Physical Science Basis. Contribution of Working Group I to the Sixth Assessment Report of the Intergovernmental Panel on Climate Change Cambridge University Press, Cambridge, United Kingdom and New York, NY, USA, pp. 33−144. https://doi.org/10.1017/9781009157896.002, 2021

Arnell, N.W., Freeman, A. and Gazzard, R.: The effect of climate change on indicators of fire danger in the UK. Environ. Res. Lett., 16(4), 044027. https://doi.org/10.1088/1748-9326/abd9f2, 2021

Arregocés, H.A., Bonivento, G.J. and Rojano, R.: Wind power potential over northern South America using ERA5-Land global reanalysis. Clean Energy, 8(2), 104-112. https://doi.org/10.1093/ce/zkad096, 2024

Atalay, I., Efe, R., Öztürk, M.: Ecology and Classification of Forests in Turkey, Proc. Soc. Behaviour. Sci., 120, 788-805, https://doi.org/10.1016/j.sbspro.2014.02.163, 2014

Avcı, M.: The floristic regions of Turkey and a geographical approach for Anatolian diagonal. Review Depart. Geogr. Univ. Istanbul, 3, 59-91. 1996

Badia, A., Serra, P. and Modugno, S.: Identifying dynamics of fire ignition probabilities in two representative Mediterranean wildland-urban interface areas. Appl.Geogr. 31(3), pp.930-940. https://doi.org/10.1016/j.apgeog.2011.01.016, 2011

Bakke, S.J., Ionita, M. and Tallaksen, L.M: Recent European drying and its link to prevailing large-scale atmospheric patterns. Sci Rep 13, 21921. https://doi.org/10.1038/s41598-023-48861-4, 2023

Barbero, R., Abatzoglou, J.T., Pimont, F., Ruffault, J. and Curt, T.: Attributing increases in fire weather to anthropogenic climate change over France. Front. Earth Sci. 8, 104. https://doi.org/10.3389/feart.2020.00104, 2020

Basse, A., Callies, D., Grötzner, A. and Pauscher, L.:. Seasonal effects in the long-term correction of short-term wind measurements using reanalysis data. Wind Energy Sci., 6(6), 1473-1490. https://doi.org/10.5194/wes-6-1473-2021, 2021

Bassler H., 'New' EU wildland firefighting force may be close to becoming a reality: https://wildfiretoday.com/new-eu-wildland-firefighting-force-may-be-close-to-becoming-a-reality/, last accessed 2 March 2026

https://doi.org/10.5194/egusphere-2026-1193
Preprint. Discussion started: 20 March 2026

Baudena, M., Santana, V.M., Baeza, M.J., Bautista, S., Eppinga, M.B., Hemerik, L., Garcia Mayor, A., Rodriguez, F., Valdecantos, A., Vallejo, V.R. and Vasques, A.: Increased aridity drives post-fire recovery of Mediterranean forests towards open shrublands. New Phytol., 225(4), 1500-1515. https://doi.org/10.1111/nph.16252, 2020

Belcher, C.M., Brown, I., Clay, G.D., Doerr, S.H., Elliott, A., Gazzard, R., Kettridge, N., Morison, J., Perry, M. and Smith, T.E.L.: UK wildfires and their climate challenges. Expert Led report prepared for the third climate change risk assessment, 2021

Biçen, T., Ayhan Arslan, A., & Vardar, A.. Regional solar and wind energy characteristics and it's energy potential in northwest of Turkey. Gümüşhane Üniversitesi Fen Bilimleri Dergisi, 12(2), 527-538. https://doi.org/10.17714/gumusfenbil.898023, 2022

Bowman, D.M., Williamson, G.J., Abatzoglou, J.T., Kolden, C.A., Cochrane, M.A. and Smith, A.M.: Human exposure and sensitivity to globally extreme wildfire events. Nat. Ecol. Evol. 1, 0058. https://doi.org/10.1038/s41559-016-0058, 2017

Brune, S., Keller, J.D. and Wahl, S.: Evaluation of wind speed estimates in reanalyses for wind energy applications. Adv. Sci. Res. 18, pp.115-126. https://doi.org/10.5194/asr-18-115-2021, 2021

Bruneua M, 2025. France's Largest Wildfire in Nearly 80 Years Contained, Say Officials: https://earth.org/frances-largest-wildfire-in-nearly-80-years-contained-say-officials/, last accessed 2nd March 2026

Calheiros, T., Nunes, J.P. and Pereira, M.G.: Recent evolution of spatial and temporal patterns of burnt areas and fire weather risk in the Iberian Peninsula. Agric. For. Meteorol., 287, 107923. https://doi.org/10.1016/j.agrformet.2020.107923, 2020

Castel-Clavera, J., Pimont, F., Opitz, T., Ruffault, J., Rivière, M. and Dupuy, J.L.: Disentangling the factors of spatio-temporal patterns of wildfire activity in south-eastern France. Int. J. Wild. Fire, 32(1), 15-28. https://doi.org/10.1071/WF22086, 2023

Chen, G., Guo, Y., Yue, X., Tong, S., Gasparrini, A., Bell, M.L., Armstrong, B., Schwartz, J., Jaakkola, J.J., Zanobetti, A. and Lavigne, E.: Mortality risk attributable to wildfire-related PM2· 5 pollution: a global time series study in 749 locations. The Lancet Planet. Health, 5(9), e579-e587. https://doi.org/10.1016/S2542-5196(21)00200-X, 2021

Chen, J. and Dai, A.: The atmosphere has become increasingly unstable during 1979–2020 over the Northern Hemisphere. Geophys. Res. Lett., 50(20), e2023GL106125. https://doi.org/10.1029/2023GL106125, 2023

Colantoni, A., Egidi, G., Quaranta, G., D'Alessandro, R., Vinci, S., Turco, R., and Salvati, L.: Sustainable land management, wildfire risk and the role of grazing in Mediterranean urban-rural interfaces: a regional approach from Greece. Land, 9(1), 21. https://doi.org/10.3390/land9010021, 2020

Copernicus, 2025. Image of the day 19/08/2025: https://www.copernicus.eu/en/media/image-day-gallery/burn-scar-aude-region-france#:~:text=A%20devastating%20wildfire%20in%20France%27s,hectares%2C%20an%20area%20…, last accessed 2nd March 2026

Costa-Saura, J.M., Bacciu, V., Sirca, C., Cappelluti, O., Spano, D. and Elia, M.: The growing link between heatwaves and megafires: evidence from southern Mediterranean countries of Europe. Nat Hazards 121, 17731–17742. https://doi.org/10.1007/s11069-025-07488-6, 2025

https://doi.org/10.5194/egusphere-2026-1193
Preprint. Discussion started: 20 March 2026

Cunningham, C.X., Williamson, G.J. and Bowman, D.M.J.S. Increasing frequency and intensity of the most extreme wildfires on Earth. Nat. Ecol. Evol. 8, 1420–1425. https://doi.org/10.1038/s41559-024-02452-2, 2024

Curt, T. and Frejaville, T.: Wildfire policy in Mediterranean France: how far is it efficient and sustainable?. Risk Anal., 38(3), 472-488. https://doi.org/10.1111/risa.12855, 2018

Davies, G.M., Legg, C.J., O'hara, R., MacDonald, A.J. and Smith, A.A.: Winter desiccation and rapid changes in the live fuel moisture content of Calluna vulgaris. Plant Ecol. Divers., 3(3), 289-299. https://doi.org/10.1080/17550874.2010.544335, 2010

De Luca, P. and Donat, M.G.: Projected changes in hot, dry, and compound hot-dry extremes over global land regions. Geophys. Res. Lett., 50(13), e2022GL102493. https://doi.org/10.1029/2022GL102493, 2023

De Onzono J.I., Spain's sees worst wildfire season since 1994 with 382,000 hectares burned so far in 2025: https://www.euronews.com/2025/08/21/spains-sees-worst-wildfire-season-since-1994-with-382000-hectares-burned-so-far-in-2025, last accessed 2nd March 2026

Di Virgilio, G., Evans, J.P., Blake, S.A., Armstrong, M., Dowdy, A.J., Sharples, J. and McRae, R.: Climate change increases the potential for extreme wildfires. Geophys. Res. Lett. 46(14), 8517-8526. https://doi.org/10.1029/2019GL083699, 2019

Díaz-Delgado, R., Lloret, F. and Pons, X.: Influence of fire severity on plant regeneration by means of remote sensing imagery. Int. J. Remote Sens. 24(8), 1751-1763. https://doi.org/10.1080/01431160210144732, 2003

Duane, A., Castellnou, M. and Brotons, L.: Towards a comprehensive look at global drivers of novel extreme wildfire events. Climatic Chang. 165, 43. https://doi.org/10.1007/s10584-021-03066-4, 2021

Dupuy, J.L., Fargeon, H., Martin-StPaul, N., Pimont, F., Ruffault, J., Guijarro, M., Hernando, C., Madrigal, J. and Fernandes, P.: Climate change impact on future wildfire danger and activity in southern Europe: a review. Annal. For. Sci. 77, 35. https://doi.org/10.1007/s13595-020-00933-5, 2020

Eisfelder, C., Uereyen, S., Asam, S., Hirner, A., Reiners, P., Huth, J., Bachofer, F., Bachmann, M., Holzwarth, S. and Kuenzer, C. Thirty-Year Analyses of Seasonal NDVI and Climatic Drivers Across Different Land Cover Types and Biogeographical Regions in Europe. IEEE J. Select. Topic. Appl. Earth Obs. Remote Sens. https://doi.org/10.1109/JSTARS.2025.3558816 2025

Ekberzade, B., Yetemen, O., Ezber, Y., Sen, O.L. and Dalfes, H.N.: Latitude or altitude as the future refugium? A case for the future of forests in Asia Minor and its surroundings. Ecol. Evol., 14(4), e11131. https://doi.org/10.1002/ece3.11131, 2024

Ekberzade, B., Görüm, T., Karabacak, F., Akay, S.S. and Şen, Ö.L.: Up in flames: the human factor behind a megafire in Mediterranean Türkiye. npj Nat. Hazards 2, 65. https://doi.org/10.1038/s44304-025-00120-4, 2025

El Garroussi, S., Di Giuseppe, F., Barnard, C. and Wetterhall, F.: Europe faces up to tenfold increase in extreme fires in a warming climate. npj Clim. Atmos. Sci. 7, 30. https://doi.org/10.1038/s41612-024-00575-8, 2024

European Commission, 2026. EFFIS Statistics Portal: https://forest-fire.emergency.copernicus.eu/apps/effis.statistics/, last accessed 2nd March 2026

https://doi.org/10.5194/egusphere-2026-1193
Preprint. Discussion started: 20 March 2026

Eyring, V., Bony, S., Meehl, G.A., Senior, C.A., Stevens, B., Stouffer, R.J. and Taylor, K.E.: Overview of the Coupled Model Intercomparison Project Phase 6 (CMIP6) experimental design and organization. Geosci. Model Dev. 9(5), 1937-1958. https://doi.org/10.5194/gmd-9-1937-2016, 2016

Fernandez-Anez, N., Krasovskiy, A., Müller, M., Vacik, H., Baetens, J., Hukić, E., Kapovic Solomun, M., Atanassova, I., Glushkova, M., Bogunović, I. and Fajković, H.: Current wildland fire patterns and challenges in Europe: A synthesis of national perspectives. Air, Soil Water Res., 14, 11786221211028185. https://doi.org/10.1177/11786221211028185, 2021

Forestry Commission: Wildfire statistics for England: Report to 2020-21. Forestry Commission England: Bristol, 2023

France 24, 2025. Portugal suffers new wildfire death as Spain beats back blazes: https://www.france24.com/en/live-news/20250823-portugal-suffers-new-wildfire-death-as-spain-beats-back-blazes, last accessed 2nd March 2026

Gagkas, Z., Campbell, G., Owen, J. and Davies, M.: Provision of analyses of Scottish fire and rescue service (SFRS) incident reporting system (IRS) data in relation to wildfire incidents. Report Prepared for Scottish Government, 2022

Galizia, L.F., Curt, T., Barbero, R. and Rodrigues, M.: Understanding fire regimes in Europe. Int. J. Wild. Fire, 31(1), 56-66. https://doi.org/10.1071/WF21081, 2022

Ganteaume, A., Barbero, R., Jappiot, M. and Maillé, E.: Understanding future changes to fires in southern Europe and their impacts on the wildland-urban interface. J. Safety Sci. Resil. 2(1), 20-29. https://doi.org/10.1016/j.jnlssr.2021.01.001, 2021

Giannaros, T.M. and Papavasileiou, G.: Changes in European fire weather extremes and related atmospheric drivers. Agric. For. Meteorol. 342, 109749. https://doi.org/10.1016/j.agrformet.2023.109749, 2023

Gouveia, C.M., Bastos, A., Trigo, R.M. and DaCamara, C.C.: Drought impacts on vegetation in the pre-and post-fire events over Iberian Peninsula. Nat. Hazard. Earth Syst. Sci. 12(10), 3123-3137. https://doi.org/10.5194/nhess-12-3123-2012, 2012

Grillakis, M., Voulgarakis, A., Rovithakis, A., Seiradakis, K.D., Koutroulis, A., Field, R.D., Kasoar, M., Papadopoulos, A. and Lazaridis, M.: Climate drivers of global wildfire burned area. Environ. Res. Lett. 17(4), 045021. https://doi.org/10.1088/1748-9326/ac5fa1, 2022

Guo, Y., Wang, J., Ge, Y. and Zhou, C.: Global expansion of wildland-urban interface intensifies human exposure to wildfire risk in the 21st century. Sci. Adv. 10(45), eado9587. https://doi.org/10.1126/sciadv.ado9587, 2024

Haas, O., Prentice, I.C. and Harrison, S.P.: Global environmental controls on wildfire burnt area, size, and intensity. Environ. Res. Lett., 17(6), 065004. https://doi.org/10.1088/1748-9326/ac6a69, 2022

Haas, O., Keeping, T., Gomez-Dans, J., Prentice, I.C. and Harrison, S.P.: The global drivers of wildfire. Frontiers in Environmental Science, 12, p.1438262. https://doi.org/10.3389/fenvs.2024.1438262, 2024

Hantson, S., Pueyo, S. and Chuvieco, E.: Global fire size distribution is driven by human impact and climate. Glob. Ecol. Biogeogr., 24(1), 77-86. https://doi.org/10.1111/geb.12246, 2015

Hargreaves, G.H. and Samani, Z.A.: Estimating potential evapotranspiration. J. Irrig. Drain. Div., 108(3), 225-230. https://doi.org/10.1061/JRCEA4.0001390, 1982

Hollingsworth, E.: Karst Regions of the World (KROW)—Populating global karst datasets and generating maps to advance the understanding of karst occurrence and protection of karst species and habitats worldwide. University of Arkansas. 2009

https://doi.org/10.5194/egusphere-2026-1193
Preprint. Discussion started: 20 March 2026

IPCC, 2021: Summary for Policymakers. In: Climate Change 2021: The Physical Science Basis. Contribution of Working Group Ito the Sixth Assessment Report of the Intergovernmental Panel on Climate Change. Camb. Univ. Press, 3−32, https://doi.org/10.1017/9781009157896.001, 2021

Ivison, K., Little, K., Orpin, A., Belcher, C.M., Clay, G.D., Doerr, S.H., Smith, T.E., Andersen, R., Graham, L.J. and Kettridge, N.: Unprecedented UK heatwave harmonised drivers of fuel moisture creating extreme temperate wildfire risk. Commun. Earth Environ. 6, 727. https://doi.org/10.1038/s43247-025-02746-8, 2025

Jacob, D., Petersen, J., Eggert, B., Alias, A., Christensen, O.B., Bouwer, L.M., Braun, A., Colette, A., Déqué, M., Georgievski, G. and Georgopoulou, E.: EURO-CORDEX: new high-resolution climate change projections for European impact research. Reg. Environ. Change 14, 563–578. https://doi.org/10.1007/s10113-013-0499-2, 2014

Jaupaj O.: Wildfires: Forecasted hazard and real exposure. A conceptual and empirical analysis of wildfires in Albania (in Albanian). Botime Impression, Tirana. [in review] 2025

Jaupaj, O., Jaupaj A.:. Wildfire hazard and activity patterns in Shkodra, Albania. Agric. Forestry, 71(3), 71-86. https://doi.org/10.17707/AgricultForest.71.3.04, 2025

Jeong, S., Ryu, Y., Gentine, P., Lian, X., Fang, J., Li, X., Dechant, B., Kong, J., Choi, W., Jiang, C. and Keenan, T.F.: Persistent global greening over the last four decades using novel long-term vegetation index data with enhanced temporal consistency. Remote Sens. Environ., 311, 114282. https://doi.org/10.1016/j.rse.2024.114282, 2024

Jeong, S., Ryu, Y., Gentine, P., Lian, X., Fang, J., Li, X., Dechant, B., Liu, J., Kong, J., Wan, L. and Choi, C.: Sustained global greening driven by continuous CO2 fertilization. https://doi.org/10.21203/rs.3.rs-8621169/v1 [preprint]

Jiang, C., Ryu, Y., Fang, H., Myneni, R., Claverie, M. and Zhu, Z.: Inconsistencies of interannual variability and trends in long-term satellite leaf area index products. Glob. chang. biol. 23(10), 4133-4146. https://doi.org/10.1111/gcb.13787, 2017

Johnston, F.H., Henderson, S.B., Chen, Y., Randerson, J.T., Marlier, M., DeFries, R.S., Kinney, P., Bowman, D.M. and Brauer, M.: Estimated global mortality attributable to smoke from landscape fires. Environ. Health Perspect., 120(5), 695. https://doi.org/10.1289/ehp.1104422, 2012

Keeley JE, Bond WJ, Bradstock RA, Pausas JG, Rundel PW. Fire in Mediterranean Ecosystems: Ecology, Evolution and Management. Camb. Univ. Press. ISBN 9781139033091, 2011.

Keeley, J.E. and Pausas, J.G.: Evolutionary ecology of fire. Annul. Rev. Ecol. Evol. Syst., 53(1), 203-225. https://doi.org/10.1146/annurev-ecolsys-102320-095612, 2022

Keeping, T., Bergin, C., Pinto, I., Ekberzade, B., Voulgarakis, A., Grillakis, M., Papavasileiou, G., Xanthopoulos, G., Lagouvardos, K., Giannaros, T. and Yucel, I. Weather conditions leading to deadly wildfires in Türkiye, Cyprus and Greece made 10 times more likely due to climate change. WWA. https://doi.org/10.25560/123302, 2025a

Keeping T., García García D., Trigo R., Santos F.L.M., Barnes C., Vahlberg M., Meyer R., Otto F., Philip S., Singh R., Casas Osorio S., Neves M., Haro P.: Extreme fire weather conditions in Spain and Portugal now common due to climate change. WWA. https://www.dx.doi.org/10.25560/123547, 2025b

https://doi.org/10.5194/egusphere-2026-1193
Preprint. Discussion started: 20 March 2026

Keesstra, S.D., Castellani, C., Lebelt, L., Breil, M., Vandecasteele, I., Pellens, N., Cerdà, A., de Rooij, L.L. and Zimmer, D.: Nature-based solutions for fire-resilient European forests. EEA. https://doi.org/10.2800/8810870, 2025

Kempf, M.: Enhanced trends in spectral greening and climate anomalies across Europe. Environmental monitoring and assessment, 195(2), 260. https://doi.org/10.1007/s10661-022-10853-8, 2023

Kirchmeier-Young, M.C., Gillett, N.P., Zwiers, F.W. and Cannon, A.J., FS Anslow: Attribution of the influence of human-induced climate change on an extreme fire season. Earth Fut. 7 2-10. https://doi.org/10.1029/2018EF001050, 2019

Kuhn-Régnier, A., Voulgarakis, A., Nowack, P., Forkel, M., Prentice, I.C. and Harrison, S.P.. Quantifying the importance of antecedent fuel-related vegetation properties for burnt area using Random Forests. Biogeosci. Discuss., 2020, 1-24. https://doi.org/10.5194/bg-18-3861-2021, 2020

Lanet, M., Li, L., Ehret, A., Turquety, S. and Le Treut, H.: Attribution of summer 2022 extreme wildfire season in Southwest France to anthropogenic climate change. npj Clim Atmos Sci 7, 267. https://doi.org/10.1038/s41612-024-00821-z, 2024

Li, S., Sparrow, S.N., Otto, F.E., Rifai, S.W., Oliveras, I., Krikken, F., Anderson, L.O., Malhi, Y., Wallom, D.: Anthropogenic climate change contribution to wildfire-prone weather conditions in the Cerrado and Arc of deforestation. Environ. Res. Lett. 16(9), 094051. https://doi/org/10.1088/1748-9326/ac1e3a, 2021

Li, X., Ault, T., Evans, C.P., Lehner, F., Carrillo, C.M., Donnelly, A., Crimmins, T.M. and Schwartz, M.D.: Growing uncertainty in projected spring onset variability in the Northern Hemisphere. Earth Syst. Sci. https://doi.org/10.1002/essoar.10512515.1, 2022

Little, K., Graham, L.J., Flannigan, M., Belcher, C.M. and Kettridge, N.: Landscape controls on fuel moisture variability in fire-prone heathland and peatland landscapes. Fire Ecol. 20, 14. https://doi.org/10.1186/s42408-024-00248-0, 2024

Little, K., Castellanos-Acuna, D., Jain, P., Graham, L., Kettridge, N. and Flannigan, M.: Persistent positive anomalies in geopotential heights drive enhanced wildfire activity across Europe. Phil. Trans. Royal Soc. B: Biol. Sci., 380(1924). https://doi.org/10.1098/rstb.2023.0455, 2025

Madhusoodanan, J.: Wildfires pose a burning problem for wines and winemakers. PNAS, 118(34), e2113327118. https://doi.org/10.1073/pnas.2113327118, 2021

Mantero, G., Morresi, D., Marzano, R., Motta, R., Mladenoff, D.J. and Garbarino, M.: The influence of land abandonment on forest disturbance regimes: a global review. Landscape Ecol. 35, 2723–2744. https://doi.org/10.1007/s10980-020-01147-w, 2020

McDowell, N., Pockman, W.T., Allen, C.D., Breshears, D.D., Cobb, N., Kolb, T., Plaut, J., Sperry, J., West, A., Williams, D.G. and Yepez, E.A.: Mechanisms of plant survival and mortality during drought: why do some plants survive while others succumb to drought?. New phytol. 178(4), 719-739. https://doi.org/10.1111/j.1469-8137.2008.02436.x, 2008

McNorton, J., Moreno, A., Turco, M., Keune, J. and Di Giuseppe, F.: Hydroclimatic Rebound Drives Extreme Fire in California's Non-Forested Ecosystems. Glob. Chang. Biol., 31(9), e70481. https://doi.org/10.1111/gcb.70481, 2025

https://doi.org/10.5194/egusphere-2026-1193
Preprint. Discussion started: 20 March 2026

Menzel, A., Sparks, T.H., Estrella, N., Koch, E., Aasa, A., Ahas, R., Alm-Kübler, K., Bissolli, P., Braslavská, O.G., Briede, A. and Chmielewski, F.M.: European phenological response to climate change matches the warming pattern. Glob. chang. biol., 12(10), 1969-1976. https://doi.org/10.1111/j.1365-2486.2006.01193.x, 2006

Mercer C., 'Nightmare' wildfire in southern France hits vineyards: https://www.decanter.com/wine-news/nightmare-wildfire-in-southern-france-hits-vineyards-563004/, last accessed 2nd March 2026

Miller, J., Touma, D. and Brunner, M.I.: Compounding preconditions of wildfires vary in time and space within Europe. Commun. Earth Environ. 6, 1005. https://doi.org/10.1038/s43247-025-02955-1, 2025

Moreira, Francisco, Olga Viedma, Margarita Arianoutsou, Thomas Curt, Nikos Koutsias, Eric Rigolot, Anna Barbati et al.: Landscape–wildfire interactions in southern Europe: implications for landscape management. J. Environ. Manag. 92(10) 2389-2402. https://doi.org/10.1016/j.jenvman.2011.06.028, 2011

Muñoz-Sabater, J., Dutra, E., Agustí-Panareda, A., Albergel, C., Arduini, G., Balsamo, G., Boussetta, S., Choulga, M., Harrigan, S., Hersbach, H. and Martens, B.: ERA5-Land: A state-of-the-art global reanalysis dataset for land applications. Earth Syst. Sci. data, 13(9), 4349-4383. https://doi.org/10.5194/essd-13-4349-2021, 2021

Murcia, J.P., Koivisto, M.J., Luzia, G., Olsen, B.T., Hahmann, A.N., Sørensen, P.E. and Als, M.: Validation of European-scale simulated wind speed and wind generation time series. Appl. Energy, 305, 117794. https://doi.org/10.1016/j.apenergy.2021.117794, 2022

Myneni, R., Knyazikhin, Y., and Park, T. 2021. MODIS/Terra Leaf Area Index/FPAR 8-Day L4 Global 500m SIN Grid V061 [Data set]. NASA Land Processes Distributed Active Archive Center: https://doi.org/10.5067/MODIS/MOD15A2H.061, last accessed 2nd March 2026

Naeher, L.P., Brauer, M., Lipsett, M., Zelikoff, J.T., Simpson, C.D., Koenig, J.Q. and Smith, K.R.: Woodsmoke health effects: a review. Inhal. Toxicol., 19(1), 67-106. https://doi.org/10.1080/08958370600985875, 2007

NFCC, 2025a. Record numbers of wildfires are putting services under huge strain, warn Fire Chiefs: https://nfcc.org.uk/record-numbers-of-wildfires-are-putting-services-under-huge-strain-warn-fire-chiefs/, last accessed 2nd March 2026

NFCC, 2025b. Wildfires position statement: https://nfcc.org.uk/our-services/position-statements/wildfires-position-statement/, last accessed 2nd March 2026

Nikonovas, T., Santín, C., Belcher, C.M., Clay, G.D., Kettridge, N., Smith, T.E. and Doerr, S.H.: Vegetation phenology as a key driver for fire occurrence in the UK and comparable humid temperate regions. Int. J. Wild. Fire, 33(10). https://doi.org/10.1071/WF23205, 2024

Olhoff, A., Christensen, J., Lamb, W.F., Pathak, M., Kuramochi, T., Fransen, T., Rogelj, J., den Elzen, M., Portugal-Pereira, J., Grant, N. and Kejun, J.: Emissions Gap Report 2024: No more hot air… please! With a massive gap between rhetoric and reality, countries draft new climate commitments. https://wedocs.unep.org/items/31ad9a4b-0c90-408e-adc0-921538ead02a, 2024

https://doi.org/10.5194/egusphere-2026-1193
Preprint. Discussion started: 20 March 2026

Ortiz A., Los incendios en Portugal han calcinado cerca de 275.000 hectáreas, casi el 3% de su territorio: https://elpais.com/internacional/2025-08-21/los-incendios-en-portugal-han-calcinado-cerca-de-275000-hectareas-casi-el-3-de-su-territorio.html, last accessed 2nd March 2026

Otto, F.E., Barnes, C., Philip, S., Kew, S., van Oldenborgh, G.J. and Vautard, R.: Formally combining different lines of evidence in extreme-event attribution. Adv. Stat. Climatol., Meteorol. Oceanogr., 10(2), 159-171. https://doi.org/10.5194/ascmo-10-159-2024, 2024

Parise M., Qiriazi P., Sala S.: Natural and anthropogenic hazards in karst areas of Albania. Nat. Hazard Earth Syst. Sci., 4(4), 569-581. https://doi.org/10.5194/nhess-4-569-2004, 2004

Parrington M, McNorton J, 2025. Extreme wildfires in summer 2025: https://www.ecmwf.int/en/newsletter/185/news/extreme-wildfires-summer-2025, last accessed 2nd March 2026

Patra, A., Oueslati, B., Chevallier, T., Renaud, P., Kervella, Y. and Dubus, L.: Evaluation of ERA5, COSMO-REA6 and CERRA in simulating wind speed along the French coastline for wind energy applications. Advances Sci. Res., 22, pp.69-85. https://doi.org/10.5194/asr-22-69-2025, 2025

Pausas, J.G. and Ribeiro, E.: The global fire–productivity relationship. Glob. Ecol. Biogeogr., 22(6), 728-736. https://doi.org/10.1111/geb.12043, 2013

Pausas, Juli G., and Santiago Fernández-Muñoz: Fire regime changes in the Western Mediterranean Basin: from fuel-limited to drought-driven fire regime. Climatic Chang.110, 1. 215-226. https://doi.org/10.1007/s10584-011-0060-6, 2012

Perry, M.C., Vanvyve, E., Betts, R.A. and Palin, E.J.: Past and future trends in fire weather for the UK. Nat. Hazard Earth Syst. Sci. 22(2), 559-575. https://doi.org/10.5194/nhess-22-559-2022, 2022

Philip, S., Kew, S., van Oldenborgh, G.J., Otto, F., Vautard, R., van Der Wiel, K., King, A., Lott, F., Arrighi, J., Singh, R. and van Aalst, M.: A protocol for probabilistic extreme event attribution analyses. Adv. Stat. Climatol. Meteorol. Oceanogr. 6(2), 177-203. https://doi.org/10.5194/ascmo-6-177-2020, 2020

Pimont, F., Fargeon, H., Opitz, T., Ruffault, J., Barbero, R., Martin-StPaul, N., Rigolot, E., Riviere, M. and Dupuy, J.L.: Prediction of regional wildfire activity in the probabilistic Bayesian framework of Firelihood. Ecol. Appl., 31(5), e02316. https://doi.org/10.1002/eap.2316, 2021

Pimont, F., Ruffault, J., Opitz, T., Fargeon, H., Barbero, R., Castel-Clavera, J., Martin-StPaul, N., Rigolot, E. and Dupuy, J.L.: Future expansion, seasonal lengthening and intensification of fire activity under climate change in southeastern France. Int. J. Wild. Fire, 32(1), 4-14. https://doi.org/10.1071/WF22103, 2023

Potter, B.E. and McEvoy, D.: Weather factors associated with extremely large fires and fire growth days. Earth Interact., 25(1), 160-176. https://doi.org/10.1175/EI-D-21-0008.1, 2021

Poynting M, Rivault E, 2025. Area burned by UK wildfires in 2025 already at annual record: https://www.bbc.co.uk/news/articles/c0m9gm3jwljo, last accessed 2nd March 2026

https://doi.org/10.5194/egusphere-2026-1193
Preprint. Discussion started: 20 March 2026

Radeloff, V.C., Helmers, D.P., Kramer, H.A., Mockrin, M.H., Alexandre, P.M., Bar-Massada, A., Butsic, V., Hawbaker, T.J., Martinuzzi, S., Syphard, A.D. and Stewart, S.I.: Rapid growth of the US wildland-urban interface raises wildfire risk. PNAS, 115(13), 3314-3319. https://doi.org/10.1073/pnas.1718850115, 2018

Ramos, A.M., Russo, A., DaCamara, C.C., Nunes, S., Sousa, P., Soares, P.M.M., Lima, M.M., Hurduc, A. and Trigo, R.M.: The compound event that triggered the destructive fires of October 2017 in Portugal. iScience, 26(3). https://doi.org/10.1016/j.isci.2023.106141, 2023

Resco de Dios, V., Camprubí, À.C., Pérez-Zanón, N., Peña, J.C., Del Castillo, E.M., Rodrigues, M., Yao, Y., Yebra, M., Vega-García, C. and Boer, M.M.: Convergence in critical fuel moisture and fire weather thresholds associated with fire activity in the pyroregions of Mediterranean Europe. Sci. Tot. Environ., 806, 151462. https://doi.org/10.1016/j.scitotenv.2021.151462, 2022

Ribes, A., Boé, J., Qasmi, S., Dubuisson, B., Douville, H. and Terray, L.: An updated assessment of past and future warming over France based on a regional observational constraint. Earth Syst. Dyn. 13(4), 1397-1415. https://doi.org/10.5194/esd-13-1397-2022, 2022

Robins A. France still battling largest wildfire in 75 years: https://www.bbc.co.uk/news/articles/cm2vk4xl204o#:~:text=A%20woman%20has%20died%20and,in%20southern%20France%20on%20Tuesday, last accessed 2nd March 2026

Rodrigues, M., Trigo, R.M., Vega-García, C. and Cardil, A.: Identifying large fire weather typologies in the Iberian Peninsula. Agric. For. Meteorol., 280, 107789. https://doi.org/10.1016/j.agrformet.2019.107789, 2020

Rodrigues, M., de Dios, V.R., Sil, Â., Camprubí, A.C. and Fernandes, P.M.: VPD-based models of dead fine fuel moisture provide best estimates in a global dataset. Agric. For. Meteorol. 346, 109868. https://doi.org/10.1016/j.agrformet.2023.109868, 2024

Rovithakis, A., Grillakis M.G., Seiradakis K.D., Giannakopoulos C., Karali A., Field R., Lazaridis M., Voulgarakis A.: Future climate change impact on wildfire danger over the Mediterranean: the case of Greece. Environ. Res. Lett. 17(4) 045022. https://doi.org/10.1088/1748-9326/ac5f94, 2022

Rovithakis, A., Burke, E., Burton, C., Kasoar, M., Grillakis, M. G., Seiradakis, K. D., Voulgarakis, A.: Estimating future wildfire burnt area over Greece using the JULES-INFERNO model, Nat. Hazards Earth Syst. Sci., 25, 3185–3200, https://doi.org/10.5194/nhess-25-3185-2025, 2025.

Ruffault, J. and Mouillot, F.: Contribution of human and biophysical factors to the spatial distribution of forest fire ignitions and large wildfires in a French Mediterranean region. Int. J. Wild. Fire, 26(6), 498-508. https://doi.org/10.1071/WF16181, 2017

Russo, A., Gouveia, C.M., Páscoa, P., DaCamara, C.C., Sousa, P.M. and Trigo, R.M.: Assessing the role of drought events on wildfires in the Iberian Peninsula. Agric. For. Meteorol., 237, 50-59. https://doi.org/10.1016/j.agrformet.2017.01.021, 2017

https://doi.org/10.5194/egusphere-2026-1193
Preprint. Discussion started: 20 March 2026

Ryu, Y., Jiang, C., Kobayashi, H. and Detto, M.: MODIS-derived global land products of shortwave radiation and diffuse and total photosynthetically active radiation at 5 km resolution from 2000. Remote Sens. Environ. 204, 812-825. https://doi.org/10.1016/j.rse.2017.09.021, 2018

Salis, Michele, Liliana Del Giudice, Roghayeh Jahdi, Fermin Alcasena-Urdiroz, Carla Scarpa, Grazia Pellizzaro, Valentina Bacciu et al. Spatial patterns and intensity of land abandonment drive wildfire hazard and likelihood in Mediterranean agropastoral areas. Land 11(11) 1942., https://doi.org/10.3390/land11111942, 2022

San-Miguel-Ayanz, Jesús, Jose Manuel Moreno, and Andrea Camia: Analysis of large fires in European Mediterranean landscapes: Lessons learned and perspectives. For. Ecol. Manag. 294: 11-22. https://doi.org/10.1016/j.foreco.2012.10.050, 2013

Sánchez-Hernández, G., Turco, M., Repeto-Deudero, I., Royé, D., Baudena, M., Montávez, J.P., Pietroiusti, R., Provenzale, A., Santin, C., Torres-Vázquez, M.Á. and Pausas, J.G.. Record-Breaking 2025 European Wildfires Concentrated in Northwest Iberia. Glob. Chang. Biol. 31(12), e70649. https://doi.org/10.1111/gcb.70649, 2025

Schumacher, D.L., Singh, J., Hauser, M., Fischer, E.M., Wild, M. and Seneviratne, S.I.: Exacerbated summer European warming not captured by climate models neglecting long-term aerosol changes. Commun Earth Environ 5, 182. https://doi.org/10.1038/s43247-024-01332-8, 2024

Schwinning, S. and Ehleringer, J.R.: Water use trade-offs and optimal adaptations to pulse-driven arid ecosystems. J. Ecol. 89(3), 464-480. https://doi.org/10.1046/j.1365-2745.2001.00576.x, 2001

Senande-Rivera, M., Insua-Costa, D. & Miguez-Macho, G. Climate change aggravated wildfire behaviour in the Iberian Peninsula in recent years. npj Clim. Atmos. Sci. 8, 19. https://doi.org/10.1038/s41612-025-00906-3, 2025

Seneviratne, S.I., X. Zhang, M. Adnan, W. Badi, C. Dereczynski, A. Di Luca, S. Ghosh, I. Iskandar, J. Kossin, S. Lewis, F. Otto, I. Pinto, M. Satoh, S.M. Vicente-Serrano, M. Wehner, and B. Zhou, 2021: Weather and Climate Extreme Events in a Changing Climate. In Climate Change 2021: The Physical Science Basis. Contribution of Working Group I to the Sixth Assessment Report of the Intergovernmental Panel on Climate Change. Camb. Univ. Press, 1513–1766, https://doi.org/10.1017/9781009157896.013, 2021

Serjani A., Hallaci H., Neziraj A., Hallaci A.: Karst and geotops of karst origin in Albania. Bull. Geol. Soc. Greece, 34(2), 811-817. https://doi.org/10.12681/bgsg.17704, 2001

Sheridan, L.M., Phillips, C., Orrell, A.C., Berg, L.K., Tinnesand, H., Rai, R.K., Zisman, S., Duplyakin, D. and Flaherty, J.E.: Validation of wind resource and energy production simulations for small wind turbines in the United States. Wind Energy Sci., 7(2), 659-676. https://doi.org/10.5194/wes-7-659-2022, 2022

Sjöström, J. and Granström, A.: A phenology-driven fire danger index for northern grasslands. Int. J. Wild. Fire, 32(9), 1332-1346. https://doi.org/10.1071/WF23013, 2023

Sousa, P.M., Trigo, R.M., Pereira, M.G., Bedia, J. and Gutiérrez, J.M.: Different approaches to model future burnt area in the Iberian Peninsula. Agric. For. Meteorol. 202, 11-25. https://doi.org/10.1016/j.agrformet.2014.11.018, 2015

https://doi.org/10.5194/egusphere-2026-1193
Preprint. Discussion started: 20 March 2026

Srock, A.F., Charney, J.J., Potter, B.E. and Goodrick, S.L.: The hot-dry-windy index: A new fire weather index. Atmos. 9(7), p.279. https://doi.org/10.3390/atmos9070279, 2018

Stephens, S.L., Collins, B.M., Fettig, C.J., Finney, M.A., Hoffman, C.M., Knapp, E.E., North, M.P., Safford, H. and Wayman, R.B.: Drought, tree mortality, and wildfire in forests adapted to frequent fire. BioSci., 68(2), 77-88. https://doi.org/10.1093/biosci/bix146, 2018

Swain, D.L., Prein, A.F., Abatzoglou, J.T., Albano, C.M., Brunner, M., Diffenbaugh, N.S., Singh, D., Skinner, C.B. and Touma, D.: Hydroclimate volatility on a warming Earth. Nat Rev Earth Environ 6, 35–50. https://doi.org/10.1038/s43017-024-00624-z, 2025

Tang, Y., Zhong, S., Luo, L., Bian, X., Heilman, W.E. and Winkler, J.: The potential impact of regional climate change on fire weather in the United States. Annal. Assoc. American Geogr., 105(1), 1-21. https://doi.org/10.1080/00045608.2014.968892, 2015

Travis, W.R.: Weather and climate extremes: Pacemakers of adaptation?. Weather Clim. Extrem., 5, pp.29-39. https://doi.org/10.1016/j.wace.2014.08.001, 2014

Trigo, R.M., Sousa, P.M., Pereira, M.G., Rasilla, D. and Gouveia, C.M.: Modelling wildfire activity in Iberia with different atmospheric circulation weather types. Int. J. Climatol., 36(7), 2761-2778. https://doi.org/10.1002/joc.3749, 2016

Van Oldenborgh, G.J., van Der Wiel, K., Kew, S., Philip, S., Otto, F., Vautard, R., King, A., Lott, F., Arrighi, J., Singh, R. and van Aalst, M., 2021. Pathways and pitfalls in extreme event attribution. Climatic Chang. 166(1), 13.. https://doi.org/10.1007/s10584-021-03071-7, 2021

Vautard, R., Van Aalst, M., Boucher, O., Drouin, A., Haustein, K., Kreienkamp, F., Van Oldenborgh, G.J., Otto, F.E., Ribes, A., Robin, Y. and Schneider, M.: Human contribution to the record-breaking June and July 2019 heatwaves in Western Europe. Environ. Res. Lett., 15(9), 094077. https://doi.org/10.1088/1748-9326/aba3d4., 2020

Vautard, R., Kadygrov, N., Iles, C., Boberg, F., Buonomo, E., Bülow, K., Coppola, E., Corre, L., van Meijgaard, E., Nogherotto, R. and Sandstad, M.: Evaluation of the large EURO-CORDEX regional climate model ensemble. J. Geophys. Res.: Atmos. 126(17), e2019JD032344. https://doi.org/10.1029/2019JD032344, 2021

Viúdez J., Interior ve una mejoría en la extinción de los incendios más graves, aunque preocupa el de Igüeña en León: https://elpais.com/espana/2025-08-28/interior-ve-una-mejoria-en-la-extincion-de-los-incendios-mas-graves-aunque-preocupa-el-de-iguena-en-leon.html, last accessed 2nd March 2026

Von der Leyen U, 2025 State of the Union Address by President von der Leyen: https://ec.europa.eu/commission/presscorner/detail/ov/SPEECH_25_2053, last accessed 2nd March 2026

Weekes, S.M. and Tomlin, A.S.: Data efficient measure-correlate-predict approaches to wind resource assessment for small-scale wind energy. Renew.Energy, 63, pp.162-171. https://doi.org/10.1016/j.renene.2013.08.033, 2014

WWF, 2025. Review of the 2025 Fire Season by WWF Greece and the FLAME Group of the National Observatory of Athens: https://www.wwf.gr/en/?20142366/Review-of-the-2025-Fire-Season-by-WWF-Greece-and-the-FLAME-Group-of-the-National-Observatory-of-

https://doi.org/10.5194/egusphere-2026-1193
Preprint. Discussion started: 20 March 2026

Athens#:~:text=Burned%20area%20during%20the%202025,burned%20area%20exceeds%2050%2C000%20hectares, last accessed 2nd March 2026